Unbundling Quantitative Easing: Taking a Cue from Treasury Auctions*

Michael Droste
Harvard University

Yuriy Gorodnichenko
UC Berkeley and NBER

Walker Ray
London School of Economics

October 26, 2020

Abstract

We study empirically and theoretically the role of preferred habitat in understanding the economic effects of the Federal Reserve's quantitative easing (QE) purchases. Using high-frequency identification and exploiting the structure of the primary market for U.S. Treasuries, we isolate demand shocks that are transmitted solely through preferred habitat channels, but otherwise mimic QE shocks. We document large "localized" yield curve effects when financial markets are disrupted. Our calibrated model, which embeds a preferred habitat model in a standard New Keynesian framework, can largely account for the observed financial effects of QE. We find that QE is modestly stimulative for output and inflation, but alternative policy designs can generate stronger effects.

Keywords: quantitative easing, monetary policy, market segmentation, treasury auctions

JEL Classification: E52, E43, E44

*We thank Michael Bauer, Rhys Bidder, Michael Fleming, Ed Knotek, Matteo Maggiori, Eric Swanson, Michael Weber, and seminar participants at Berkeley, New York Fed, Cleveland Fed, San Francisco Fed, ASU, DEC, CMC, and Northwestern for comments on an earlier version of the paper. We are grateful to Maxime Sauzet for excellent research assistance.

1 Introduction

Demand for safe assets, and U.S. Treasuries in particular, plays a central role in the macro-financial landscape. Over the past decade, a new feature has been introduced to the landscape: large-scale asset purchases (LSAPs) implemented by central banks, representing a sharp increase in demand for safe assets. The most salient of these is the quantitative easing (QE) programs carried out by the Federal Reserve, which originated during the global financial crisis and reemerged during the COVID19 crisis. Apart from the massive scale of these purchases, the Federal Reserve disproportionately bought long-maturity government debt, thus departing from the practice of having the distribution of its portfolio close to the distribution of outstanding debt (Figure 1).

While evaluating the first rounds of QE, Ben Bernanke, the chair of the Fed at the time, observed, "The problem with QE is it works in practice but it doesn't work in theory." Indeed, QE was successful in reducing short- and long-term interest rates, which motivated the redeployment of QE during the COVID19 crisis, but the mechanism behind this reaction is still not well understood. For example, standard macro-financial models imply that the demand for assets such as Treasuries is determined solely by economic agents' intertemporal consumption decisions, which does not capture the sources of demand shifts initiated by the Fed. Although the workhorse macroeconomic models cannot readily explain the workings of the QE, several explanations have been put forth. For instance, QE could be effective because it signaled to the markets that the Fed was serious about keeping short-term interest rates low for a long time (forward guidance). Or, perhaps the Fed exploited frictions (limited arbitrage and market segmentation) in the financial markets by purchasing securities in a particular segment. Alternatively, by buying assets on a massive scale, the Fed could signal a poor state of the economy which pushed interest rates down ("Delphic" effect; see Campbell et al. (2012) for more details). Given the paucity of QE events, it has proven remarkably hard to provide clear empirical evidence for each theory, as well as to assess the relative contributions of the proposed channels. Indeed, many channels were likely active during QE rounds and the reactions to QE were observed in a particular state of the economy, which potentially confounds identification and interpretation.

The objective of this paper is to unbundle QE by focusing on one channel: market segmentation and *preferred habitat*, which posits that certain investors have preferences for specific maturities. To this end, we take the following approach. First, we identify shifts in *private* demand for Treasuries that mimic QE, but are independent of the other channels discussed above. Next, we analyze the propagation of demand shocks across financial markets. In particular, we assess the ability of preferred habitat theory to rationalize the observed responses, and we confirm key predictions regarding pass-through of demand shocks in and out of financial crises. Informed by our empirical analysis, we then

develop and calibrate a general-equilibrium macroeconomic model designed to study QE policies. Our model shows that the preferred habitat channel accounts for the bulk of the observed response to QE in financial markets. Finally, while QE has modest stimulative effects on output and inflation in our model, we explore counterfactual alternative QE implementations that can help improve the design of future asset purchases.

Our analysis starts with the key insight that the mechanism through which market segmentation and preferred habitat forces operate is not the source of Treasury quantity shocks *per se*, but rather how marginal investors in the market for Treasury debt absorb these shocks. Hence, our goal is to identify demand shifts for Treasuries that are independent of all QE propagation mechanisms besides preferred habitat. To accomplish this, we utilize the primary market for Treasuries. Despite the fact that this is venue through which the Treasury issues debt (a supply-side action), the institutional structure of Treasury auctions has a number of desirable features for identifying shocks on the demand-side of the market.

First, similar to the empirical literature measuring the effects of monetary policy (e.g., Bernanke and Kuttner (2005), Gürkaynak et al. (2007), Gorodnichenko and Weber (2016)), we can use high-frequency (intraday) changes in Treasury yields in small windows around the close of Treasury auctions to identify unexpected shocks to demand for Treasuries. The key for identification is that the Treasury announces all of the "supply" information (e.g. security characteristics such as the maturity, as well as the amount of newly offered and outstanding securities) many days before the close of the auction. Moreover, the Treasury seeks to minimize supply-induced surprises by following a so-called "regular and predictable" issuance policy (see Garbade (2007)). Because all of the supply information is known and priced in by the market before the close of the auction, the release of the auction results reveal unexpected shifts in demand alone. The high-frequency focus and the timing of Treasury auctions allow us to rule out a host of confounding factors and identify unexpected shifts in demand.

Second, although the auctions are not as large as the QE rounds, in recent years the Treasury sold nearly $200 billion per month in notes and bonds, and received half a trillion in bids. Because the primary market for Treasuries is a convenient venue for investors who wish to purchase large amounts of government securities, the release of Treasury auction results can reveal potentially large shifts in demand for Treasuries. The surprise movements in the yields are reasonably large and persistent, with effect on yields typically lasting for many weeks following the auction.

Third, we document that demand shocks are driven by institutional investors such as foreign monetary authorities, investment funds, insurance companies and the like. We show that these shocks are not driven by changes in expectations about inflation, output, or other broad market conditions. Therefore, variation during Treasury auctions can help us to isolate the effect of *idiosyncratic* purchases in specific asset segments on the level

and shape of the yield curve, which is difficult to achieve by examining only QE events.

Finally, in sharp contrast to QE events, Treasury auctions are frequent and information spans many decades.[1] This gives us an opportunity for crisper inference and to study state-dependence in the effect of targeted purchases of assets (e.g., crisis vs. non-crisis states), which is instrumental for understanding how QE-like programs can work in normal times. Importantly, because Treasury auctions for specific maturities are spread over time, we can identify changes in demand for government debt of specific maturities. As a result, we can trace how a shock in one part of the yield curve propagates to other parts of the yield curve. In this sense, we have natural experiments which can mimic targeted purchases of the Fed during QE programs.

Utilizing our auction demand shocks, we assess empirically the "localization hypothesis," a characteristic prediction of preferred habitat theory and a key diagnostic for our subsequent quantitative, model-based analyses. Put simply, this hypothesis predicts that when bond markets are functioning well, demand shocks for either short- or long-maturity bonds will have similar effects on the yield curve. However, when financial intermediaries' risk-bearing capacity is low, they are unwilling to smooth out the price impact of demand shocks, and hence bond markets become more segmented: the location of the demand shock in maturity space matters and the effects on the yield curve are bigger for bonds of similar maturities. Informed by theory, we derive a simple regression specification that tests for equality of the relative response of the yield curve following auctions of short- and long-maturity debt. We find strong evidence in favor of localized yield curve effects during financial crisis periods, thus suggesting potentially powerful effects of QE on yields. However, during normal times, we cannot reject that the relative response of the yield curve is identical when comparing short- and long-maturity auctions, which points to weak (if any) effects of QE on bond markets.

Building on Vayanos and Vila (2009, 2020) and Ray (2019), we develop a theoretical model to rationalize the empirical responses of the yield curve to shocks in demand for Treasury securities. We use the model to run policy experiments to better understand the effects of QE on financial markets and the broader economy. When calibrated to match unconditional moments of the yield curve, we find that our model closely matches the empirical reactions of the yield curve to *private* demand shocks in crisis and non-crisis times (untargeted in the calibration). Furthermore, our results provide a quantitative sense of how much QE programs could influence interest rates through the preferred habitat channel. Specifically, when fed a shock calibrated to mimic QE1 in size and duration, our model generates movements in the yield curve remarkably close to the movements observed in the data. This result is consistent with the view that QE works mainly via market segmentation and preferred habitat, and that the *net* effect of other

[1] Availability of high-quality intraday data for the secondary market of Treasuries constrains our estimation sample to 1995-2017.

channels is small.

In the next step, we use the calibrated model to assess the ability of QE1 to influence output and inflation in crisis times. We find that the $300 billion purchase of Treasury debt increases output and inflation by the magnitudes that are only somewhat larger than a 25-basis-point cut in the policy rate during non-crisis times. That is, QE is expansionary but the effects are relatively modest. However, the macroeconomic effects of QE are sensitive to the implementation details of the program. In particular, holding the securities on the balance sheet longer (and making this clear to markets on announcement) boosts the stimulative power of QE significantly. We also show that QE may have unintended consequences: uncertainty surrounding the Fed's asset purchases themselves may lead to excess macroeconomic volatility. Finally, the expansionary effects of QE fall precipitously when undertaken during periods when bond markets are relatively healthy. Taken together, this suggests that QE should remain in policymakers' toolkit, but must be utilized with caution: QE is best undertaken during periods of severe financial distress; and clear communication regarding the size and duration of asset purchases is key to achieving stimulative outcomes while avoiding inducing excess financial and macroeconomic volatility.

Our study contributes to several strands of previous research. The first literature examines theoretically (e.g., Vayanos and Vila (2009), Greenwood and Vayanos (2014), Greenwood et al. (2016), Ray (2019), King (2019a) and empirically (e.g., Krishnamurthy and Vissing-Jorgensen (2012), Hamilton and Wu (2012), Kaminska and Zinna (2020)) determinants of demand for government debt by focusing on departures from the "expectations hypothesis" (e.g., limited arbitrage, market segmentation). Relative to this literature, we make progress in several dimensions. First, in the spirit of Kuttner (2001) and Bernanke and Kuttner (2005), we use intraday data around Treasury auctions to provide sharp identification of unanticipated demand shocks. This allows us to develop clean empirical tests of the theory and obtain precise estimates. In contrast, previous empirical research largely relies on time series methods estimating affine term structure models for interest rates. Second, we use a calibrated model not only to quantitatively analyze interest rate movements in response to demand shocks and QE, but also to map these reactions to macroeconomic outcomes for the purpose of evaluating the effect of QE programs on output and inflation. Third, we explicitly focus on how variation in risk-bearing capacity influences responses of the yield curve to shocks in demand for Treasury debt. This focus allows us to examine the effectiveness of QE programs in both crisis and non-crisis times; therefore, our results can help inform policymakers about the potential of quantitative easing to become a "conventional" tool.

The second literature studies the effects of QE programs in the U.S. and other countries (see Martin and Milas (2012) for a survey) and in particular how market segmentation interacts with QE programs (e.g. D'Amico and King (2013), Li and Wei (2013), Cahill et al.

(2013), King (2019b)). While most of these studies focus on market movements around QE announcements (e.g., Krishnamurthy and Vissing-Jorgensen (2012), Chodorow-Reich (2014)), we instead focus on market movements around Treasury auctions rather than on the Fed's purchases of Treasuries. This focus permits cleaner identification of demand shocks so that we can isolate preferred habitat from other channels (e.g., forward guidance, "Delphic" effects, etc.) in our analysis of QE. In addition, we have a longer time series dimension in Treasury auctions (QE events and the Fed's QE purchases did not exist before the Great Recession) and so we can study normal and crisis times. Finally, we move beyond the analysis of market reactions to purchases of Treasuries and shed light on the macroeconomic implications of preferred habitat broadly speaking (in addition to its connections with QE) and on the importance of various elements of QE design.

The third literature investigates how yields move around Treasury auctions (e.g., Lou et al. (2013), Fleming and Liu (2016)) and respond to variation in demand (e.g., Cammack (1991), Beetsma et al. (2016, 2018), Forest (2018)). Unlike this literature, our focus is not studying Treasury auctions directly; rather, we utilize the institutional structure of the primary market for Treasuries to better understand the mechanisms behind QE. Hence, relative to this literature, we *structurally* link demand shocks measured at Treasury auctions to a general equilibrium preferred habitat model. Furthermore, we study not only how variation in demand at an auction influences the pricing of the bond (or very similar bonds in the secondary market), but also how this variation spills over to all other bonds along the term structure, and further across other asset markets. With the exception of Beetsma et al. (2016), this literature focuses on periods of financial calm, while we focus on how variation in risk-bearing capacity of financial intermediaries in and out of financial crises affects the spillovers.

Finally, we contribute to the emergent literature on macroeconomic effects of QE. Specifically, our paper is related to recent efforts to move beyond case studies (e.g. Bernanke et al. (2004)) and provide more quantitative analyses. For example, in the spirit of Fieldhouse et al. (2018) and Di Maggio et al. (2020), we use QE-like events (rather than QE directly) and rich cross-sectional variation to obtain sharp identification and precise estimates. These estimates directly inform our calibrated structural general equilibrium model, which we use to assess the effects of QE on output and inflation. On the theory side, our work is related to Sims and Wu (2020), Gertler and Karadi (2011), Karadi and Nakov (2020), Cúrdia and Woodford (2011), Carlstrom et al. (2017), and Chen et al. (2012). In contrast to these works, we embed a financial model of the entire term structure of interest rates within a dynamic model of the macroeconomy. Further, we focus on the interaction of preferred habitat with limited risk-bearing capacity in bond markets as the core mechanism behind QE effects, rather than on reserve requirements or moral hazard/enforcement constraints on banks. Quantitatively, our estimates are in line with those in the literature that find QE was modestly effective at stimulating the

economy. We further stress the state-dependent nature of QE's effectiveness in and out of financial crises.

2 Data and Institutional Details

In this section we describe the primary sources of our data and present basic statistics. First, we describe the U.S. Treasury auctions for U.S. government notes and bonds (coupon-bearing nominal securities). Second, we describe the details of the data regarding intraday secondary-market Treasury prices.

2.1 Primary Market for Treasury Securities

The Treasury sells newly issued securities to the public on a regular basis through auctions. In recent years, 2-, 3-, 5- and 7-year notes are auctioned monthly. 10-year notes and 30-year bonds are auctioned in February, May, August and November with reopenings in the other 8 months. The frequency of auctions evolves over time. For example, 30-year bonds were not issued between 1999 and 2006 and were issued only twice a year between 1993 and 1999; and 20-year bonds were auctioned in May 2020, the first time since 1986.

There are two types of bids: noncompetitive and competitive. Noncompetitive bidders agree to accept the terms settled at the auction, and are typically limited to $5 million per bidder. Competitive bidders submit the amount they would like to purchase and the price (the interest rate) at which they would like to make the purchase. For each competitive bidder, the submitted amount cannot be greater than 35% of the amount offered at the auction.

Auction participants include primary dealers, other non-primary brokers and dealers, investment funds (for example, pension, hedge, mutual), insurance companies, depository institutions, foreign and international entities (governmental and private), the Federal Reserve (System Open Market Account), and individuals. These participants are classified into three groups. The first group is Primary Dealers (brokers and banks) that trade on their accounts with the Federal Reserve Bank of New York. This group typically buys the largest share of auctioned debt and is required to participate in every Treasury auction. The second group is Direct Bidders: non-primary dealers submitting bids for their own proprietary accounts. The third group is Indirect Bidders who submit competitive bids via a direct submitter, including Foreign and International Monetary Authorities placing bids through the Federal Reserve Bank of New York.[2]

[2]Additionally the Federal Reserve System purchases securities for its System Open Market Account (SOMA). Starting in 1997, the SOMA amount was changed from being listed within the announced offering amount to being additions to the announced offering amount. That is, if the Treasury auctions $15 billion in bonds and the Federal Reserve would like to purchase $1 billion in the auction, the Treasury issues $16 billion in bonds. This change was made so that the Treasury would be able to provide better information to the market about the amount of securities actually available for sale to the public.

Additionally, the Treasury divides investors into the following classes: Investment Funds (mutual funds, money market funds, hedge funds, money managers, and investment advisors); Pension and Retirement Funds and Insurance Companies (pension and retirement funds, state and local pension funds, life insurance companies, casualty and liability insurance companies, and other insurance companies); Depository Institutions (banks, savings and loan associations, credit unions, and commercial bank investment accounts); Individuals (individuals, partnerships, personal trusts, estates, non-profit and tax-exempt organizations, and foundations); Dealers and Brokers (primary dealers, other commercial bank dealer departments, and other non-bank dealers and brokers); Foreign and International (private foreign entities, non-private foreign entities placing tenders external of the Federal Reserve Bank of New York (FRBNY), and official foreign entities placing tenders through FRBNY); Federal Reserve System (the Federal Reserve Banks System Open Market Account (SOMA)); Other (represents the residual from categories not specified in investor class descriptions above). Fleming (2007) describes in greater detail the breakdown by types and class of bidders.

As detailed in Figure 2, there are four stages of a Treasury auction:[3]

1. *Announcement*: A few days before an auction, the Treasury releases all the pertinent information regarding the upcoming auction. An announcement includes security information (maturity, CUSIP identifier, schedule of coupon payments, etc.) as well as the amount offered, the bidding closing times, which class of bidders can participate, and other information describing the rules of the auction.

   Figure 3a presents a typical announcement. At this auction, the Treasury offers $16 billion in 30-year bonds. This is a new auction (that is, the Treasury does not reopen a previous auction) with the maximum award (that is, maximum allocation to a bidder) of $5.6 billion.

2. *Bidding*: After the announcement, individuals and institutions may submit bids up until the closing times of the auction. The announcement in Figure 3a stipulated that non-competitive bids should be submitted by 12:00 p.m., while the deadline for competitive bids is 1:00 p.m.

3. *Results*: Most Treasury note and bond auctions close at 1:00 p.m. Competitive bids are accepted in ascending order (in terms of yields) after the auction closes until the quantity meets the amount offered minus the amount of non-competitive bids. All bidders receive the same yield as the highest accepted bid. Once the auction closes and the winning bids are determined, the information regarding the results is released immediately. Besides the winning yield, the Treasury announces various aggregate

[3]See Driessen (2016) for details on the design of Treasury auctions. Garbade (2007) provides historical details regarding the manner in which the Treasury has conducted auctions.

statistics regarding the bidding. Beginning in the early 2000s, auction results are released within minutes of the close of the auction (see Garbade and Ingber (2005)).

Figure 3b presents a typical announcement about auction results, which corresponds to the auction announcement presented in Figure 3a. The demand (tendered) for the security was $33.3 billion, most of the bids came from primary dealers ($23.7 billion), $489.9 million was bought by the Federal Reserve (SOMA), and a relatively low amount was bought via non-competitive bids ($14.8 million). The "bid-to-cover", the ratio of all bids received to all bids accepted, was $33.3/$16.0=2.08. The interest rate, corresponding to the winning yield, was set at 3.75 percent per year.

4. *Issuance*: A few days after the close of an auction, the Treasury delivers the securities and charges the winning bidders for payment of the security. At this point the winning bidders can hold the security to maturity and receive coupon payments, or sell the security on the secondary market.

Data from the announcements and results of every auction since late 1979 are available from TreasuryDirect.gov. Data regarding amounts accepted and tendered by bidder type (Primary Dealer, Direct, and Indirect) are available starting in 2003. Additionally, the Treasury provides information regarding allotment by investor class (Investment Funds, Individuals, etc) starting in 2000.

2.2 Intraday Treasury Yields

Once a Treasury security auction is complete, the security is issued to the winner bidders, at which point the security is free to trade on the secondary market. Treasuries trade in the over-the-counter market, the largest and most active debt market in the world. Additionally, following the announcement of an auction but before issuance, there is a forward market for newly auctioned Treasuries. The forward contracts mature on the same day as the securities are issued, and hence this market is referred to as the "when-issued market." Our data on secondary-market yields (including when-issued yields) comes from GovPX, for the period 1995-2017. GovPX offers comprehensive intraday coverage of all outstanding US Treasury securities. We use changes in intraday Treasury yields in order to construct market-based measures of demand surprises occurring during Treasury auctions.[4]

[4]In an earlier version of the paper, we used Treasury futures to construct auction demand shocks. Treasury futures provide a natural market-based measure of unexpected shifts in Treasury prices; but in practice, secondary-market Treasury yields around auctions contain essentially no predictable movements. Additionally, Treasury futures cannot be tied directly to a specific bond issue at the CUSIP level, and the futures markets are less liquid than the secondary over-the-counter Treasury market. For these reasons, we focus our analysis on demand shocks constructed using secondary-market Treasury yields; however, our results are robust to using futures. See Gorodnichenko and Ray (2017).

2.3 Summary Statistics

In our analysis we focus on Treasury note and bond auctions. We exclude inflation protected securities (TIPS) and floating rate notes (FRNs) because these securities have different structural arrangements than simple coupon-bearing nominal securities. We also exclude Treasury bills (zero-coupon securities with maturity one year or less) because the QE programs mainly bought long-maturity nominal U.S. government debt.

Figure 4 plots the number and size of note and bond auctions per year in our sample, broken up by maturity. The number of auctions is relatively stable throughout the 1980s to mid 1990s. In the face of declining government debt, the number and size of auctions temporarily fell in the late 1990s and early 2000s, which also coincides with the termination of new issuances of 30-year bonds. After the Great Recession, the number of auctions increased significantly.

Table 1 presents summary statistics for all note and bond auctions since 1979, and the subsample 1995-2017 for which we have intraday Treasury yields. Since 1995, a typical offering is about $20 billion which generates more than $50 billion in demand so that the bid-to-cover ratio is approximately 2.6. The largest source of demand for Treasuries is primary dealers (their bid-to-cover ratio is ≈2) but other types of bidders also account a large fraction of auction offerings. Primary dealers purchase approximately 60 percent of auctioned Treasuries with the rest split equally between investment funds and foreign buyers.

There is considerable variation in the offered amounts (standard deviation is ≈$9 billion) as well as the level and composition of demand (standard deviation for the bid-to-cover ratio is ≈0.5 and the standard deviation of bid-to-cover ratio for primary dealers is 0.35). In our sample of Treasury note and bond auctions, the median maturity is 5 years. The winning yield ("high yield") is on average close to 3 percent per year with standard deviation of 1.9 percentage points.[5]

3 Quantifying Demand Shocks

In this section, we describe how we measure the surprise movements in Treasury yields around Treasury auctions and document properties of these surprises. Our key assumption is that within small enough windows around the close and release of Treasury auction results, shifts in Treasury yields reflect unexpected changes in market beliefs about the demand for Treasuries with a specific maturity. Indeed, the Treasury announces an offered amount well before an auction happens, thus fixing supply in advance of investor bidding.

[5]Between 1999-2015 when the data are available, the Fed purchased Treasuries through SOMA in approximately two thirds of auctions; when doing so they purchased an average of $2.3 billion (standard deviation of $2 billion). Note that these purchases are not included in the amounts offered to the public, and do not affect the winning bids.

Hence, between the announcement and close of the auction, Treasury yields should move only in response to unexpected changes in demand conditions. By focusing our analysis on a narrow window around the close of an auction and the release of the auction results, we likely isolate variation only due to unexpected shifts in demand for this specific auction. As a result, we can identify a demand shock for a specific maturity and then use this shock to trace the reaction of Treasury yields for the given maturity and for other maturities as well as reactions for other prices in financial markets.

3.1 Shock Construction

Let $y_{t,pre}^{(m)}, y_{t,post}^{(m)}$ be the Treasury yields before and after the close of the auction on date t with maturity m. We measure the surprise movements in Treasury yields as:

$$D_t^{(m)} = y_{t,post}^{(m)} - y_{t,pre}^{(m)}. \tag{1}$$

For all auctions, $y_{t,pre}^{(m)}$ is the last yield observed 10 minutes before the close of the auction,[6] while $y_{t,post}^{(m)}$ is the first yield observed 10 minutes following the release of the auction results. In our sample, auctions typically close at 1:00PM, or less frequently at 11:30AM. However, the time between the close of the auction and the release of the results is a function of how long it takes the Treasury to compile the results. The Treasury began releasing results much faster in the early 2000s, but in the 1990s auction results frequently took over an hour after the close of the auction to be released. Unlike the close of the auction, the time at which the results are released is not reported by the Treasury. However, wire reports from Bloomberg allow for an upper bound on the release time. Note that we use small symmetric windows around the events to eliminate predictable movements in prices identified in Lou et al. (2013) and Fleming and Liu (2016). Indeed, Fleming and Liu (2016) show that these predictable movements extend to the hours before and after the auction, but near the close of the auction and release of the results the price movements are reactions to the surprises regarding the demand observed at the auction. Hence, the use of small intraday windows is key to identifying unanticipated demand shocks.[7]

If the date t auction is a re-opening of a previously issued security, we use secondary-market market yields to construct our shocks. If the date t auction is instead a newly

[6] While it is conventional for event studies to assume that $y_{t,pre}^{(m)}$ incorporates *all* information available at the time (i.e., financial markets are efficient), a weaker assumption suffices for our analysis: relative to (potentially imperfect) market expectations, auction results contain new information.

[7] Of course, market-based measures are only effective when the markets in question are functioning well. Although the Treasury market is one of the largest and most liquid in the world, it is still possible that investors are able to manipulate the market. For instance, in 2015, the U.S. Department of Justice launched a probe to investigate whether various financial companies (most of which are primary dealers of U.S. Treasury securities) participated in a conspiracy to manipulate the secondary and futures markets for Treasuries; the class-action lawsuit is ongoing. However, as shown below our shocks show no evidence of manipulation.

issued security, we use yields from the "when-issued" market.

Figure 5 plots the time series of our constructed shock measures, with summary statistics presented in Table 2. Panels A and B of Table 2 report summary statistics for $D_t^{(m)}$ shocks during auction dates, both polling across maturities as well as separately by maturity. The mean values of the shocks are close to zero (and statistical tests do not reject the null of zero means), suggesting that surprises are not systematic and do not contain predictable movements.[8] In our sample period, the standard deviation of $D_t^{(m)}$ increases in maturity m and ranges from 1.3 basis points for 2-year maturity to 3.3 basis points for 30-year maturity. For comparison, Chodorow-Reich (2014) estimates that the largest intraday movements in yields following a QE announcement occurred after the Fed announced its purchases of Treasuries on March 18, 2009, whereby Treasury rates (five-year maturity) fell by 23 basis points. Panels C and D present statistics separately for periods of expansion/recession, and for periods of a binding/non-binding ZLB. Demand shocks appear to be more volatile during busts compared to booms.

To verify that these shocks are not spurious we also report (Panel E of Table 2) movements in Treasury yields on non-auction days (for days without auctions, the same "pre" and "post" windows are used as auctions in the same period). In all cases, the variance of the shocks on auction dates is larger than on non-auction dates. This pattern further suggests that surprise auction results influence secondary-market Treasury yields.

3.2 Narrative Evidence

To provide a better understanding of what forces are behind these surprise movements, Figure 6 plots the 30-year Treasury yields during two 30-year Treasury bond auctions.

The first is from December 9, 2010. This auction was a reopening of previously issued 30-year bonds from the month prior. The 30-year Treasury yields are relatively stable in the lead up to the close of the auction. After the auction closes and results are released, yields dropped sharply and immediately. The Financial Times wrote:

> "Large domestic financial institutions and foreign central banks were big buyers at an auction of 30-year US Treasury bonds on Thursday. 'Investors weren't messing around...You don't get the opportunity to buy large amounts of paper outside the auctions and 'real money' were aggressive buyers.'"

The second is from an auction of newly issued bonds on August 11, 2011. Once again, when-issued yields were relatively stable in the lead up to the close of the auction, but

[8] There is evidence that the when-issued market systematically trades at lower yields than the winning yield at the auction (see e.g. Fleming and Liu (2016)). However, as evidenced by Table 2, our demand shocks do not contain any such systematic biases because we focus exclusively on the changes in secondary-market yields. Additionally, Appendix Figure C1 compares auction shocks constructed using Treasury futures and yields. The two shock series are highly correlated, showing that secondary-market yield movements in these small windows around auctions do not contain any predictable movements.

after the close and release of the auction results, yields immediately rose. The Financial Times wrote:

> "An auction of 30-year US Treasury bonds saw weak demand...bidders such as pension funds, insurers and foreign governments shied away. 'There's not too many ways you can slice this one, it was a very poorly bid auction.'"

We interpret the two example auctions as follows. Before the auction closes, the market information set consists of all the supply information, both for outstanding securities as well as the amount on offer for the current 30-year auction. The 30-year Treasury yields reflect beliefs about the expected path of short-term interest rates, inflation expectations, and demand for long-maturity Treasury securities. After the auction closes and the results are released, the only update to the information set is the news regarding the bidding that took place in the auction, which solely reflects demand for Treasury debt. The change in the 30-year yields reflects this unexpected shift in beliefs about Treasury demand. The contemporaneous articles in the financial press further suggest that the important driver of the demand shifts arise from foreign and domestic institutional investors.

The narrative evidence from the financial press also highlights why auctions can have important elements of price discovery: when investors wish to purchase large amounts of Treasuries to meet their needs, they may prefer to use auctions rather than attempting to make substantial transactions on the secondary market. As a result, auctions reveal new information about demand that is not already reflected in over-the-counter secondary market trades.[9]

3.3 Demand Determinants

Our assumption is that $D_t^{(m)}$ captures unexpected shifts in the demand for Treasuries. We further hypothesize that these shocks are particularly driven by demand shifts arising from institutional investors. Figure 6 and the corresponding reporting in the financial press provided some narrative evidence in this direction. However, $D_t^{(m)}$ is a market-based measure and hence is an equilibrium response to the underlying shifts in demand. Because the mapping from shifts in demand to changes in Treasury yields may be complex, it is important to establish that the market interpretation of changes in demand is actually related to observable movements in demand.

One of the most commonly reported statistics in the financial press is the bid-to-cover ratio. It is a natural measure of the demand at a given auction: the higher is the bid-to-cover ratio, the higher is demand. The bin scatter plot in Figure 7 shows that the

[9]We could not find any reference in the press about monetary policy (or leaked information about future monetary policy) being a source of unexpected movements. Consistent with this observation, we do not find any statistical power of surprise movements in Treasury yields around Treasury auctions to predict future monetary policy.

bid-to-cover ratio (after controlling for its four own lags) is a strong predictor of our measure of demand shocks. Table 3 presents more formal evidence by regressing our shocks on measures of demand reported at the auction:

$$D_t^{(m)} = \alpha^{(m)} + \beta^{(m)} X_t^{(m)} + \varepsilon_t^{(m)} \tag{2}$$

This specification is estimated separately for auctions of different maturities in columns (1)-(6). For example, column (1) restricts the sample to include only auctions of 2-year notes and column (2) restricts the sample to include only auctions of notes with 3-year maturity. Column (7) reports results when we pool across maturities and impose that $\beta^{(m)}$ is the same across maturities m. Consistent with our interpretation of our intraday yield changes as a measure of unexpected demand shocks, the results show that the bid-to-cover ratio is strongly negatively associated with $D_t^{(m)}$. That is, a higher bid-to-cover ratio at a given auction predicts a larger intraday fall in Treasury yields following the close of the auction.

Panel B repeats the regressions from Panel A, but explicitly decomposes the bid-to-cover ratio into "expected" and "surprise" components. For these regressions, we first estimate a univariate AR(4) model of the bid-to-cover ratio, separately for each maturity group. This AR(4) model helps us to filter out predictable, low-frequency variation in demand for Treasuries in the primary market. We then construct the fitted (expected) and residual (surprise) values of the bid-to-cover ratio, and regress $D_t^{(m)}$ on these expected and surprise components. We find that the variation in our demand shocks is determined by the surprise component of the bid-to-cover ratio, and is unaffected by expected movements in the bid-to-cover ratio. Further, the effect of a surprise increase in the bid-to-cover ratio is economically large. For example, a one standard deviation (0.5) increase in the bid-to-cover ratio (after controlling for its own four lags) in a Treasury auction for 30-year bonds leads to a $5.36 \times 0.5 = 2.7$ basis point decline in 30-year Treasury yields.[10]

In order to assess sensitivity of our demand shocks to changes in demand by bidder type, Panel C reports estimates of equation (2) using the bid-to-cover ratio of Indirect Bidders, Direct Bidders, and Primary Dealers. The sensitivity of surprises $D_t^{(m)}$ to unexpected demand of indirect bidders increases with maturity. For example, a unit increase in the bid-to-cover ratio for indirect bidders decreases the yields of 2-year Treasuries by 4.7 basis points, and the yields of 30-year Treasuries by 15.8 basis points. Direct bidders exhibit the same pattern, although the coefficients are smaller and not always statistically significant. The sensitivity to changes in the bid-to-cover ratio coming from Primary Dealers is smaller still. When we pool across maturities, demand of Direct and especially Indirect Bidders generates *ceteris paribus* more variation in Treasury yields than demand

[10]We found that controlling for other variables (e.g., policy uncertainty constructed in Baker et al. (2016)) in equation (2) does not materially change our estimates.

of Primary Dealers, although for all bidder types an increase in bidder demand implies a decline in intraday yields $D_t^{(m)}$.

Panel D uses additional investor allotment data from the Treasury to break down the amount accepted by types of bidders: Investment Funds, Foreign, Dealers, and remaining smaller investors classes (which we aggregate into a "Miscellaneous" category). Since the fractions by group add up to one, we set Dealers as the leave-out category. The estimated coefficients suggest that as the fraction accepted for investment funds and foreign buyers increases, $D_t^{(m)}$ declines. The coefficients for the Miscellaneous category are generally smaller and less robust.

These results indicate that, indeed, a key determinant of $D_t^{(m)}$ surprises is movements in demand conditions as proxied by the bid-to-cover ratio. Furthermore, we observe that the demand from institutional investors is important in accounting for variation in $D_t^{(m)}$.

3.4 Comovement Across Markets

We now turn to analyzing how our demand shocks for Treasuries propagate across other financial markets. We measure the impact of demand shocks on other asset prices by running simple bivariate regressions:

$$y_t = \gamma + \phi D_t + u_t \tag{3}$$

where y_t is the change in the price or yield of some asset on auction date t and D_t is the measure of demand constructed above. To simplify the presentation, we pool across all auction maturities but the results are robust to estimating equation (3) separately by maturity groups.

Where available, we use intraday changes within the same time window as our shocks D_t. However we also examine changes at the daily frequency, partly due to data limitations but also because daily changes may pick up responses in other asset markets that don't occur immediately. A strong correlation between D_t and y_t signals either that D_t and y_t have a common determinant (e.g., changes in inflation expectations alter the behavior of bids in Treasury auctions and change prices of inflation swaps) or that y_t is a channel of propagation for D_t shocks (e.g., unexpected prices in an auction result in repricing of Treasuries in the secondary market). To preserve space, we focus on the OLS estimates of equation (3).[11]

Panel A of Table 4 reports results for debt markets. The dependent variable in the first row is the intraday change in the Exchange Traded Funds (ETF) "LQD," which tracks the iBoxx Liquid Investment Grade Index. The coefficient should be interpreted as the impact in log points of a one basis point increase in D_t. We observe a strong reaction to

[11] We report very similar instrumental variable estimates (using unexpected changes in the bid-to-cover ratio as instrumental variables) in Appendix Table C1.

the Treasury demand shock, accounting for more than 50 percent of variation observed in corporate bond ETF prices during the short windows around the close and release of the Treasury auction results.

The next rows report the results for the daily change in corporate bond yields, as measured by Moody's Aaa, Moody's Baa, and Bank of America's C corporate yield indices. Consistent with the intraday results, our demand shocks have a strong effect on relatively safe corporate bonds. Moreover, the pass-through of our demand shocks to corporate bond yields is nearly one-to-one. However, using daily rather than intraday changes as the dependent variable leads to a decline in R^2s, which underscores the benefits of using intraday data. On the other hand, our demand shocks have almost no effect on riskier corporate debt.[12]

As expected, yields in the secondary market react strongly to the demand shock. Furthermore, this reaction is persistent in spite of the fact that our shocks are constructed from intraday movements. Figure 8 plots the contemporaneous reaction of 10-year Treasury spot rates (top panel) and the Aaa corporate bond yields (bottom panel) to our shocks D_t, as well as the reactions up to 60 days in the future. The reaction remains strongly statistically significant over three weeks later, while the point estimate is quite stable even 2 months later. To provide a perspective on the magnitude of this persistence, Figure 8 also plots the change in yields following the QE1 announcement on March 18, 2009 (normalized such that the change on impact is equal to 1). Consistent with Wright (2012) and Greenlaw et al. (2018), yields had returned to roughly their starting point within a few months. Hence, the persistence of the effect of auction demand shocks on yields is comparable to QE.

Panel B of Table 4 reports results for equities. Rows 1 and 2 report the results for the intraday change in ETFs tracking the S&P 500 and the Russell 2000 indices. Rows 3 and 4 are for the daily changes in these indices. Although the estimated slope is generally positive, the estimate is typically insignifcant. Moreover, the quantitative importance is small, as the auction demand shocks account for a tiny share of variation in equities.

Panel C of Table 4 presents results for inflation expectations and commodities. The dependent variable in row 1 is the intraday change in the ETF "GLD," which tracks the price of Gold Bullion. Row 2 reports results for the daily change in the S&P Total Commodity Index. For the Commodity Index we do not find a significant correlation with D_t. For Gold, while the relationship is statistically significant, the R^2 is very low. Rows 3 and 4 report the results for the daily change in inflation expectations implied by inflation swaps at the 10-year and 2-year horizon. We observe that demand shocks for Treasuries do not generate significant movements in inflation expectations.[13] Hence, high-frequency

[12]Note that the LQD ETF is measured in terms of price, while the bond indices are measured in terms of yields; hence, the different signs of the coefficients are expected since prices and yields move in opposite directions.

[13]To further explore the robustness of this finding, we plot reactions of inflation swap rates at all

demand shifts are not driven by changes in inflation expectations and not propagated by changes in inflation expectation. This finding is intuitive because, for example, changes in demand of institutional investors are unlikely to generate future fluctuations in the rate of U.S. inflation.

Panel D of Table 4 reports results for various bond spreads and credit default swaps. The first row reports results for the daily change in the Moody's Baa-Aaa corporate yield spread. Rows 2 and 3 use daily changes in two CDS indices from Credit Market Analysis (CMA) that track the automotive industry (a highly cyclical industry) and banks (a proxy for the financial sector). These three measures proxy for expectations about future output and market conditions. We find that surprise movements D_t have no tangible effect on these measures, consistent with the view that D_t shocks do not capture superior information of Treasury auction bidders about future recessions and the like. In row 4, we document that D_t shocks are not associated with VIX (a measure of market perceptions about future volatility). Hence, it is unlikely that there is a common force that moves D_t and volatility or that D_t shocks propagate via volatility. In short, as with the case of inflation expectations, these null results provide further evidence that our demand shocks are not being driven by changes in expectations regarding output, liquidity, default risk, or volatility.

4 Channels of Treasury Demand Shocks

The results of Tables 3 and 4 allow for some broad observations. First, given our high-frequency approach and the institutional structure of Treasury auctions, we know that our constructed shocks are only driven by new information regarding the demand side of the market. Second, these shifts are largely driven by shifts in the demand arising from institutional investors. Third, these demand shocks from the primary market for Treasuries propagate to the corporate debt market. Finally, these demand shifts are not driven by some underlying shift in macroeconomic expectations (such as flight to quality or inflation expectations) that may move demand for Treasuries at all maturities.

However, it still remains the case that a variety of unobserved factors can generate movements in yields and so one should not interpret $D_t^{(m)}$ as structural shocks.[14] Despite this limitation, the properties of $D_t^{(m)}$ shocks allow us to study how unexpected demand

available maturities in Appendix Figure C2. We find that the change in the inflation expectation term structure exhibits little reaction to D_t.

[14]To highlight this caveat, we plot sensitivities for select asset prices estimated over rolling windows in Figure C3. The sensitivity of LQD prices, Aaa interest rates, and Baa-Aaa spread is relatively stable over time. On the other hand, the sensitivity of S&P500 flips sign from positive in the late 1990s to generally negative since the early 2000s, which is consistent with Campbell et al. (2014). Although we do not have long-time series of inflation expectations (or assets used for hedging against inflation), we observe that during the Great Recession in the U.S., inflation expectations and D_t moved in opposite directions while in normal time these two series are approximately uncorrelated.

interventions at specific maturities propagate to other maturities. Building on recent theoretical work, in this section we develop a model of the propagation mechanisms of Treasury demand shocks and test (and confirm) key implications of the theory.

What do spillovers across the yield curve look like? To provide some examples, Figure 9 plots the changes in the entire the yield curve following auctions of 30-year and 10-year Treasuries for four dates. Using intraday yield changes in all traded Treasuries during small windows around specific auctions, each panel of the figure plots the change in yields (as estimated from local mean smoothing regressions) across all maturities on a given date. On December 9, 2010 (upper left panel), there was unexpectedly strong demand (as measured by changes in our demand shock $D_t^{(30y)}$) during an auction of 30-year Treasuries. We observe that, although the whole yield curve shifted down, the strongest reaction was for long maturities. Similarly, on August 11, 2011 (upper right panel) there was unexpectedly weak demand during another 30-year auction. The entire yield curve shifts up, and the effect is increasing in magnitude as the maturity approaches 30 years.

We find a similar pattern following the 10-year auction on August 12, 2009 (bottom left panel). Unexpectedly weak demand at the auction is associated with increases in yields across the entire term structure, but the largest effects are observed for maturities of 10 years or greater. However, this contrasts with the pattern observed following another 10-year auction on January 11, 2017 (bottom right panel). In this case, unexpectedly strong demand puts downward pressure on the yield curve, but the largest effects are for intermediate maturities around 5 years; as the maturity increases, the effect becomes attenuated. These cases illustrate that the propagation of demand shocks across maturities does not amount to simple upward or downward "parallel" shifts.

This raises the question: to what extent do Treasury demand shocks have local effects? In other words, does the location of the demand shock in maturity space matter? Are the impacts state-dependent? The auctions in Figure 9 provide suggestive evidence that the location can in fact matter. To systematically characterize the impact of these demand shocks, we now examine the impact on the term structure of Treasury rates through the lens of the *preferred habitat* model of investor demand.

4.1 Preferred Habitat Theory in a Nutshell

We now develop key testable predictions of preferred habitat theory regarding the propagation of demand shocks. Our analysis is based on the model originally proposed in Vayanos and Vila (2009) and embedded in a general equilibrium New Keynesian setting as in Ray (2019). Here we briefly describe the equations for determining equilibrium in these models; details are in the Appendix. The key idea is the existence of "clientèle" investors who have idiosyncratic demand ("preferred habitat") for Treasuries of specific maturities. For example, pension funds can have a preference for long-maturity Treasuries

to better match the maturity structure of pension liabilities. The other side of the market are risk-averse arbitrageurs such as global hedge funds and dealers, who smooth out these preferred-habitat demand shocks. Fluctuations in the yield curve lead to changes in consumption due to the borrowing decisions of households. The model formalizes the interaction of preferred-habitat investors with arbitrageurs, and how these interactions have spillover effects in the real economy.

Bond markets: Zero coupon bonds of maturity $\tau \in (0, T)$ are available in zero net supply. Arbitrageurs have mean-variance preferences and allocate their wealth W_t to holdings $X_t^{(\tau)}$ across τ bonds, subject to their budget constraint:

$$\max_{\left\{X_t^{(\tau)}\right\}_{\tau=0}^{T}} \quad E_t \, \mathrm{d}W_t - \frac{a}{2} Var_t \, \mathrm{d}W_t \tag{4}$$

$$\text{s.t.} \quad \mathrm{d}W_t = \left(W_t - \int_0^T X_t^{(\tau)} \, \mathrm{d}\tau \right) r_t \, \mathrm{d}t + \int_0^T X_t^{(\tau)} \frac{\mathrm{d}P_t^{(\tau)}}{P_t^{(\tau)}} \, \mathrm{d}\tau \tag{5}$$

where $P_t^{(\tau)}$ is the price of a τ-maturity bond, and r_t is the short rate set by the monetary authority. The parameter a governs the risk-return trade-off that arbitrageurs face. This parameter can be taken literally as a risk aversion parameter, or more generally can be thought of as a proxy for factors that lead to the imperfect risk-bearing capacity of arbitrageurs. For tractability, we take a as time-invariant, although one would expect a to increase in periods of financial distress; we will analyze (in a comparative statics sense) how the predictions of the model depend on the risk-bearing capacity of arbitrageurs.[15]

On the other side of the market is a continuum of habitat investors, who specialize in bonds of specific maturities. These investors are assumed to respond to bond prices (or equivalently, yields) through the following demand curves:

$$Z_t^{(\tau)} = -\alpha(\tau) \log P_t^{(\tau)} - \sum_{k=1}^{K} \theta^k(\tau) \beta_t^k. \tag{6}$$

The function $\alpha(\tau)$ is the semi-elasticity of a τ-habitat investor's demand. $\left\{\beta_t^k\right\}_{k=0}^{K}$ are time-varying demand shocks, and the functions $\theta^k(\tau)$ govern how these demand shocks lead to changes in demand from τ-habitat investors. Market clearing implies that in equilibrium, arbitrageurs take the opposite positions of habitat investors: $X_t^{(\tau)} = Z_t^{(\tau)}$.

Macroeconomic dynamics: Inflation π_t, the output gap x_t, and the central bank's policy rate r_t are determined by a familiar set of "three-equation" New Keynesian rela-

[15] He and Krishnamurthy (2013), Kyle and Xiong (2001) and others show how risk aversion can be endogenously higher in times of crises.

tionships:

$$\mathrm{d}\pi_t = (\rho\pi_t - \delta x_t)\,\mathrm{d}t\,, \tag{7}$$

$$\mathrm{d}x_t = \varsigma^{-1}\left(\tilde{r}_t - \pi_t - \bar{r}\right)\mathrm{d}t\,, \tag{8}$$

$$\mathrm{d}r_t = -\kappa_r(r_t - \phi_\pi\pi_t - \phi_x x_t - r^*)\,\mathrm{d}t + \sigma_r\,\mathrm{d}B_{r,t}\,. \tag{9}$$

Equation (7) is the standard New Keynesian Phillips curve. ρ is the discount rate and δ governs the degree of price stickiness. Equation (8) is a modified New Keynesian IS curve, where the output gap depends on an "effective" borrowing rate $\tilde{r}_t \equiv \int_0^T \eta(\tau) y_t^{(\tau)}\,\mathrm{d}\tau$, which depends on the entire term structure of interest rates. $\eta(\tau)$ is a weighting function, ς^{-1} is the intertemporal elasticity of substitution, and $\bar{r}$ is the "natural" real borrowing rate. Equation (9) is a Taylor rule, with persistence in the policy rate. ϕ_π and ϕ_x govern the response of the policy rate to inflation and the output gap, while κ_r is a mean-reversion parameter. r^* is the central bank's target policy rate (set such that the economy features a zero inflation and output gap steady state).

As in Vayanos and Vila (2009), the model features an affine term structure in the state variables. Following Ray (2019), one can show that the dynamics of the economy are governed by

$$\begin{bmatrix}\mathbf{y}_t & \mathbf{x}_t\end{bmatrix}^\top \equiv \mathbf{Y}_t = -\boldsymbol{\Upsilon}\left(\mathbf{Y}_t - \overline{\mathbf{Y}}\right)\mathrm{d}t + \boldsymbol{\sigma}\,\mathrm{d}\mathbf{B}_t\,, \tag{10}$$

where the vector $\mathbf{y}_t$ includes state variables (the habitat demand factors and the persistent policy rate) and $\mathbf{x}_t$ includes the non-predetermined variables (inflation and the output gap), the matrix $\boldsymbol{\sigma}$ depends on structural parameters, and the dynamics matrix $\boldsymbol{\Upsilon}$ is determined as a fixed point that produces equilibrium dynamics in the bond market consistent with equilibrium dynamics of the macroeconomy and vice versa. Note that this formulation also allows for correlation of idiosyncratic habitat demand factors and the macro fundamentals.

This model of preferred habitat bond markets provides insights into the observations of Figure 6. In particular, one of the characteristic predictions of preferred habitat theory, first formalized in Vayanos and Vila (2009), is the *localization hypothesis*. When arbitrageur risk-bearing capacity is high, demand shocks have *global* effects on the yield curve. That is, the relative response of the interest rates across the yield curve does not depend on where in maturity space the demand shock occurs. However, as arbitrageur risk-bearing capacity declines, the spillovers of demand shocks become more *localized*. That is, the relative response of interest rates becomes more concentrated on parts of the yield curve that are closer in maturity space to where the demand shock occurs.

The intuition for the localization hypothesis is as follows: when arbitrageurs are nearly risk-neutral, macroeconomic fundamentals affecting the path of the short rate are by far the dominant factor in determining of the term structure of interest rates. Hence, when

arbitrageurs hold bonds, the main source of risk to which they are exposed is short rate fluctuations. Demand shocks that re-allocate bonds away from arbitrageurs reduce their exposure to short rate risk, and hence decrease the compensation arbitrageurs require to hold bonds. Since all bonds are sensitive to short rate risk, any such demand shock will push down yields of all bonds. Importantly, this mechanism is independent of the location (in maturity space) of the demand shock.[16]

As arbitrageur risk aversion increases, demand shocks become more prominent as additional sources of risk. Arbitrageurs try to limit their exposure to these sources of risk, leading to less propagation from the location of the demand shock to other parts of the term structure. Arbitrageurs become less willing to integrate bond markets across maturities, and hence the response of the yield curve becomes more localized around the location (in maturity space) of a given demand shock.

4.2 Localization Regression Specification

As shown in Section 3, our high-frequency identification strategy allows us to isolate the reactions of the yield curve to Treasury demand shocks alone, ruling out any other shocks during these small windows around auctions.[17] Hence, following the close and release of an auction at date t, we have that

$$\mathbf{y}_t^{post} - \mathbf{y}_t^{pre} \approx \begin{bmatrix} 0 & \dots & 0 & \left(\beta_t^{k,post} - \beta_t^{k,pre}\right) & 0 & \dots & 0 \end{bmatrix}^\top$$

In other words, the only structural shock corresponds to movements in a particular demand factor β_t^k, while the remaining fundamentals remain unchanged. Therefore, observed changes in yields in the small window following the auction at date t represent the equilibrium response to the given demand factor.

To link the change in fundamentals (which we do not observe) to the change in yields (which we observe), consider a version of the model with the following habitat demand factors: a "short" factor β_t^s and "long" factor β_t^ℓ such that

$$\int_0^T \theta^s(\tau)\,\mathrm{d}\tau = \int_0^T \theta^\ell(\tau)\,\mathrm{d}\tau \tag{11}$$

$$\exists \tau' : \quad \theta^s(\tau) < \theta^\ell(\tau) \iff \tau > \tau' \tag{12}$$

That is, the factors have the same overall magnitude across maturities (equation (11)),

[16] In this example, the location of a demand shock will impact the size of the effect on the yield curve, but not the shape of the response of the yield curve. Hence, the relative effects of a demand shock on the yield curve is independent of the location of the shock.

[17] The change in the bid-to-cover ratio is a proxy for structural demand shifts, but we do not have a high-frequency market-based measure of the expected bid-to-cover before and after an auction. We return to the possibility of utilizing the bid-to-cover ratio to test the localization hypothesis in robustness checks.

but the short factor is more concentrated in bonds of short maturities relative to the long factor (equation (12)). Note that this does not require the assumption that the long factor β_t^ℓ only affects demand for long maturities; indeed, changes in β_t^ℓ will shift demand for bonds of all maturities τ such that $\theta^\ell(\tau) \neq 0$. In other words, as long as $\theta^k(\tau) \neq 0$ for some maturity τ, we allow for a "hard-wired," direct response of yields for this maturity to factor k. In this sense, the demand factors imply "correlated" changes in demand across the term structure: a short factor can directly move demand for short- and long-maturity bonds and a long factor can directly move demand for short- and long-maturity bonds. We only require (equation (12)) that, relative to the short factor β_t^s, the long factor has a larger direct effect on demand for bonds with long maturities.

In this context, the localization hypothesis involves the differential responses of the entire yield curve to movements in the short and long demand factors. We can formally state a version of the localization hypothesis as follows. When arbitrageur risk-bearing capacity is high ($a \approx 0$), the relative response of the yield curve is the same for both factors. On the other hand, when risk-bearing capacity is low ($a \gg 0$), then long demand shocks have relatively larger effects on long-maturity yields and *vice versa* for short demand shocks. This logic implies:

$$\text{If } a \approx 0 \ : \frac{\partial y_t^{(\tau)} \Big/ \partial \beta_t^s}{\partial y_t^{(\tau^*)} \Big/ \partial \beta_t^s} \approx \frac{\partial y_t^{(\tau)} \Big/ \partial \beta_t^\ell}{\partial y_t^{(\tau^*)} \Big/ \partial \beta_t^\ell} \tag{13}$$

$$\text{If } a \gg 0 \ : \tau > \tau^* \iff \frac{\partial y_t^{(\tau)} \Big/ \partial \beta_t^s}{\partial y_t^{(\tau^*)} \Big/ \partial \beta_t^s} < \frac{\partial y_t^{(\tau)} \Big/ \partial \beta_t^\ell}{\partial y_t^{(\tau^*)} \Big/ \partial \beta_t^\ell} \tag{14}$$

where τ^* is some arbitrary "baseline" maturity (and unrelated to τ') and $\frac{\partial y_t^{(\tau)}}{\partial \beta_t^k}$ is the response of τ-maturity yields to the demand shock $k \in \{s, \ell\}$.[18] Hence, these expression make statements about the movements of the yield curve to short and long demand shocks, *relative* to movements in some fixed maturity τ^*. Specifically, equation (13) states that even if $\theta^k(\tau) \neq \theta^k(\tau^*)$ (i.e., direct responses are different across maturities for a given factor) and $\theta^s(\tau) \neq \theta^\ell(\tau)$ (i.e., direct responses for a given maturity are different across factors), arbitrageurs with low risk aversion ($a \approx 0$) ensure that the *equilibrium* scaled responses of yields are approximately the same for short and long factors. In contrast, equation (14) states that when risk aversion is high, arbitrageurs do not smooth out demand shocks and the scaled responses of yields depend on where the direct impact of a factor is concentrated. In particular, if the long factor has a larger direct effect on demand for long maturities than the short factor, then in equilibrium, the scaled response of yields for longer maturities is larger for the long factor than for the short factor.

[18] Section A in the Appendix discusses sufficient conditions and formally derives the localization predictions of the model.

This insight allows us to arrive at a simple, theory-based regression specification that can test the localization hypothesis using only high-frequency changes in yields around auctions $D_t^{(\tau)} = y_t^{(\tau),post} - y_t^{(\tau),pre}$, which are data analogues of $\partial y_t^{(\tau)} \Big/ \partial \beta_t^s$:

$$D_t^{(\tau)} = \alpha^{(\tau)} + \gamma_s^{(\tau)} \mathbf{I}(m_t = short) D_t^{(\tau^*)} + \gamma_\ell^{(\tau)} \mathbf{I}(m_t = long) D_t^{(\tau^*)} + \varepsilon_t^{(\tau)} \tag{15}$$

where $\mathbf{I}(m_t = short)$ is an indicator variable equal to one if there is an auction of short-maturity bonds on date t, $\mathbf{I}(m_t = long)$ is an indicator variable equal to one if there is an auction of long-maturity bonds on date t. We estimate equation (15) for all maturities τ, holding τ^* fixed.

Coefficients $\hat{\gamma}_s^{(\tau)}$ and $\hat{\gamma}_\ell^{(\tau)}$ measure the relative effect of demand shocks for short and long-maturity auctions respectively. Now we can restate the localization hypothesis formally as a function of the coefficients $\gamma_s^{(\tau)}, \gamma_\ell^{(\tau)}$, and risk aversion a as follows: i) As risk aversion $a \to 0$, $\left|\gamma_s^{(\tau)} - \gamma_\ell^{(\tau)}\right| \to 0$ for all maturities τ; ii) When risk aversion is high ($a \gg 0$), then $\gamma_s^{(\tau)} > \gamma_\ell^{(\tau)}$ if $\tau < \tau^*$ and $\gamma_s^{(\tau)} < \gamma_\ell^{(\tau)}$ if $\tau > \tau^*$.

4.3 Empirical Localization Results

To test the state-dependent localization hypothesis, we estimate specification (15) separately for two subsamples: a "non-crisis" period (when risk aversion a is low), and a "crisis" period (when risk aversion a is high). Testing for the equality of coefficients $\hat{\gamma}_s^{(\tau)}$ and $\hat{\gamma}_\ell^{(\tau)}$ in each subsample shows whether demand shocks have more localized effects when risk aversion is high. In our baseline estimates, we take the "crisis" period to be 2008-2012. We divide the auctions into short-maturity (maturity of 5 years or less) and long-maturity (maturity of 7 years or greater). As we discuss later, the results are robust to alternative choices.

Since we construct $D_t^{(\tau)}$ from secondary-market yields, we do not have measures for all maturities τ at all times. Hence, for our approach we conduct rolling regressions (across maturities), including yields for maturities within ± 2 years for each maturity $\tau \leq 20$ years and within ± 4 years for each maturity $\tau > 20$ year. Given that the choice of benchmark maturity τ^* is arbitrary, we set $\tau^* = 3$, with an eye towards applying our results to QE in order to focus on the differential effects of intermediate and long-maturity yields.

The top panel of Figure 10 plots the estimates of $\hat{\gamma}_s^{(\tau)}$ and $\hat{\gamma}_\ell^{(\tau)}$ for the non-crisis sample. The estimated responses follow a similar hump-shaped pattern peaking at intermediate maturities (around roughly 5-7 years), and then declining and stabilizing for longer term maturities (with a possible slight uptick for very long (20+ years) maturities). In general, we cannot reject equality of $\hat{\gamma}_s^{(\tau)}$ and $\hat{\gamma}_\ell^{(\tau)}$ (Appendix Figure C4 reports p-values). This finding is consistent with the first prediction of the localization hypothesis: during periods of financial calm, the relative effects of demand shocks for short- and long-maturity bonds

are identical.

When we estimate specification (15) on the crisis sample, we observe a strikingly different pattern (the bottom panel of Figure 10). In response to shocks in demand for short- and long-maturity Treasuries, both $\hat{\gamma}_s^{(\tau)}$ and $\hat{\gamma}_\ell^{(\tau)}$ increase rapidly for $\tau < \tau^*$, with the $\hat{\gamma}_s^{(\tau)}$ estimates increasing somewhat more quickly than $\hat{\gamma}_\ell^{(\tau)}$. Once we move to maturities greater than τ^*, the estimates quickly diverge. Specifically, in response to shocks in demand for short-maturity Treasuries, the yields for maturities greater than τ^* fall relative to the yield response for τ^* (as shown by the estimates of $\hat{\gamma}_s^{(\tau)}$). On the other hand, in response shocks in demand for long-maturity Treasuries, yields for maturities $\tau > \tau^*$ continue to increase relative to the benchmark maturity τ^* (as shown by the estimates of $\hat{\gamma}_\ell^{(\tau)}$). For maturities of 20 to 30 years, the relative response of yields to long-maturity demand shocks ($\hat{\gamma}_\ell^{(\tau)}$) is over twice as large as the response of yields to short-maturity demand shocks ($\hat{\gamma}_s^{(\tau)}$). We can strongly (at the 0.1% level) reject the null of $\hat{\gamma}_s^{(\tau)}$ and $\hat{\gamma}_\ell^{(\tau)}$ being equal (Appendix Figure C4 reports p-values). Hence, consistent with our second theoretical prediction, we find more pronounced localization effects in crisis times when risk-aversion a is elevated.

These results are consistent with the key predictions of our preferred habitat framework: during "normal" periods when financial risk-bearing capacity is high, demand shocks for short- and long-maturity securities have relatively similar impacts on the yield curve. During periods of financial distress when risk-bearing capacity is low, the impacts are more localized: the impact of short-maturity demand shocks are largest for short maturities, while the impact of long-maturity demand shocks peaks at the long end of the term structure. These results provide support for the view that during financial crises, arbitrageurs are less willing or able to integrate bond markets.[19]

The localization results are robust to a variety of alternative assumptions. In the interest of space, we provide summaries for a few key robustness specifications in this section. First, we explore the sensitivity of our results to using alternative measures of financial distress. Specifically, we consider two alternatives: i) an aggregate "intermediary capital ratio," a market-based measure of financial distress (low intermediary capital ratios are associated with lower risk-bearing capacity) described in He et al. (2016); ii) a narrative-based measure of financial crisis from Romer and Romer (2017) (higher values of the crisis indicator are associated with lower risk-bearing capacity). Both of these alternatives generate results similar to our baseline findings (see Appendix Figures C5 through

[19]Correlated shocks to demand could be an alternative explanation of localization effects. Note that correlated shocks alone do not negate the predictions of the model. However, if the correlation structure changes in crisis and demand shocks become *less* correlated across maturities, one may also rationalize stronger localization effects in crisis. We do not find evidence to support this explanation. Specifically, for each period (crisis sample period vs. non-crisis sample period), we have time series of bid-to-cover ratios for Treasury auctions with a given maturity. We estimate the correlation matrix of these time series for each period and test equality of the correlation matrices across the periods. We cannot reject equality of the matrices (p-value is 0.25).

C9). Second, our results are robust to using different cutoffs for separating auctions into short and long maturities. For example, when we use 10 years (rather than 7 years in the baseline) as the cut-off for long-maturity auctions, the results (Appendix Figure C10) still strongly support the localization hypothesis and, if anything, the point estimates for the "non-crisis" period are even more similar than in our baseline specification. Third, as we discussed above, the choice of the benchmark maturity τ^* is arbitrary in our framework. To verify that this choice is indeed immaterial for our results, we experiment with values other than $\tau^* = 3$ and find similar results (e.g. Appendix Figure C11 reports estimates for $\tau^* = 6$). Fourth, our results are nearly identical when dropping auctions that occurred during the weeks of QE announcements (Appendix Figure C12).

Finally, we also considered an alternative regression specification to test the localization hypothesis. Our auction data provides a proxy for structural demand shocks: movements in the bid-to-cover ratio. However, the bid-to-cover ratio is only a crude proxy, because the value reported following an auction does not solely reflect new demand information revealed following the close of the auction. Nevertheless, it is informative to run the following regression:

$$D_t^{(\tau)} = \alpha^{(\tau)} + \nu_s^{(\tau)} \mathbf{I}(m_t = short)\tilde{\beta}_t + \nu_\ell^{(\tau)} \mathbf{I}(m_t = long)\tilde{\beta}_t + \varepsilon_t^{(\tau)} \tag{16}$$

where $\tilde{\beta}_t$ is the residualized ("surprise") bid-to-cover ratio following an auction at date t (controlling for its own four lags, as in Table 3). We further flip the sign of the bid-to-cover ratio, in order to make the estimates more comparable to our baseline specification. Note that unlike specification (15), the estimates $\hat{\nu}_s^{(\tau)}, \hat{\nu}_\ell^{(\tau)}$ measure the absolute response of the yield curve to the short and long demand factors (proxies), as opposed to the relative response. Hence, unlike the baseline specification (15), the formal test of the localization hypothesis is not as straightforward using specification (16) (recall that the localization hypothesis is about relative movements in yields across the term structure). Nevertheless, we see strong patterns of localization in the "crisis" estimates, but little evidence of localization in the "non-crisis" estimates. In the non-crisis subsample estimates (the top panel of Appendix Figure C13), the response to both short- and long-maturity demand follows a similar hump-shaped pattern: the response is increasing from short to intermediate maturities, peaking around $\tau = 5$ to $\tau = 10$ before declining (though there is some evidence that long demand shocks have larger effects on very long-maturity yields). On the other hand, the estimates from the crisis subsample (the bottom panel of Appendix Figure C13) exhibit significant differences across short and long estimates: the response to short demand shocks remains hump-shaped, but peaks for short maturities before quickly declining. Conversely, the response to long demand shocks increases almost without fail as the maturity increases, peaking at very long maturities.

Since the mechanism for the market segmentation channel is the same regardless of

the source of demand shifts (recall that the preferred habitat channel is about how private arbitrageurs absorb demand shifts rather than about the source of the demand shocks), our results already offer important lessons for central banks undertaking QE. For example, if the Fed is trying to decrease long-maturity Treasury rates relative to shorter-maturity rates, our findings suggest that QE policies that directly purchase long-maturity Treasuries should be highly effective during financial crises. Indeed, the Fed may have a menu of options in terms of where it can intervene in the maturity space to hit the yield at a target maturity. But if the Fed is trying to move the entire term structure of interest rates, during periods of high financial distress the Fed will have to be active in purchasing Treasuries throughout the yield curve.

5 Implications for Quantitative Easing

In this section, we use our theoretical framework to make further progress in several directions. First, we use a calibrated version of our model to quantify the role of preferred habitat in rationalizing the response of asset prices to the QE announcement. Second, we use the model to evaluate the effectiveness of QE for macroeconomic stabilization purposes. Third, we consider alternative implementations of QE to inform policymakers about trade-offs associated with various designs of QE.

5.1 Model Calibration

Table 5 describes the calibration used in our numerical exercises. Panel A describes the calibration used for the macroeconomic parameters, which we set using standard values used in the literature.[20] The rest of the model is less standard and so requires more explanation.

The functional forms of the habitat elasticity function $\alpha(\tau)$, habitat demand functions $\theta^k(\tau)$, and effective borrowing weights $\eta(\tau)$ are based on Ray (2019) and Vayanos and Vila (2020) and take the following exponential forms:

$$\alpha(\tau) = \alpha_0 \exp(-\alpha_1 \tau) \tag{17}$$

$$\theta^k(\tau) = \theta_0 \tau (\theta_1^k)^2 \exp\left(-\theta_1^k \tau\right) \tag{18}$$

$$\eta(\tau) = \tau \eta_1^2 \exp(-\eta_1 \tau) \tag{19}$$

Equation (17) implies that the habitat investor elasticity with respect to (log) price is declining with maturity, and is single-peaked with respect to yields. Similarly, equations (18) and (19) imply that the demand factor and borrowing weights are single-peaked

[20] Additional parameters (e.g., $\bar{r}, r^*$) determine the steady state of the economy, but do not affect how the economy reacts to shocks and hence are not required for the analysis that follows.

functions. These functional forms allow us some flexibility in capturing key modeling features, such as demand shocks targeted in specific areas of maturity space, without significantly increasing the dimensionality of the problem. Additionally, the exponential expressions improve the numerical properties of the model. Note that the functions $\theta^k(\tau)$ and effective borrowing weights $\eta(\tau)$ are parameterized such that they integrate to θ_0 and 1, respectively. Thus, the parameters α_0, θ_0 govern the overall size of the habitat elasticity and demand functions, while $\alpha_1, \theta_1^k, \eta_1$ govern the shape as a function of maturity: a lower value of these parameters imply that more of the weight of these functions lies at longer maturities.

As in Ray (2019), the weighting function in the effective borrowing rate $\eta(\tau)$ is parameterized to roughly match the outstanding amounts of government securities by maturity: $\eta_1 = 1.7$, which reflects the fact that a large portion of outstanding Treasury debt is short-term.

To map the model to our estimates in the previous section, we set the number of demand factors $K = 2$, corresponding to short- and long-maturity auctions. In order to impose more discipline on the model, we assume the habitat demand shocks β_t^s, β_t^ℓ are identical, except for the shape of the demand factor functions $\theta^s(\tau)$ and $\theta^\ell(\tau)$. Specifically, we set $\theta_1^s = 1.25$ and $\theta_1^\ell = 0.25$ such that the short factor is concentrated in short maturities less than 5 years, while the long factor has more weight in intermediate and long maturities above 7 years, as in our regression analysis in Section 4. For the habitat elasticity function, we set the parameter $\alpha_1 = 0.1$ such that the habitat elasticity with respect to yields ($\equiv \tau \cdot \alpha(\tau)$) is maximized for the 10-year maturity, which is often taken as a key benchmark yield.

We also assume that the habitat demand factors are independent from one another, but may respond to the short rate (as in King (2019a)):

$$\mathrm{d}\beta_t^k = -\left(\kappa_\beta \beta_t^k + \phi_{r,\beta} r_t\right) \mathrm{d}t + \sigma_\beta \, \mathrm{d}B_{\beta^k,t}$$

Because both $\alpha(\tau)$ and $\theta(\tau)$ enter the solution multiplicatively with risk aversion a and shock volatility $\boldsymbol{\sigma}$, they are only identified up to a scaling factor. We normalize all of the variances equal to one another: $\sigma_r = \sigma_{\beta^s} = \sigma_{\beta^\ell} \equiv \sigma$. The remaining objects to calibrate are therefore $a\sigma^2 \cdot \alpha_0$, $a\sigma^2 \cdot \theta_0$, κ_β, and $\phi_{r,\beta}$, which govern how the model deviates from risk-neutrality and how demand shocks propagate. We jointly estimate these parameters in a moment-matching exercise. Specifically, we target a set of unconditional moments: term structure regression coefficients from Fama and Bliss (1987) (FB) and Campbell and Shiller (1991) (CS). These unconditional moments are informative about how the slope of the yield curve predicts excess returns and realized changes in yields. This in turn is informative about deviations from the expectations hypothesis and risk-neutral pricing. While we can allow these objects to vary across "crisis" and "non-crisis" regimes,

we impose that κ_β and $\phi_{r,\beta}$ are the same across the regimes and allow only $a \cdot \alpha_0$ and $a \cdot \theta_0$ to vary across the regimes; that is, our "non-crisis" and "crisis" model calibrations differ only in the estimates of risk-adjusted parameters.

Given that the number of observations in the "non-crisis" period is vastly larger than the number of observations in the "crisis" period, we recover κ_β and $\phi_{r,\beta}$ from the "non-crisis" sample. Calibration of $a \cdot \alpha_0$ and $a \cdot \theta_0$ for the "crisis" period is reported in Panel D of Table 5. We find (see Appendix Figure C14) that our model can match the FB and CS coefficients quite well in "non-crisis" times (characterized by smaller deviations from the expectations hypothesis) and in "crisis" times (characterized by greater deviations, which is accomplished by increasing the risk-adjusted estimates of $a \cdot \alpha_0$ and $a \cdot \theta_0$).

To further assess the fit of the model, we generate the model-implied regression coefficients from equation (15) as a type of "out-of-sample" test of the model. Recall the coefficients show the relative responses of the yield curve to shocks in demand for short and long maturities, and are untargeted in the calibration. Figure 11 plots the model-implied coefficients from the "non-crisis" and "crisis" calibrations, showing that the model performs well at matching the empirical responses we found in Section 4. Thus, our calibrated model not only picks up the qualitative change in how demand shocks affect yields in and out of financial crises, but is also suitable for quantitative analyses.

5.2 Response of the Yield Curve to QE1

As observed by Chairman Bernanke, the mechanisms behind the reaction of asset prices to quantitative easing are poorly understood. To assess the contribution of the preferred habit theory to the observed reaction, we feed a "QE1" shock into our model, compute predicted responses of yields at different maturities, and compare predictions to actual changes in yields.

We focus on QE1 because it was arguably the "cleanest" LSAP shock: there are a clear set of policy announcement events, and the observed response to these events are unlikely to be plagued by anticipation issues relative to later rounds of QE. In terms of magnitude, QE1 involved purchasing roughly $300 billion Treasuries, concentrated in Treasuries with maturities over 5 years. Compared with the typical fluctuations in bids at auctions, QE1 therefore represents a ten-fold increase in purchases relative to a typical demand shock at Treasury auctions. Krishnamurthy and Vissing-Jorgensen (2011) report the cumulative change in the yield curve following the 5 major QE1 event dates. We use this change as the empirical response of the yield curve to QE1.

To mimic the actual QE1 shock in the model, we assume that this shock was completely unexpected ("MIT shock"), and that afterwards markets expected purchases to be unwound slowly and deterministically:

$$\mathrm{d}\beta_t^{QE} = -\kappa_{QE}\beta_t^{QE}\,\mathrm{d}t \tag{20}$$

We set the inertia parameter $\kappa_{QE} = 0.1$. This magnitude roughly implies that markets expected the Fed to hold its purchases to maturity (more precisely, the half-life of the purchases is roughly 7 years). Ex-post, the Treasuries purchased as part of the Fed's QE programs were held on the balance sheet for a very long time, and holdings remained elevated well beyond 7 years. However, this does not imply that markets expected this ex-ante.[21] We explore the sensitivity of this assumption below. Finally, we assume that QE1 does not resolve distress in the financial markets and thus we hold the model regime fixed at "crisis." Hence, the goal of the exercise is to see how far the preferred habitat channel of QE alone can go in explaining the observed response to QE1.

Figure 12 plots the cumulative change observed in the data and predicted in the model. The remarkable consistency between the responses suggests that the actual market reaction to QE1 announcements is consistent with the predictions of a preferred habitat model and the behavior of the market in response to observed shifts in private demand for Treasuries. This finding implies that the *net* effect of other channels of QE (e.g., inflation expectations, forward guidance, signaling) could be smaller than thought before. Consistent with this observation, Krishnamurthy and Vissing-Jorgensen (2011) document that there was little movement in 5-year inflation expectations in response to QE1 announcements.

5.3 Macroeconomic Effects of Quantitative Easing

While there is extensive research documenting the responses of financial markets to rounds of QE, little is known about how much QE affected the broader economy because QE events are so infrequent. We cannot shed more light on this using regression analysis or similar tools, but we can use our calibrated model to quantify the macroeconomic effects and compare them with the effects one can achieve by using conventional policy tools. Specifically, we analyze the effects of QE in crisis times relative to a typical 25 basis point monetary policy cut undertaken in non-crisis times.

Note that the dynamics of the model following a policy shock feature simple, monotonic ("AR(1)-like") mean reversion to the steady state. Since the persistence of shocks is similar for QE and conventional policy, without loss of generality we focus on the macroeconomic responses on impact and report QE-induced responses as a multiple of the responses to conventional policy shocks.

Our baseline calibration implies that in terms of macroeconomic effects, the Treasury

[21] The actual purchases of Treasuries during QE1 were planned to take place over the 6 months following the March 2009 announcement. The FOMC statements during this time do not make any reference to selling these securities off, but state that the FOMC will "carefully monitor the size and composition of the Federal Reserve's balance sheet in light of evolving financial and economic developments." Eventually, the FOMC made clear their policy of Treasury reinvestment. For instance, in Chariman Bernanke's July 2010 report to Congress, he stated that "the proceeds from maturing Treasury securities are being reinvested in new issues of Treasury securities with similar maturities."

purchases of QE1 (approximately increase the balance sheet of the central bank by $\frac{300bn}{15trl} \approx$ 2% of GDP) were roughly comparable to a typical monetary policy shock. Specifically, QE1 boosts output by a factor of 1.20 and inflation by a factor of 1.27, relative to a 25 basis point cut in the policy rate during non-crisis periods. In other words, if a conventional policy shock raises output by 1 percentage point, QE1 raises output by 1.2 percentage points. This magnitude is comparable to the estimate in Sims and Wu (2020) reporting that, in a model where QE works via enforcement/reserve constraints on banks, a 25-basis-point cut in the policy rate in normal times is approximately equivalent to increasing the balance sheet of the central bank by 1 percent of output.

5.4 Alternative Designs of Quantitative Easing

Can policymakers make QE more powerful? And what, if any, are the potential downside risks of QE? To address this question, we explore how variations in the implementation of large-scale asset purchases can influence the power of this tool to move output and inflation. In particular, we explore the sensitivity to the rate at which QE purchases are unwound, the uncertainty associated with QE, and the degree of financial distress present during QE. To preview our results (reported in Figure 13), QE effects are sensitive to the implementation details of the purchases.

Unwinding: One practical question for policymakers is how long central banks should hold assets accumulated during QE rounds. While this issue has been explored–but seemingly not resolved with a consensus recommendation (e.g., Sims and Wu (2020) and Karadi and Nakov (2020))–in models emphasizing reserve requirements/moral hazard constraints on banks as a key channel for QE, little is known in a preferred habitat macroeconomic context. To this end, we vary κ_{QE} in equation (20), which governs the unwinding process, to investigate how the duration of holdings affects output and inflation. The top panel of Figure 13 shows that relative to the baseline calibration (the vertical dotted line), the macroeconomic effects roughly double if markets expected QE1 to be unwound more slowly ($\kappa_{QE} \approx 0.05$, implying a half-life of about 14 years). If instead markets expect QE1 to be unwound more quickly ($\kappa_{QE} \approx 0.4$, implying a half-life of about 2 years), then the macroeconomic effects are less than half as large as the baseline. This result is intuitive: if the Fed were to purchase a large amount of Treasuries but then quickly sell those securities back, we would not expect to observe large macroeconomic effects. Rather, it is the cumulative size of QE over time that matters.

Hence, policymakers should be clear about how long the central bank expects to hold the securities on its balance sheet. To the extent that the policymaker is planning to unwind their asset holdings very slowly, providing a type of "forward guidance" regarding the expected path of purchases can potentially increase the immediate effectiveness of these policies if markets do not fully anticipate how long the QE program will last.

Uncertainty: Recall that we assume QE was a one-off shock, completely unanticipated by markets. This may be an accurate representation of the first round of quantitative easing, but a decade later it is clear that large-scale asset purchases are here to stay. Hence, it is likely that markets now consider the possibility of future QE shocks. To model the recurrent nature of QE, we modify equation (20) and instead assume that QE shocks are described by the following equation:

$$\mathrm{d}\beta_t^{QE} = -\kappa_{QE}\beta_t^{QE}\,\mathrm{d}t + \sigma_{QE}\,\mathrm{d}B_{QE,t} \tag{21}$$

Hence, whenever $\sigma_{QE} > 0$, QE shocks themselves may lead to additional macroeconomic volatility. Further, risk-averse arbitrageurs must hedge against QE risk, in addition to fundamental sources of risk in the economy.

The middle panel of Figure 13 explores the change in long-run volatility of output and inflation change as a function of the volatility of QE shocks. $\sigma_{QE} = 0$ is our baseline estimate (marked by the vertical dotted line); the x-axis is the volatility of QE shocks relative to the volatility of habitat demand shocks $\frac{\sigma_{QE}}{\sigma_\beta}$; the y-axis is the increase in percent of the long-run variance of output and inflation. The results provide an important note of caution for central bankers: increased uncertainty regarding QE leads to increased volatility of inflation and output. In other words, although policymakers may desire the added flexibility of discretionary QE tools, the downside is that this increases the uncertainty surrounding these policy tools. If instead policymakers provide clear communication regarding the expected path of QE purchases, this should reduce market uncertainty and prevent volatility spillovers from QE into the real economy. This provides support for the use of QE rules or forward guidance regarding asset purchases in the spirit of Ray (2019) and Greenwood et al. (2016).

Risk Appetite: As we discussed above, the power of QE to affect yields at target maturities is high in crisis times and weak in non-crisis times. Consistent with this insight, the bottom panel of Figure 13 shows that the transmission depends roughly linearly on the risk aversion of arbitrageurs. Given that our baseline calibration for "crisis" corresponds to the Great Recession, one has to have a financial crisis of truly unprecedented proportions to materially increase the power of QE-based tools. On the other hand, normal times are characterized by much lower values of risk aversion. As a result, the balance of risks appears to be somewhat one-sided: it is difficult to raise the power of QE beyond what was achieved during the Great Recession but it is relatively easy to reduce the power as soon as financial panics calm down. This logic suggests that QE is less effective as a "conventional" tool to the extent that "conventional" entails well-functioning financial markets. QE may remain in the central bankers' toolkit, but should only be utilized during periods of financial distress.

6 Concluding Remarks

Quantitative easing during the recent global financial crisis was a massive policy experiment. The deployment of QE in response to the COVID19 crisis is a testament of policymakers' belief that the experiment worked. But to understand which channels are responsible for the workings of QE, we need to unbundle these channels so that future policy can be designed to maximize the effectiveness of QE-like tools in crisis and non-crisis times. We focus on the "preferred habitat" channel, which posits that, because of market segmentation and limited arbitrage, interest rates for a given maturity range may be influenced by targeted buying or selling of assets within this range ("localization effect").

We utilize Treasury auctions of government debt to identify Treasury demand shocks arising from changes in institutional investor demand to study how shocks in one maturity segment propagate to other segments, and how this propagation is affected by financial markets conditions. These shocks provide us with variation that is not related to some prominent theories of how QE works (e.g., inflation expectations, forward guidance, or signaling) and instead allow us to focus on the role of preferred habitat mechanisms. Crucially, these mechanisms are dependent on how *private* agents in the market for Treasury debt absorb these demand shocks, regardless of the source of these shocks. Therefore, we can use this variation to inform and evaluate our general-equilibrium macroeconomic model that embeds financial markets with preferred habitat and then use this model to assess the quantitative importance of preferred habit for QE rounds as well as alternative designs of QE

We find that localization effects are stronger when markets are segmented (e.g. due to a crisis) than when markets are integrated. Through the lens of our model, we show that the magnitude of these localization effects is large enough to account for the entirety of interest rate movements in response to QE announcements, consistent with the view that QE programs worked mainly via market segmentation. Policy experiments in the calibrated model suggest that QE can be a useful policy tool in crises: a QE1 shock during crisis stimulates output and inflation by the magnitudes that roughly correspond to movements in response to a 25 basis point cut in the policy rate during normal times. However, the effect of QE on asset prices and hence the broader economy weakens if the holding period of assets purchases by a central bank is short or financial markets are well-functioning; further, there is the risk that uncertainty about future QE rounds leads to excess macroeconomic volatility.

Our analysis is a step in a broader research agenda to better understand the interactions of monetary policy, financial markets, and the macroeconomy. "A legacy of the [financial] crisis," Fed Chairman Powell explained in 2019, "is that policymakers now have a broader range of tested tools to turn to" in the next crisis. COVID19 has now provided

such an opportunity, but the unique and unprecedented challenges of the pandemic emphasize the urgent need for a reassessment of what policies work, and precisely how they work. This paper sheds light on how Treasury demand shocks and QE propagate through bond markets into the broader macroeconomy. The COVID19 crisis has not only thrown into stark relief the significance of this topic, but also highlighted more broadly many unanswered questions regarding the workings of the Treasury market, a bedrock of the modern financial system. For example, the crisis induced a major sell-off of Treasuries by a large swath of investors in March of 2020, leading to a deterioration of conditions in the Treasury market. The Fed's rapid interventions (including massive purchases of assets) resumed the normal functioning of the markets, but important questions about market segmentation, liquidity, and the like remain to be answered. "What can be done to improve Treasury market functioning over the longer term so that this market can withstand a large shock to demand or supply?" the Fed's Vice Chair for Supervision Quarles asked and continued with, "I will simply raise that question, but not attempt to answer it here."

References

Baker, S. R., Bloom, N., and Davis, S. J. (2016). Measuring Economic Policy Uncertainty. *The Quarterly Journal of Economics*, 131(4):1593–1636.

Beetsma, R., Giuliodori, M., de Jong, F., and Widijanto, D. (2016). Price effects of sovereign debt auctions in the euro-zone: The role of the crisis. *Journal of Financial Intermediation*, 25(C):30–53.

Beetsma, R., Giuliodori, M., Hanson, J., and de Jong, F. (2018). Bid-to-cover and yield changes around public debt auctions in the euro area. *Journal of Banking & Finance*, 87(C):118–134.

Bernanke, B. S. and Kuttner, K. N. (2005). What Explains the Stock Market's Reaction to Federal Reserve Policy? *Journal of Finance*, 60(3):1221–1257.

Bernanke, B. S., Reinhart, V. R., and Sack, B. P. (2004). Monetary Policy Alternatives at the Zero Bound: An Empirical Assessment. *Brookings Papers on Economic Activity*, 35(2):1–100.

Cahill, M. E., D'Amico, S., Li, C., and Sears, J. S. (2013). Duration risk versus local supply channel in Treasury yields: evidence from the Federal Reserve's asset purchase announcements. Finance and Economics Discussion Series 2013-35, Board of Governors of the Federal Reserve System (U.S.).

Cammack, E. B. (1991). Evidence on Bidding Strategies and the Information in Treasury Bill Auctions. *Journal of Political Economy*, 99(1):100–130.

Campbell, J. R., Evans, C. L., Fisher, J. D., and Justiniano, A. (2012). Macroeconomic Effects of Federal Reserve Forward Guidance. *Brookings Papers on Economic Activity*, 43(1 (Spring):1–80.

Campbell, J. Y., Pflueger, C., and Viceira, L. M. (2014). Monetary Policy Drivers of Bond and Equity Risks. NBER Working Papers 20070, National Bureau of Economic Research, Inc.

Campbell, J. Y. and Shiller, R. J. (1991). Yield Spreads and Interest Rate Movements: A Bird's Eye View. *Review of Economic Studies*, 58(3):495–514.

Carlstrom, C. T., Fuerst, T. S., and Paustian, M. (2017). Targeting Long Rates in a Model with Segmented Markets. *American Economic Journal: Macroeconomics*, 9(1):205–242.

Chen, H., Cúrdia, V., and Ferrero, A. (2012). The Macroeconomic Effects of Large-scale Asset Purchase Programmes. *Economic Journal*, 122(564):289–315.

Chodorow-Reich, G. (2014). Effects of Unconventional Monetary Policy on Financial Institutions. *Brookings Papers on Economic Activity*, 45(1 (Spring)):155–227.

Cúrdia, V. and Woodford, M. (2011). The central-bank balance sheet as an instrument of monetarypolicy. *Journal of Monetary Economics*, 58(1):54–79.

D'Amico, S. and King, T. B. (2013). Flow and stock effects of large-scale treasury purchases: Evidence on the importance of local supply. *Journal of Financial Economics*, 108(2):425–448.

Di Maggio, M., Kermani, A., and Palmer, C. J. (2020). How Quantitative Easing Works: Evidence on the Refinancing Channel. *Review of Economic Studies*, 87(3):1498–1528.

Driessen, G. A. (2016). How treasury issues debt. *Congressional Research Service Report R40767*.

Fama, E. F. and Bliss, R. R. (1987). The Information in Long-Maturity Forward Rates. *American Economic Review*, 77(4):680–692.

Fieldhouse, A. J., Mertens, K., and Ravn, M. O. (2018). The Macroeconomic Effects of Government Asset Purchases: Evidence from Postwar U.S. Housing Credit Policy. *The Quarterly Journal of Economics*, 133(3):1503–1560.

Fleming, M. J. (2007). Who buys treasury securities at auction? *Federal Reserve Bank of New York Current Issues in Economics and Finance*, 13(1).

Fleming, M. J. and Liu, W. (2016). Intraday pricing and liquidity effects of us treasury auctions.

Forest, J. J. (2018). The Effect of Treasury Auction Results on Interest Rates: The 1990s Experience. Technical report, University of Massachusetts - Amherst.

Garbade, K. D. (2007). The Emergence of "Regular and Predictable" as a Treasury Debt Management Strategy. *FRBNY Economic Policy Review*, (March):53–71.

Garbade, K. D. and Ingber, J. F. (2005). The Treasury auction process: objectives, structure, and recent acquisitions. *Current Issues in Economics and Finance*, 11(Feb).

Gertler, M. and Karadi, P. (2011). A model of unconventional monetary policy. *Journal of Monetary Economics*, 58(1):17 – 34. Carnegie-Rochester Conference Series on Public Policy: The Future of Central Banking April 16-17, 2010.

Gorodnichenko, Y. and Ray, W. (2017). The Effects of Quantitative Easing: Taking a Cue from Treasury Auctions. NBER Working Papers 24122, National Bureau of Economic Research, Inc.

Gorodnichenko, Y. and Weber, M. (2016). Are Sticky Prices Costly? Evidence from the Stock Market. *American Economic Review*, 106(1):165–199.

Greenlaw, D., Hamilton, J. D., Harris, E., and West, K. D. (2018). A Skeptical View of the Impact of the Fed's Balance Sheet. NBER Working Papers 24687, National Bureau of Economic Research, Inc.

Greenwood, R., Hanson, S. G., and Vayanos, D. (2016). Forward Guidance in the Yield Curve: Short Rates versus Bond Supply. In Albagli, E., Saravia, D., and Woodford, M., editors, *Monetary Policy through Asset Markets: Lessons from Unconventional Measures and Implications for an Integrated World*, volume 24 of *Central Banking, Analysis, and Economic Policies Book Series*, chapter 2, pages 011–062. Central Bank of Chile.

Greenwood, R. and Vayanos, D. (2014). Bond supply and excess bond returns. *Review of Financial Studies*, 27(3):663–713.

Gürkaynak, R. S., Sack, B., and Wright, J. H. (2007). The U.S. Treasury yield curve: 1961 to the present. *Journal of Monetary Economics*, 54(8):2291 – 2304.

Hamilton, J. D. and Wu, J. C. (2012). The Effectiveness of Alternative Monetary Policy Tools in a Zero Lower Bound Environment. *Journal of Money, Credit and Banking*, 44:3–46.

He, Z., Kelly, B., and Manela, A. (2016). Intermediary asset pricing: New evidence from many asset classes. Working Paper 21920, National Bureau of Economic Research.

He, Z. and Krishnamurthy, A. (2013). Intermediary Asset Pricing. *American Economic Review*, 103(2):732–770.

Kaminska, I. and Zinna, G. (2020). Official demand for u.s. debt: Implications for u.s. real rates. *Journal of Money, Credit and Banking*, 52(2-3):323–364.

Karadi, P. and Nakov, A. (2020). Effectiveness and addictiveness of quantitative easing. *Journal of Monetary Economics*.

King, T. (2019a). Duration Effects in Macro-Finance Models of the Term Structure. Technical report.

King, T. B. (2019b). Expectation and duration at the effective lower bound. *Journal of Financial Economics*, 134(3):736–760.

Krishnamurthy, A. and Vissing-Jorgensen, A. (2011). The effects of quantitative easing on interest rates: Channels and implications for policy. *Brookings Papers on Economic Activity*, (2 (Fall)):215–265.

Krishnamurthy, A. and Vissing-Jorgensen, A. (2012). The aggregate demand for Treasury debt. *Journal of Political Economy*, 120(2):233–267.

Kuttner, K. N. (2001). Monetary policy surprises and interest rates: Evidence from the Fed funds futures market. *Journal of Monetary Economics*, 47(3):523–544.

Kyle, A. S. and Xiong, W. (2001). Contagion as a Wealth Effect. *Journal of Finance*, 56(4):1401–1440.

Li, C. and Wei, M. (2013). Term Structure Modeling with Supply Factors and the Federal Reserve's Large-Scale Asset Purchase Progarms. *International Journal of Central Banking*, 9(1):3–39.

Lou, D., Yan, H., and Zhang, J. (2013). Anticipated and Repeated Shocks in Liquid Markets. *Review of Financial Studies*, 26(8):1891–1912.

Martin, C. and Milas, C. (2012). Quantitative easing: a sceptical survey. *Oxford Review of Economic Policy*, 28(4):750–764.

Ray, W. (2019). Monetary policy and the limits to arbitrage: Insights from a new keynesian preferred habitat model. Working paper.

Romer, C. D. and Romer, D. H. (2017). New evidence on the aftermath of financial crises in advanced countries. *American Economic Review*, 107(10):3072–3118.

Sims, E. and Wu, J. C. (2020). Evaluating central banks' tool kit: Past, present, and future. *Journal of Monetary Economics*.

Vayanos, D. and Vila, J.-L. (2009). A preferred-habitat model of the term structure of interest rates. Working Paper 15487, National Bureau of Economic Research.

Vayanos, D. and Vila, J.-L. (2020). A preferred-habitat model of the term structure of interest rates. *Econometrica*.

Wright, J. H. (2012). What does monetary policy do to long-term interest rates at the zero lower bound?*. *The Economic Journal*, 122(564):F447–F466.

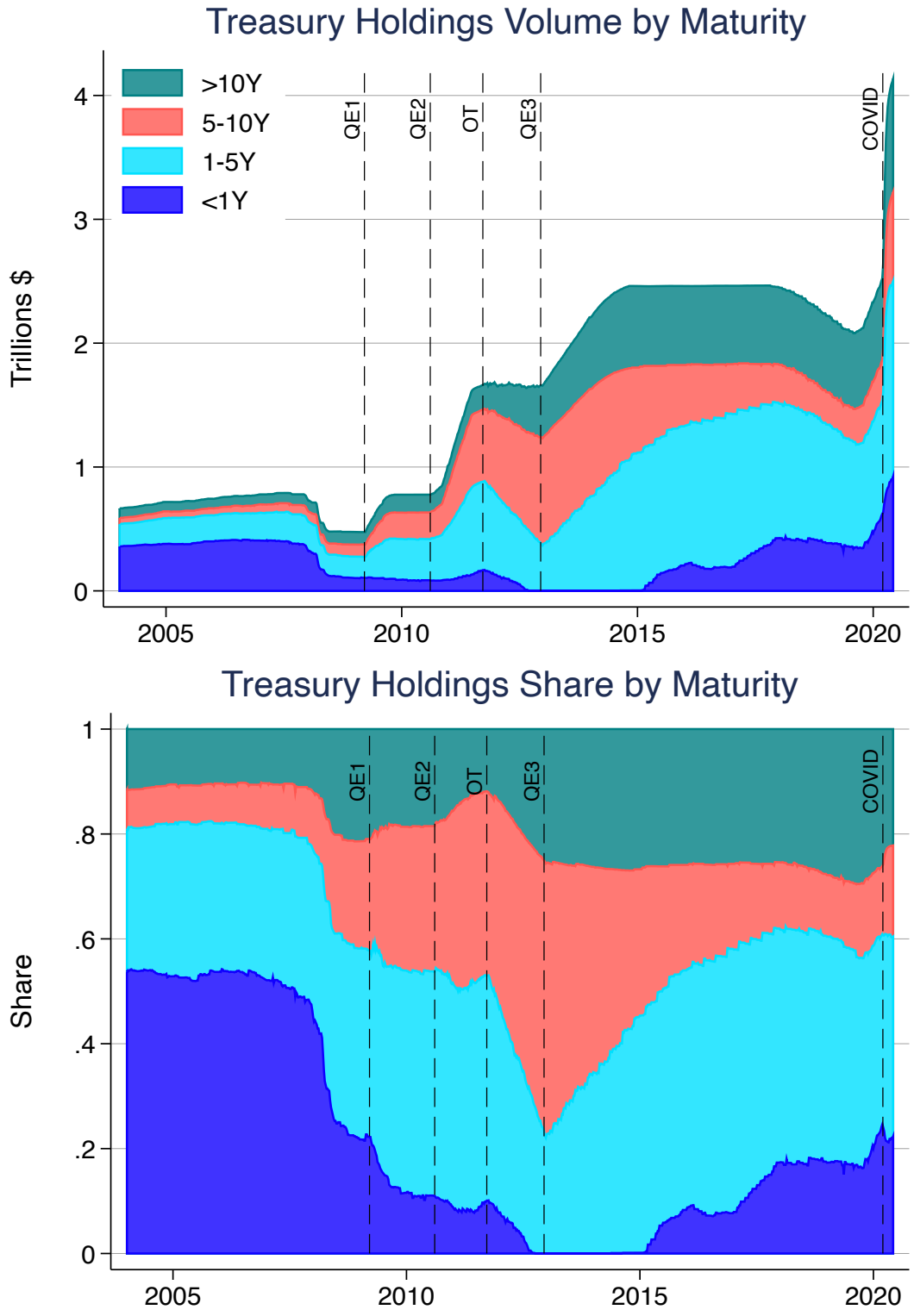

Figure 1: Federal Reserve Holdings of U.S. Government Debt

Notes: QE1 denotes time when the Fed announced its decision to buy U.S. Treasuries as a part of the first round of quantitative easing. QE2 denotes the announcement of the second round of quantitative easing. QE3 denotes the time when the Fed announced its purchases of U.S. Treasuries as a part of the third round of quantitative easing. OT denotes the announcement of "Operation Twist". COVID denotes the announcement of the large-scale asset purchases undertaken to combat the financial disruptions caused by the COVID-19 pandemic.

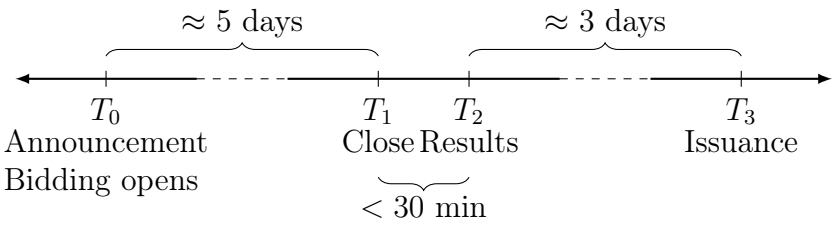

Figure 2: Auction Timing

Notes: Timeline of the events occurring during a representative Treasury auction.

August 03, 2011 202-504-3550

TREASURY OFFERING ANNOUNCEMENT [1]

Term and Type of Security	30-Year Bond
Offering Amount	$16,000,000,000
Currently Outstanding	$0
CUSIP Number	912810QS0
Auction Date	August 11, 2011
Original Issue Date	August 15, 2011
Issue Date	August 15, 2011
Maturity Date	August 15, 2041
Dated Date	August 15, 2011
Series	Bonds of August 2041
Yield	Determined at Auction
Interest Rate	Determined at Auction
Interest Payment Dates	February 15 and August 15
Accrued Interest from 08/15/2011 to 08/15/2011	None
Premium or Discount	Determined at Auction
Minimum Amount Required for STRIPS	$100
Corpus CUSIP Number	912803DT7
Additional TINT(s) Due Date(s) and	August 15, 2041
CUSIP Number(s)	912834KP2
Maximum Award	$5,600,000,000
Maximum Recognized Bid at a Single Yield	$5,600,000,000
NLP Reporting Threshold	$5,600,000,000
NLP Exclusion Amount	$0
Minimum Bid Amount and Multiples	$100
Competitive Bid Yield Increments [2]	0.001%
Maximum Noncompetitive Award	$5,000,000
Eligible for Holding in Treasury Direct Systems	Yes
Eligible for Holding in Legacy Treasury Direct	No
Estimated Amount of Maturing Coupon Securities Held by the Public	$24,430,000,000
Maturing Date	August 15, 2011
SOMA Holdings Maturing	$2,205,000,000
SOMA Amounts Included in Offering Amount	No
FIMA Amounts Included in Offering Amount [3]	Yes
Noncompetitive Closing Time	12:00 Noon ET
Competitive Closing Time	1:00 p.m. ET

(a) Announcement

August 11, 2011 202-504-3550

TREASURY AUCTION RESULTS

Term and Type of Security	30-Year Bond
CUSIP Number	912810QS0
Series	Bonds of August 2041
Interest Rate	3-3/4%
High Yield[1]	3.750%
Allotted at High	41.74%
Price	100.000000
Accrued Interest per $1,000	None
Median Yield[2]	3.629%
Low Yield[3]	3.537%
Issue Date	August 15, 2011
Maturity Date	August 15, 2041
Original Issue Date	August 15, 2011
Dated Date	August 15, 2011

	Tendered	**Accepted**
Competitive	$33,305,800,000	$15,985,160,000
Noncompetitive	$14,855,600	$14,855,600
FIMA (Noncompetitive)	$0	$0
Subtotal[4]	**$33,320,655,600**	**$16,000,015,600**[5]
SOMA	$489,928,400	$489,928,400
Total	**$33,810,584,000**	**$16,489,944,000**

	Tendered	**Accepted**
Primary Dealer[6]	$23,734,000,000	$10,921,532,000
Direct Bidder[7]	$6,567,000,000	$3,119,654,000
Indirect Bidder[8]	$3,004,800,000	$1,943,974,000
Total Competitive	**$33,305,800,000**	**$15,985,160,000**

(b) Results

Figure 3: Example of Auction Press Releases

Notes: Press releases from the Treasury for an auction of 30-year bonds. Source: TreasuryDirect.

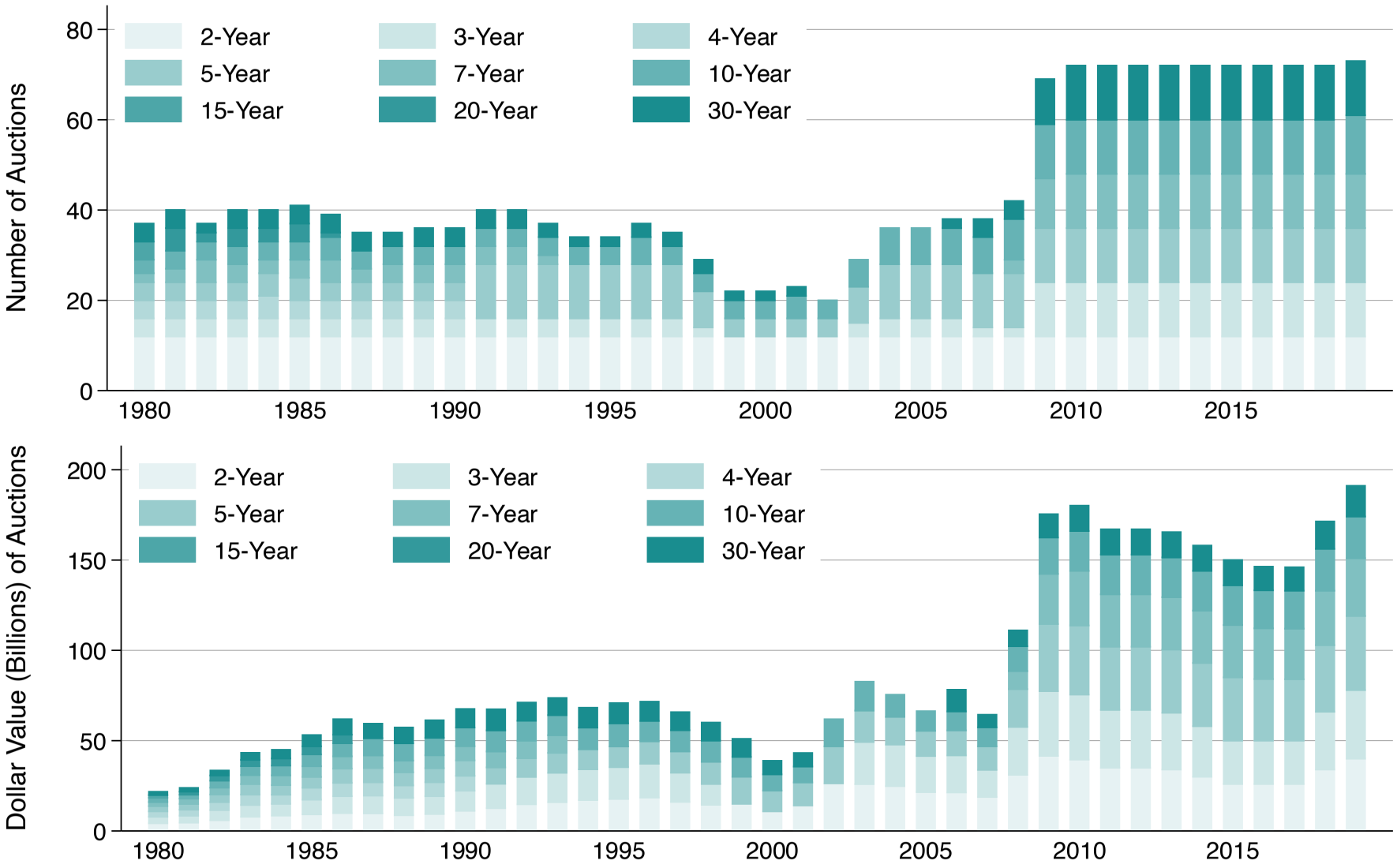

Figure 4: Number and Size of Auctions per Year

Notes: the number (top panel) and dollar value (bottom panel) of note and bond Treasury auctions per year by term length. The number of auctions temporarily fell in the late 1990s and early 2000s (during which time the Treasury ceased issuing 7- and 30-year securities). After the Great Recession, the number and size of auctions increased sharply. Since 2010, the Treasury has held auctions every month for maturities $m = 2, 3, 5, 7, 10, 30$ years.

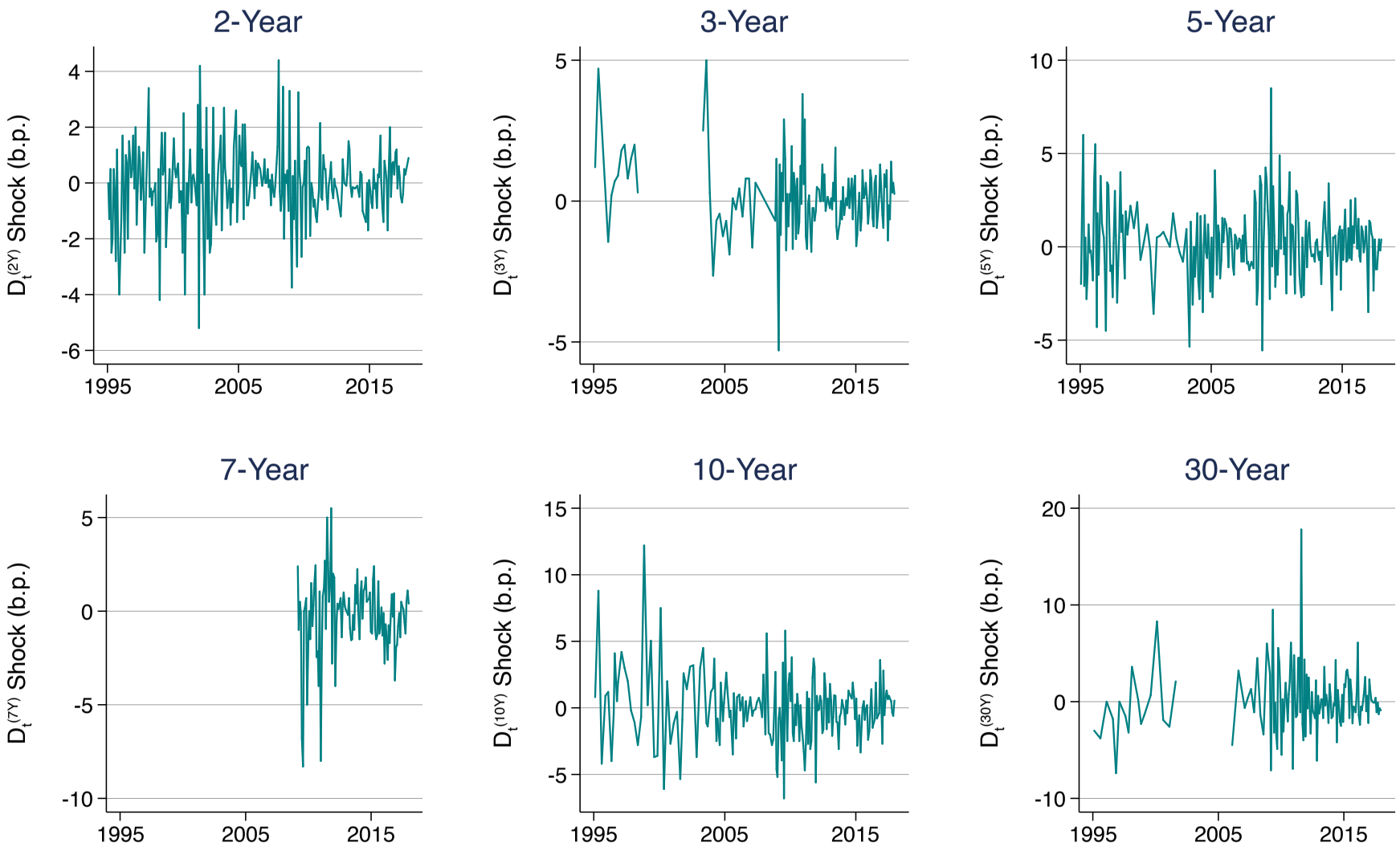

Figure 5: Time Series of Surprises Movements in Treasury Yields

Notes: Plots of the times series of intraday yield shocks following the close of Treasury auctions. Shocks $D_t^{(m)}$ are plotted separately for auctions of maturities $m = 2, 3, 5, 7, 10, 30$ years (in basis points). Gaps in the time series of 3-year, 7-year, and 30-year shocks correspond to temporary halts newly issued securities of these maturities; see Figure 4.

Figure 6: Intraday Treasury Yield Movements

Notes: The top panel plots intraday movements during the 30-year auction on December 9, 2010. An auction for reopened 30-year Treasury bonds closed at 1:00pm (first vertical line), and results were released shortly after (second vertical line). Immediately following the release, yields of the associated security in secondary-market trading fell sharply. The bottom panel plots intraday movements during the 30-year auction on August 11, 2011. An auction for newly-issued 30-year Treasury bonds closed at 1:00pm (first vertical line), and results were released shortly after (second vertical line). Immediately following the release, yields of the corresponding when-issued trading rose sharply

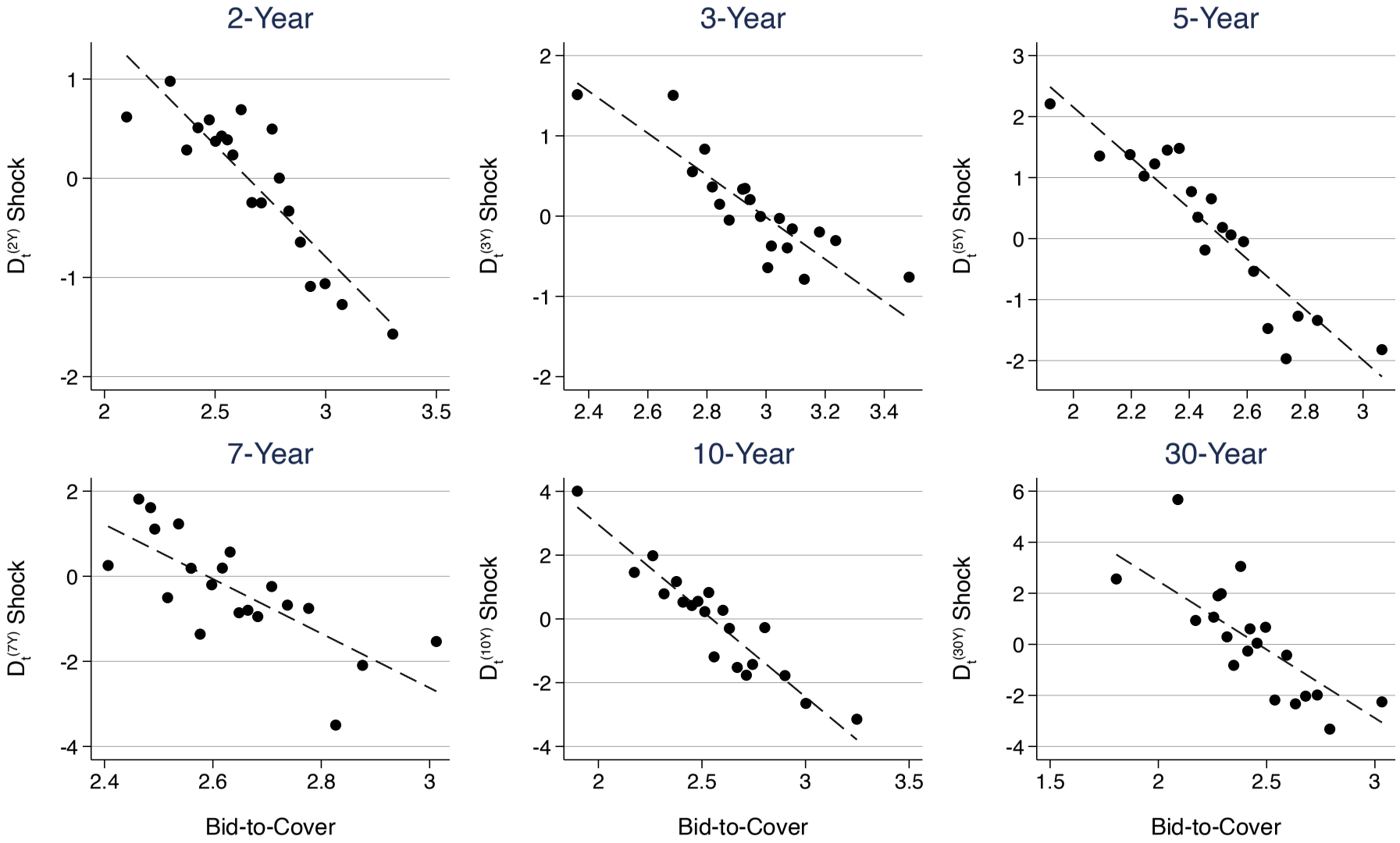

Figure 7: Demand Shocks and the Bid-to-Cover

Notes: Bin scatter plot comparing demand shocks and the bid-to-cover ratio from the auction. The bid-to-cover is the ratio of the dollar value of bids received to those accepted at a given auction. Four lags of the bid-to-cover are included; the residuals are plotted. Demand shocks $D_t^{(m)}$ for maturities $m = 2, 3, 5, 7, 10, 30$ years are reported in basis points.

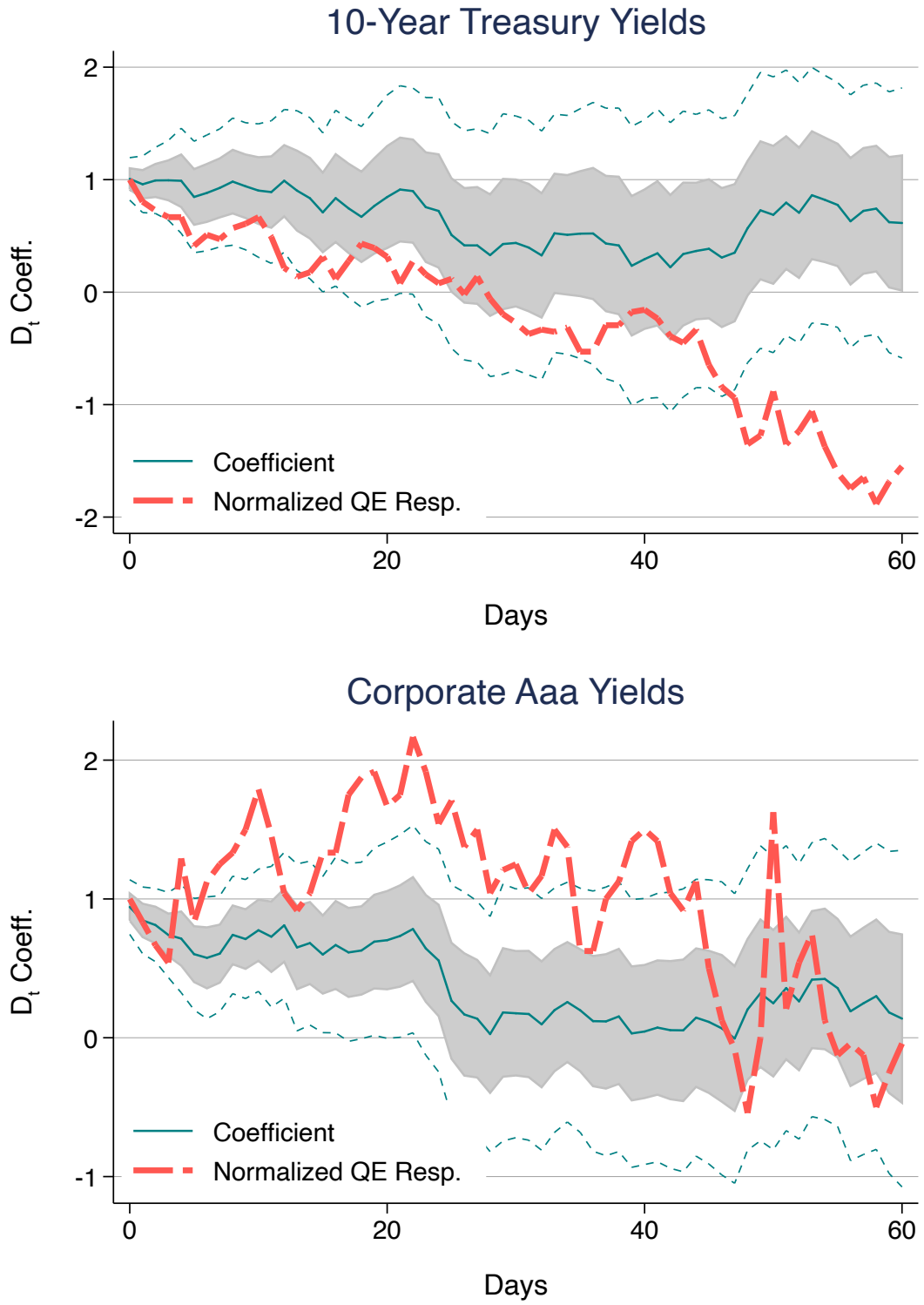

Figure 8: Long-Difference Response to Demand Shocks

Notes: Responses of 10-year Treasury spot rates (top panel) and Moody's Aaa yields (bottom panel) to demand shocks D_t (pooled across maturities). We compute "long-difference" regressions: on an auction date t, the dependent variable is $y_{t+h} - y_{t-1}$, the change h days after the auction relative to the day before the auction. The solid line plots the coefficients from regressions for $h = 0, \ldots, 60$; the shaded region and dotted lines correspond to one- and two-standard error (Newey-West, 9 lags) confidence bands. The dashed line compares the long-horizon effects of the March 2009 QE1 FOMC announcement (normalized so that the impact on announcement is one).

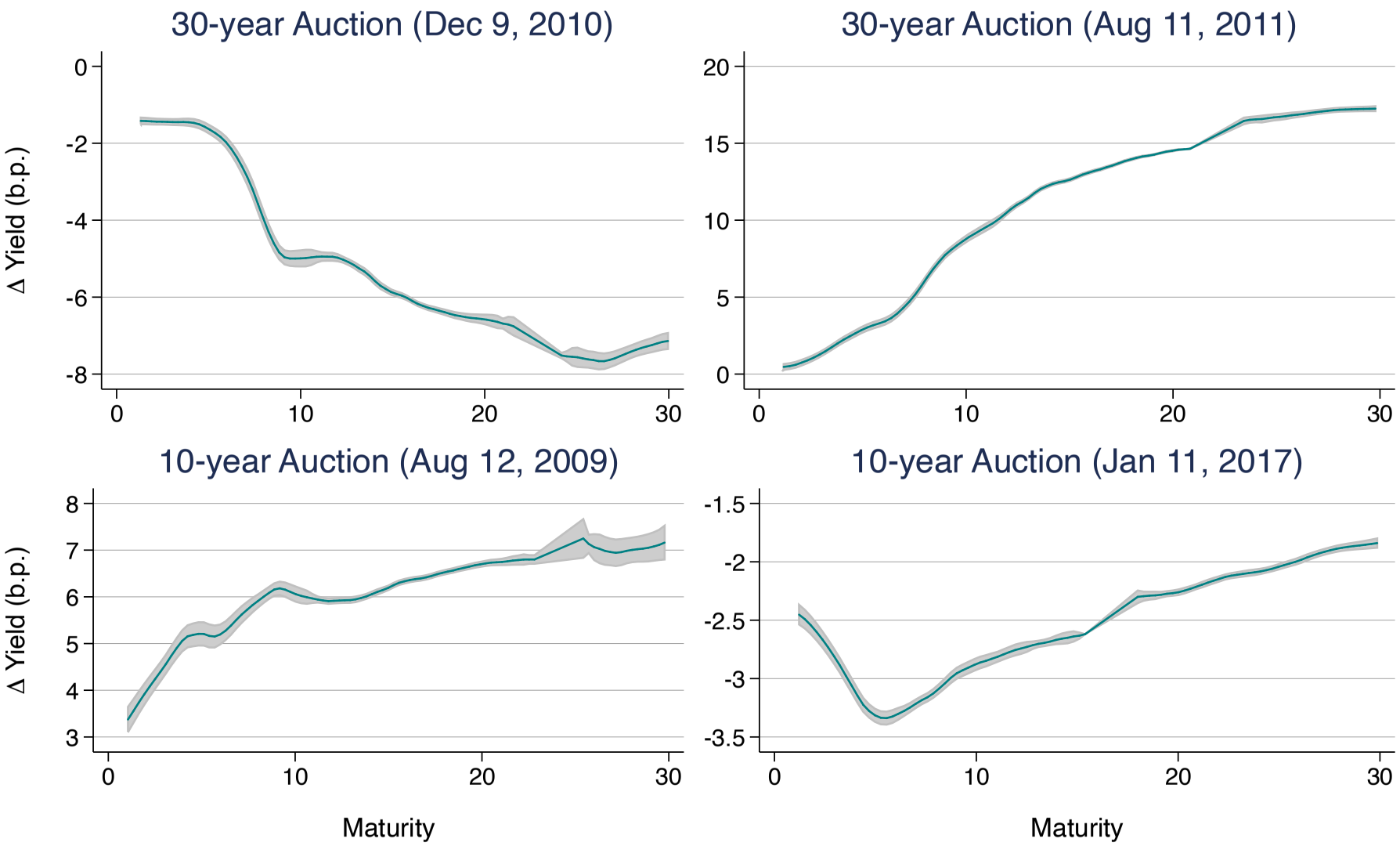

Figure 9: Changes in Yield Curves Following Treasury Auctions

Notes: Intraday changes in the yield curve following 30-year auctions on December 9, 2010 and August 11, 2011 (top panels) and following 10-year auctions on August 12, 2009 and January 11, 2017 (bottom panels). The change in yields (in basis points) are from all traded bills, notes, and bonds in the secondary market. The solid line represents the point estimates of local-mean smoothing regressions across maturities, while the shaded regions represent two standard error confidence intervals.

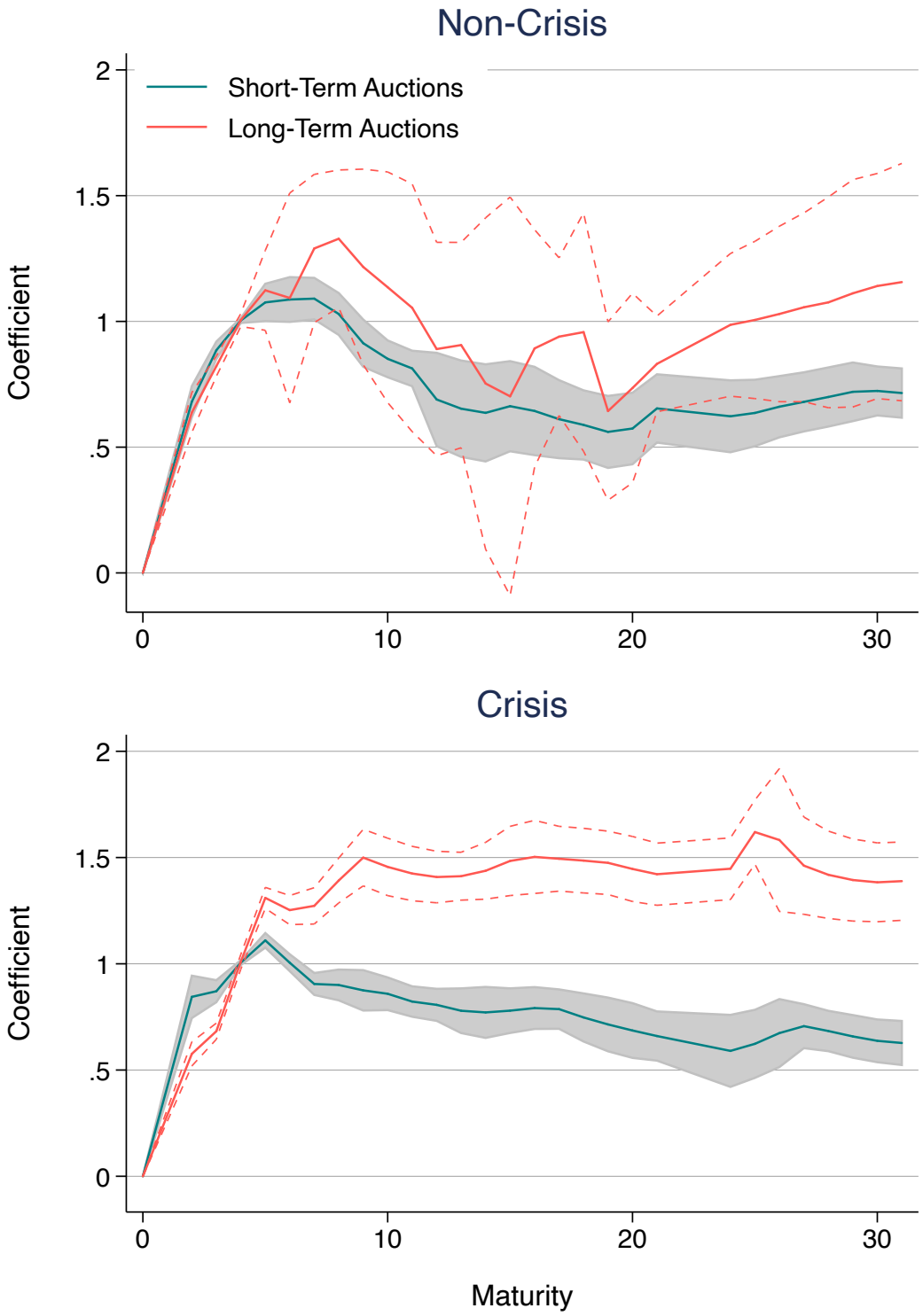

Figure 10: Localization Regression Results

Notes: Plots of the regression coefficients from regression equation (15). The top panel compares estimates from short- and long-maturity auctions during non-crisis periods; the bottom panel compares these estimates during crisis periods. 2 standard error (Newey-West, 9 lags) confidence intervals are included.

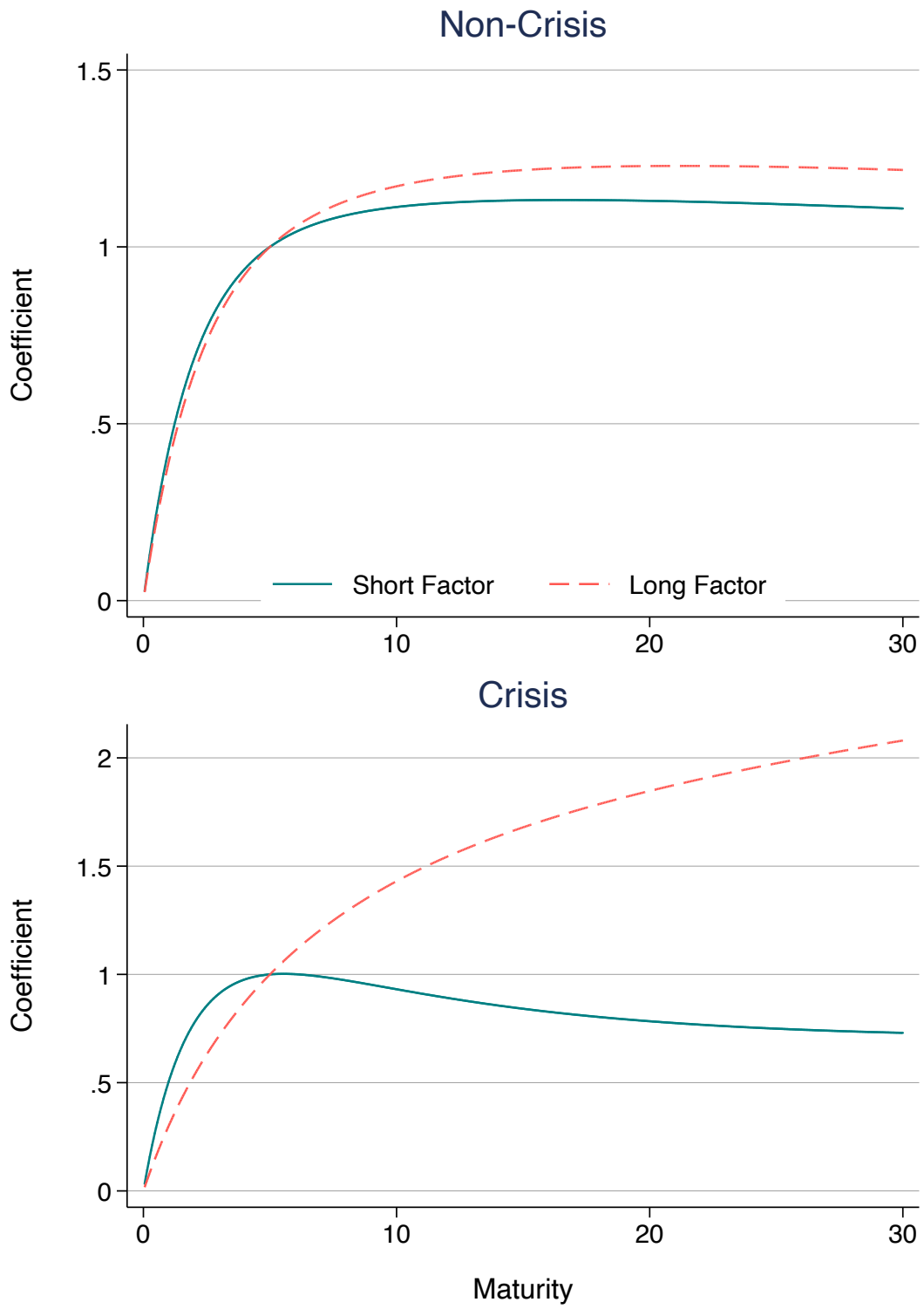

Figure 11: Model-Implied Localization Regression Coefficients

Notes: Model-implied coefficients from regression equation (15). The top panel plots the coefficients from the model calibrated to non-crisis periods, while the bottom panel plots the coefficients from the model calibrated to crisis periods. The empirical analogues are plotted in Figure 10.

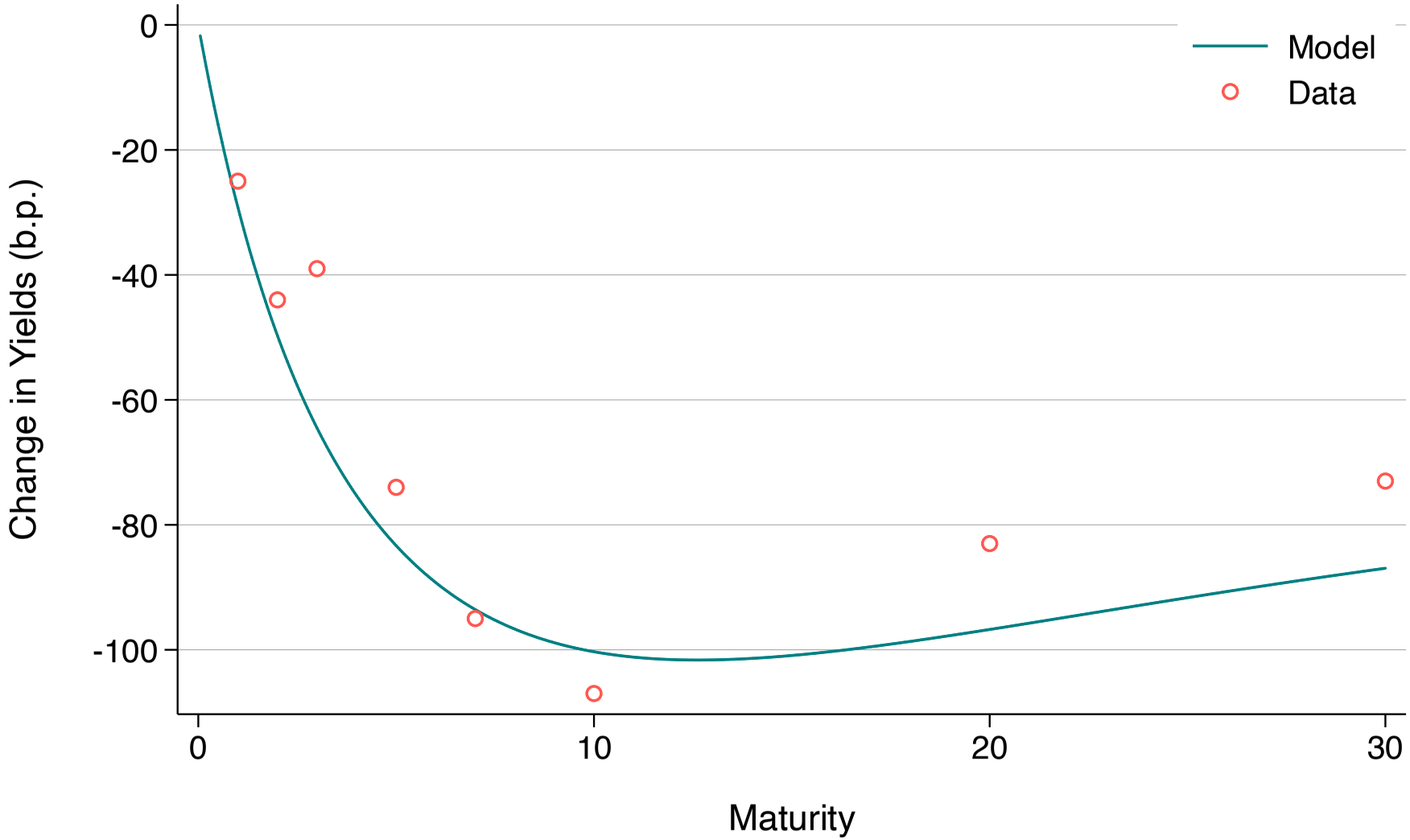

Figure 12: Model-Implied Response to QE1

Notes: Comparison of the observed (cumulative) yield reactions to QE1 and the model-implied change in yields following a QE1 shock. The empirical response is constructed as in Krishnamurthy and Vissing-Jorgensen (2011), and consists of the sum of the two-day changes in yields following all the major QE1 announcements.

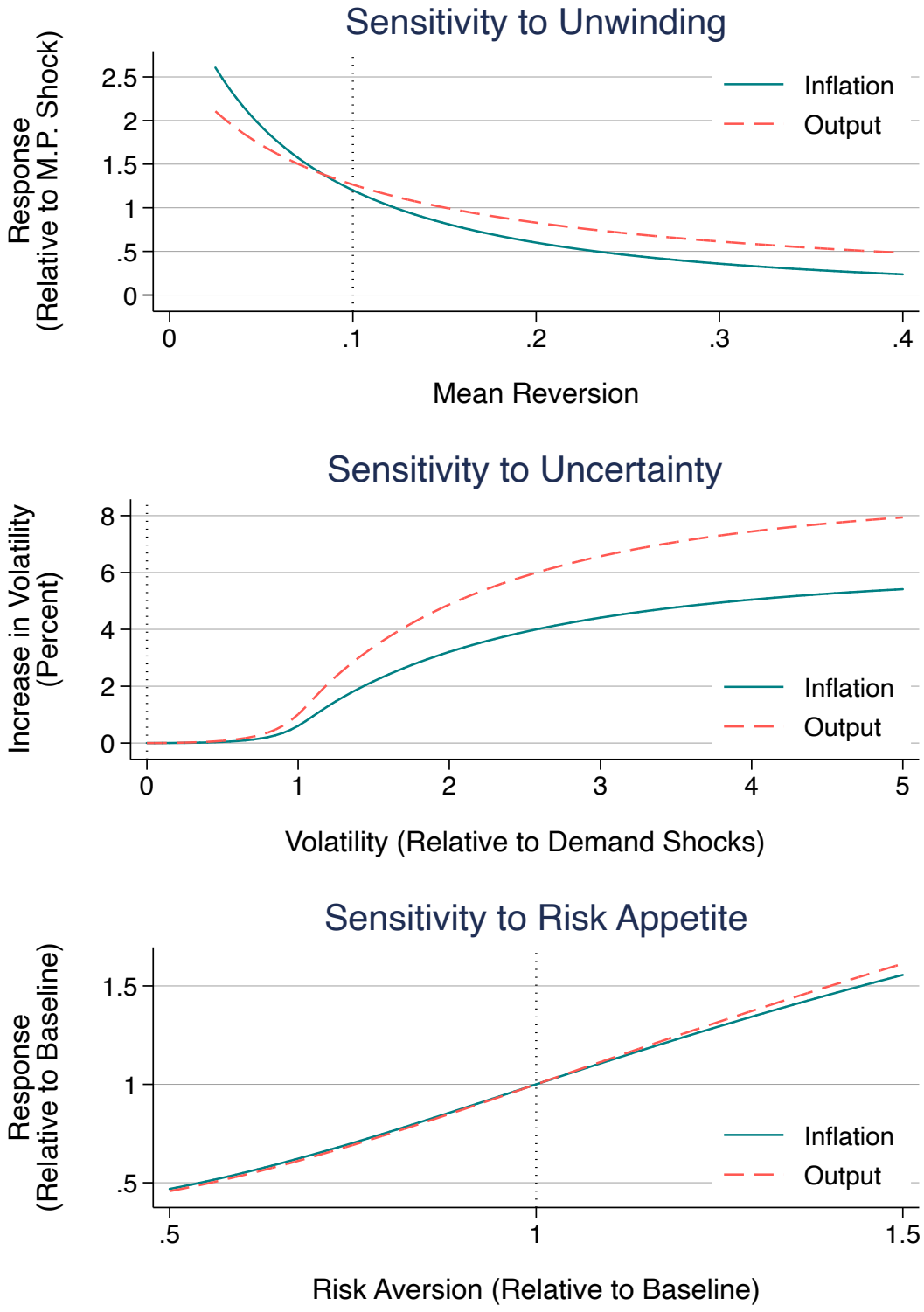

Figure 13: Policy Sensitivity Analysis

Notes: The top panel plots the impact of the QE shock in the model on output and inflation (relative to a monetary policy shock) as a function of the mean reversion of the QE shock (κ_{QE} in equation (20)) The middle panel plots the change in long-run volatility of output and inflation as a function of the volatility of QE shocks (σ_{QE} in equation (21)). The bottom panel plots the impact of QE on output and inflation as a function of arbitrageur risk aversion (a in equation (4)).

Table 1: Auction Summary Statistics

	Mean	Median	Std. Dev.	Min	Max
Panel A: All auctions					
Offering Amount (billions)	18.82	16.00	10.75	0.03	44.00
Total Tendered (billions)	51.41	40.80	32.27	0.09	160.96
Term (Years)	8.03	5.00	8.61	2.00	30.25
High Yield	4.87	3.90	3.63	0.22	16.28
Bid-to-Cover	2.58	2.54	0.48	1.22	5.88
Panel B: 1995-2017					
Offering Amount (billions)	22.51	22.00	8.99	5.00	44.00
Total Tendered (billions)	62.18	57.91	30.12	11.35	160.96
Term (Years)	8.09	5.00	8.60	2.00	30.25
High Yield	2.99	2.67	1.84	0.22	7.79
Bid-to-Cover	2.61	2.58	0.46	1.22	4.07
Bid-to-Cover by type$^\sharp$					
Direct Bidders	0.22	0.21	0.17	0.00	0.85
Indirect Bidders	0.53	0.53	0.17	0.03	1.05
Primary Delears	1.93	1.88	0.34	0.98	3.12
Fraction Accepted by type†					
Depository Institutions	0.01	0.00	0.02	0.00	0.32
Individuals	0.01	0.00	0.02	0.00	0.19
Dealers	0.54	0.53	0.16	0.12	0.98
Pensions	0.00	0.00	0.01	0.00	0.21
Investment Funds	0.26	0.23	0.17	0.00	0.74
Foreign	0.19	0.18	0.09	0.00	0.61
Other	0.00	0.00	0.01	0.00	0.13

Notes: Summary statistics for Treasury note and bond auctions. † indicates that the moments are computed for 2000 onward, the period for which these data are available. ♯ indicates that the moments are computed from 2003 onward, the period for which these data are available.

Table 2: Treasury Yield Shocks Summary Statistics

	Mean	Med.	Std. Dev.	Min	Max	Obs.
Panel A: Auction shocks						
D_t	0.03	0.00	2.12	-8.30	17.80	1047
Panel B: Maturity						
$D_t^{(2Y)}$	-0.06	0.00	1.39	-5.20	4.40	256
$D_t^{(3Y)}$	0.15	0.10	1.32	-5.30	5.00	134
$D_t^{(5Y)}$	0.20	0.30	1.94	-5.55	8.50	233
$D_t^{(7Y)}$	-0.28	0.05	2.10	-8.30	5.50	106
$D_t^{(10Y)}$	-0.04	-0.05	2.55	-6.80	12.20	186
$D_t^{(30Y)}$	0.09	-0.15	3.28	-7.40	17.80	132
Panel C: Economic regime						
Expansion	0.03	0.00	2.03	-8.30	17.80	963
Recession	-0.07	-0.05	2.95	-7.10	9.50	84
Panel D: Monetary regime						
Non-ZLB	0.08	0.10	2.02	-7.40	12.20	563
ZLB	-0.03	0.00	2.23	-8.30	17.80	484
Panel E: Non-auction						
$\tilde{D}_t^{(2Y)}$	-0.07	0.00	1.32	-19.20	11.00	1225
$\tilde{D}_t^{(5Y)}$	-0.01	0.00	1.13	-17.40	12.90	1924
$\tilde{D}_t^{(10Y)}$	-0.01	0.00	1.03	-13.30	8.90	2151
$\tilde{D}_t^{(30Y)}$	0.01	0.00	0.92	-8.50	5.60	1914

Notes: Shocks $D_t = y_{t,post} - y_{t,pre}$ are the intraday change in Treasury yields before and after the close of an auction (in basis points). For newly issued securities, the yields are from when-issued trades. For reopened securities, the yields are from secondary-market trades. Panel B reports statistics for shocks $D_t^{(m)} = y_{t,post}^{(m)} - y_{t,pre}^{(m)}$ separately for major maturities $m = 2, 3, 5, 7, 10, 30$ years. Panels C and D report statistics separately for recessions/expansions and binding/non-binding ZLB periods, respectively. Panel E reports synthetic shocks on non-auction dates $\tilde{D}_t^{(m)} = y_{t,post}^{(m)} - y_{t,pre}^{(m)}$ using the same intraday windows around 1PM on non-auction dates. The yields are from secondary-market trades for on-the-run securities for maturities $m = 2, 5, 10, 30$ years.

Table 3: Demand Shocks and Measures of Demand

	(1) $D_t^{(2Y)}$	(2) $D_t^{(3Y)}$	(3) $D_t^{(5Y)}$	(4) $D_t^{(7Y)}$	(5) $D_t^{(10Y)}$	(6) $D_t^{(30Y)}$	(7) Pool D_t
Panel A: Total bid-to-cover ratio							
Bid-to-Cover	-0.57***	-0.91**	-2.50***	-3.06***	-3.05***	-4.69***	-1.68***
	(0.15)	(0.37)	(0.51)	(0.72)	(0.49)	(1.09)	(0.22)
Obs.	256	134	233	106	186	132	1047
R^2	0.06	0.11	0.20	0.09	0.26	0.20	0.12
Panel B: Expected and unexpected bid-to-cover							
Fitted	-0.03	-0.09	0.27	1.72	-0.40	-2.58	-0.11
	(0.14)	(0.37)	(0.62)	(2.44)	(0.51)	(1.89)	(0.16)
Residual	-2.25***	-2.62***	-4.15***	-6.40***	-5.40***	-5.36***	-3.97***
	(0.43)	(0.34)	(0.56)	(1.17)	(0.83)	(1.71)	(0.37)
Obs.	252	130	229	102	182	128	1023
R^2	0.22	0.26	0.34	0.22	0.43	0.22	0.26
Panel C: Bid-to-cover by bidder type							
Indirect	-4.72***	-3.01***	-8.82***	-13.22***	-8.38***	-15.79***	-8.42***
	(0.62)	(0.71)	(1.24)	(1.71)	(0.90)	(2.68)	(0.84)
Direct	-2.51**	-3.24***	-2.75	-4.88**	-3.66**	-6.38***	-3.61***
	(1.00)	(0.97)	(1.78)	(2.42)	(1.63)	(1.91)	(0.72)
Primary	-0.42	-1.35**	-2.97***	-0.09	-3.36***	-4.10**	-2.22***
	(0.52)	(0.61)	(0.77)	(1.49)	(0.68)	(1.73)	(0.42)
Obs.	159	117	168	102	146	111	803
R^2	0.46	0.39	0.48	0.59	0.50	0.53	0.39
Panel D: Fraction accepted by bidder type							
Invest. Fund	-6.61***	-6.33***	-9.78***	-15.10***	-9.62***	-17.83***	-10.49***
	(1.37)	(1.48)	(1.94)	(2.70)	(1.65)	(4.40)	(1.17)
Foreign	-6.89***	-3.90**	-10.43***	-16.35***	-9.61***	-17.56***	-9.50***
	(1.52)	(1.60)	(2.04)	(2.56)	(2.41)	(5.15)	(1.15)
Misc.	-6.35**	-6.87	-6.89***	3.92	11.98	-13.00**	-6.88***
	(2.88)	(7.58)	(2.31)	(6.53)	(10.66)	(6.44)	(2.12)
Obs.	197	117	181	102	160	115	872
R^2	0.27	0.22	0.30	0.49	0.31	0.41	0.24

Notes: Regressions of demand shocks $D_t^{(m)}$ on the bid-to-cover ratio and fractions accepted, total and broken up by bidder type. Columns (1)-(6) restrict the sample to include only auctions of maturities $m = 2, 3, 5, 7, 10, 30$ years; column (7) pools across all auctions. In Panels A, C, and D, four lags of the dependent variables are included but not reported; in Panel B, the fitted values and residuals of an AR(4) are both used as dependent variables. Newey-West (9 lags) standard errors in parentheses.

Table 4: Asset Price Reactions to Demand Shocks at Treasury Auctions

Asset type	Estimate (s.e.)	Obs.	R^2	Sample
	(1)	(2)	(3)	(4)
Panel A: Corporate debt				
LQD	-3.93***	830	0.59	2002-2017
	(0.15)			
Corp. Aaa†	0.94***	1040	0.14	1995-2017
	(0.10)			
Corp. Baa†	0.96***	1040	0.15	1995-2017
	(0.10)			
Corp. C†	0.23	973	0.00	1997-2017
	(0.39)			
Panel B: Equities				
SPY	-0.23	1033	0.00	1995-2017
	(0.52)			
IWM	0.18	876	0.00	2000-2017
	(0.58)			
SP500†	3.61	974	0.00	1995-2016
	(2.74)			
Russell 2000†	6.26*	974	0.01	1995-2016
	(3.25)			
Panel C: Inflation and commodities				
GLD	-1.16***	775	0.02	2004-2017
	(0.36)			
GSCI†	-1.20	974	0.00	1995-2016
	(2.74)			
10Y Infl. Swap†	0.02	724	0.00	2004-2016
	(0.08)			
2Y Infl. Swap†	0.04	724	0.00	2004-2016
	(0.17)			
Panel D: Spreads and credit default swaps				
Aaa-Baa†	0.02	1040	0.00	1995-2017
	(0.03)			
LIBOR-OIS†	0.03	737	0.00	2003-2016
	(0.04)			
Auto CDS†	-0.60	733	0.00	2004-2016
	(2.65)			
Bank CDS†	-0.23	733	0.01	2004-2016
	(0.16)			
VIX†	-0.04	1040	0.00	1995-2017
	(0.03)			

Notes: Regressions of asset price changes on demand shocks D_t (pooled across maturities). † denotes that changes are at the daily frequency; otherwise, changes are measured over the same intraday window corresponding to the auction demand shocks. The intraday changes are from ETFs that track various underlying securities or indices: LQD (corporate debt); SPY (S&P 500); IWM (Russell 2000); GLD (gold bullion). Daily series: Aaa, Baa, C (Moody's and B of A corporate debt yield indices); S&P 500, Russell 2000 (equity indices); GSCI (S&P Total Commodity Index); 10- and 2-year inflation swaps; Auto and Bank credit default swap indices; LIBOR-OIS (3-month USD LIBOR-Overnight Index Swap spread); VIX (implied volatility index). Newey-West (9 lags) standard errors in parentheses.

Table 5: Calibration

Parameter	Value	Description
Panel A: Macroeconomic Dynamics		
ρ	0.04	Discount Factor
ς^{-1}	1.0	Intertemporal Elasticity
δ	0.1	Nominal Rigidity
ϕ_π	1.5	Inflation Taylor Coeff.
ϕ_x	0.25	Output Taylor Coeff.
κ_r	0.1	Monetary Policy Inertia
σ	0.0025	Monetary Shock Vol.
Panel B: Effective Borrowing Rate		
η_1	1.7	Weight Scaling Factor
Panel C: Term Structure		
θ_1^s	1.25	Short Factor Location
θ_1^ℓ	0.25	Long Factor Location
α_1	0.1	Habitat Elasticity Shape
κ_β	0.469	Demand Factor Inertia
$\phi_{r,\beta}$	-0.372	Demand Short Rate Response
$a\sigma^2 \cdot \alpha_0$	0	Habitat Elasticity Size
$a\sigma^2 \cdot \theta_0$	0.0654	Demand Factor Size
Panel D: Term Structure (Crisis)		
$a\sigma^2 \cdot \alpha_0$	0.000457	Habitat Elasticity Size
$a\sigma^2 \cdot \theta_0$	0.273	Demand Factor Size
Panel E: QE1 Shock		
θ_1^{QE}	0.75	QE1 Shock Location
κ_{QE}	0.1	QE1 Shock Intertia

Notes: Calibrated and estimated parameters used in the numerical simulations.

Appendix A Model Details

This section briefly lays out the details of the model, characterizes the solution of the model, and proves the key localization results of Section 4.

A.1 Characterizing the Solution

Following Ray (2019), under rational expectations the state variables evolve according to

$$\mathbf{y}_t = -\mathbf{\Gamma}(\mathbf{y}_t - \overline{\mathbf{y}})\,\mathrm{d}t + \boldsymbol{\sigma}\,\mathrm{d}\mathbf{B}_t \tag{A1}$$

where

$$\mathbf{\Gamma} = \mathbf{Q}_{11}\mathbf{\Lambda}_1\mathbf{Q}_{11}^{-1} \tag{A2}$$

and $\mathbf{Q}_{11}, \mathbf{\Lambda}_1$ are the blocks of eigenvector and eigenvalue matrices of $\mathbf{\Upsilon}$ from equation (10) associated with the state variables $\mathbf{y}_t$. In general, the short rate is given by $\mathbf{y}_t^\top \mathbf{e}_r$ for some vector $\mathbf{e}_r$, but we simplify and assume that the short rate r_t is ordered first in $\mathbf{y}_t$, so $\mathbf{e}_r = \mathbf{e}_1$, the first standard normal basis vector (zeros everywhere except one as the first element).

As in Vayanos and Vila (2009) and Ray (2019), we focus on equilibria in which (log) bond prices are affine functions of the state variables:

$$-\log P_t^{(\tau)} = \mathbf{y}_t^\top \mathbf{A}(\tau) + C(\tau)$$

Let $\mathbf{\Sigma} = \boldsymbol{\sigma}\boldsymbol{\sigma}^\top$ and define

$$\tilde{\mathbf{X}} = \int_0^T \alpha(\tau)\mathbf{A}(\tau)\mathbf{A}(\tau)^\top \,\mathrm{d}\tau$$
$$\tilde{\mathbf{Y}} = \int_0^T \mathbf{\Theta}(\tau)\mathbf{A}(\tau)^\top \,\mathrm{d}\tau$$

where $\mathbf{\Theta}(\tau) = \begin{bmatrix} 0 & \dots & \theta^k(\tau) & \dots \end{bmatrix}^\top$ stacks the $\theta^k(\tau)$ demand functions from equation (6). Note that the zero as the first element captures the fact that habitat demand does not respond directly to movements in the short rate: $\mathbf{e}_r^\top \mathbf{\Theta}(\tau) = 0$.

Then equilibrium is characterized by a root of the following equation $H : \mathbb{R}^{J\times J} \to \mathbb{R}^{J\times J}$ which characterizes the affine coefficient function $\mathbf{A} : \mathbb{R} \to \mathbb{R}^J$:

$$H(\mathbf{M}) = \mathbf{\Gamma}^\top - a \cdot \left\{\tilde{\mathbf{Y}} - \tilde{\mathbf{X}}\right\} \mathbf{\Sigma} - \mathbf{M} \tag{A3}$$

$$\mathbf{A}(0) = \mathbf{0}, \;\; \mathbf{A}'(\tau) + \mathbf{M}\mathbf{A}(\tau) = \mathbf{e}_r \tag{A4}$$

where a is the risk aversion of the arbitraguers (from equation (4)). Because the matrices $\tilde{\mathbf{X}}, \tilde{\mathbf{Y}}$ themselves depend on $\mathbf{A}(\tau)$, the solution for $\mathbf{M}$ involves a fixed point problem with

no simple analytical solution.

A.2 Laplace Solutions

Many of the results hold under general functional form assumptions regarding the habitat investor functions $\alpha(\tau)$ and $\theta^k(\tau)$. However, in order to simplify the proofs (and to link the results with the calibrated numerical model), we make the following functional form assumptions:

$$\begin{aligned}\alpha(\tau;\alpha_0,\alpha_1) &\equiv \alpha_0 \exp(-\alpha_1\tau)\\ \theta^k(\tau;\theta_0,\theta_1) &\equiv \theta_0^k(\theta_1^k)^2\tau\exp\left(-\theta_1^k\tau\right)\end{aligned}$$

Note that $\theta^k(\tau) > 0$ and is single-peaked, with a maximum at $\tau = \frac{1}{\theta_1^k}$. Hence, for any two demand factors j and k, $\theta_1^j > \theta_1^k$ implies that demand factor j is more concentrated in short-maturity bonds compared to demand factor k.

Approximating the maximum maturity $T \to \infty$, the model can be solved more easily using Laplace transforms. Define the Laplace transform $\mathcal{A}(s) \equiv \mathcal{L}\left\{\mathbf{A}(\tau)\right\}(s)$. Then equation (A4) implies:

$$\begin{aligned}s\mathcal{A}(s) + \mathbf{M}\mathcal{A}(s) - \frac{1}{s}\mathbf{e}_r &= \mathbf{0}\\ \implies \mathcal{A}(s) &= \left[s\mathbf{I}+\mathbf{M}\right]^{-1}\left[\frac{1}{s}\mathbf{e}_r\right]\\ \implies \mathcal{A}'(s) &= -\left[s\mathbf{I}+\mathbf{M}\right]^{-1}\left[\frac{1}{s^2}\mathbf{e}_r + \mathcal{A}(s)\right]\\ \implies \mathcal{A}^{(n)}(s) &= \left[s\mathbf{I}+\mathbf{M}\right]^{-1}\left[\frac{(-1)^n n!}{s^{n+1}}\mathbf{e}_r - n\mathcal{A}^{(n-1)}(s)\right]\end{aligned}$$

Additionally, define $\mathbf{X}(\tau) \equiv \mathbf{A}(\tau)\mathbf{A}(\tau)^\top$. Note that from equation (A4) we can write

$$\begin{aligned}\mathbf{A}'(\tau)\mathbf{A}(\tau)^\top + \mathbf{A}(\tau)\mathbf{A}'(\tau)^\top + \mathbf{M}\mathbf{X}(\tau) + \mathbf{X}(\tau)\mathbf{M}^\top &= \mathbf{e}_r\mathbf{A}(\tau)^\top + \mathbf{A}(\tau)\mathbf{e}_r^\top\\ \iff \mathbf{X}'(\tau) + \mathbf{M}\mathbf{X}(\tau) + \mathbf{X}(\tau)\mathbf{M}^\top &= \mathbf{e}_r\mathbf{A}(\tau)^\top + \mathbf{A}(\tau)\mathbf{e}_r^\top\end{aligned}$$

Define the Laplace transform $\mathcal{X}(s) \equiv \mathcal{L}\left\{\mathbf{X}(\tau)\right\}(s)$. Then $\mathcal{X}(s)$ is characterized by the following Lyapunov equation:

$$\left[\frac{1}{2}s\mathbf{I}+\mathbf{M}\right]\mathcal{X}(s) + \mathcal{X}(s)\left[\frac{1}{2}s\mathbf{I}+\mathbf{M}\right]^\top = \mathbf{e}_r\mathcal{A}(s)^\top + \mathcal{A}(s)\mathbf{e}_r^\top$$

A sufficient (but not necessary) condition for a unique solution $\mathcal{X}(s)$ is if the eigenvalues of $\mathbf{M}$ have positive real parts. The analytical solution of the general Lyapunov equation $AX + XA^\top = Q$ is given by $\operatorname{vec} X = (A \oplus A)^{-1}\operatorname{vec} Q$. When A is diagonal, $X_{ij} = \frac{Q_{ij}}{a_{ii}+a_{jj}}$.

With these definitions, the matrices $\tilde{\mathbf{X}}, \tilde{\mathbf{X}}$ in equation (A3) are given by

$$\begin{aligned}
\int_0^T \alpha(\tau)\mathbf{A}(\tau)\mathbf{A}(\tau)^\top \,\mathrm{d}\tau &= \alpha_0 \mathcal{X}(\alpha_1) \equiv \tilde{\mathbf{X}} \\
\int_0^T \theta_k(\tau)\mathbf{A}(\tau)^\top \,\mathrm{d}\tau &= -\theta_{0k}\theta_{1k}^2 \mathcal{A}'(\theta_{1k})^\top \\
\implies \int_0^T \mathbf{\Theta}(\tau)\mathbf{A}(\tau)^\top \,\mathrm{d}\tau &= \begin{bmatrix} \vdots \\ -\theta_{0k}\theta_{1k}^2 \mathcal{A}'(\theta_{1k})^\top \\ \vdots \end{bmatrix} \equiv \tilde{\mathbf{Y}}
\end{aligned}$$

We can characterize the behavior of the model as a function of risk aversion by deriving the derivatives of the equilibrium model objects with respect to a.

$$\frac{\mathrm{d}}{\mathrm{d}a}(H(\mathbf{M})) = \frac{\mathrm{d}}{\mathrm{d}a}(\mathbf{\Gamma})^\top - \left\{\frac{\mathrm{d}}{\mathrm{d}a}\left(\tilde{\mathbf{Y}}\right) - \frac{\mathrm{d}}{\mathrm{d}a}\left(\tilde{\mathbf{X}}\right)\right\}(a \cdot \mathbf{\Sigma}) - \left\{\tilde{\mathbf{Y}} - \tilde{\mathbf{X}}\right\}\mathbf{\Sigma} - \frac{\mathrm{d}}{\mathrm{d}a}(\mathbf{M}) \tag{A5}$$

Setting equation (A5) to zero implicitly defines $\frac{\mathrm{d}\mathbf{M}}{\mathrm{d}a}$ (though like equation (A3), in general the solution is a fixed point problem with no simple analytical solution).

Inductively, higher order derivatives are given by:

$$\begin{aligned}
\frac{\mathrm{d}^n}{\mathrm{d}a^n}(H(\mathbf{M})) = \frac{\mathrm{d}^n}{\mathrm{d}a^n}(\mathbf{\Gamma})^\top - \left\{\frac{\mathrm{d}^n}{\mathrm{d}a^n}\left(\tilde{\mathbf{Y}}\right) - \frac{\mathrm{d}^n}{\mathrm{d}a^n}\left(\tilde{\mathbf{X}}\right)\right\}(a \cdot \mathbf{\Sigma}) - \\
n\left\{\frac{\mathrm{d}^{n-1}}{\mathrm{d}a^{n-1}}\left(\tilde{\mathbf{Y}}\right) - \frac{\mathrm{d}^{n-1}}{\mathrm{d}a^{n-1}}\left(\tilde{\mathbf{X}}\right)\right\}\mathbf{\Sigma} - \frac{\mathrm{d}^n}{\mathrm{d}a^n}(\mathbf{M})
\end{aligned}$$

Note that

$$\begin{aligned}
\frac{\mathrm{d}}{\mathrm{d}a}(\mathcal{A}(s)) &= -\left[s\mathbf{I} + \mathbf{M}\right]^{-1} \frac{\mathrm{d}}{\mathrm{d}a}(\mathbf{M})\mathcal{A}(s) \\
\implies \frac{\mathrm{d}^n}{\mathrm{d}a^n}(\mathcal{A}(s)) &= -\left[s\mathbf{I} + \mathbf{M}\right]^{-1} \sum_{k=0}^{n-1} \binom{n}{k} \frac{\mathrm{d}^{n-k}}{\mathrm{d}a^{n-k}}(\mathbf{M}) \frac{\mathrm{d}^k}{\mathrm{d}a^k}(\mathcal{A}(s)) \\
\frac{\mathrm{d}}{\mathrm{d}a}(\mathcal{A}'(s)) &= -\left[s\mathbf{I} + \mathbf{M}\right]^{-1} \left(\frac{\mathrm{d}}{\mathrm{d}a}(\mathbf{M})\mathcal{A}'(s) + \frac{\mathrm{d}}{\mathrm{d}a}(\mathcal{A}(s))\right) \\
\implies \frac{\mathrm{d}^n}{\mathrm{d}a^n}(\mathcal{A}'(s)) &= -\left[s\mathbf{I} + \mathbf{M}\right]^{-1} \left(\frac{\mathrm{d}^n}{\mathrm{d}a^n}(\mathcal{A}(s)) + \sum_{k=0}^{n-1} \binom{n}{k} \frac{\mathrm{d}^{n-k}}{\mathrm{d}a^{n-k}}(\mathbf{M}) \frac{\mathrm{d}^k}{\mathrm{d}a^k}(\mathcal{A}'(s))\right)
\end{aligned}$$

Higher order derivatives for $\tilde{\mathbf{Y}}$ are obtained directly:

$$\frac{\mathrm{d}^n}{\mathrm{d}a^n}\left(\tilde{\mathbf{Y}}\right) = \begin{bmatrix} \vdots \\ -\theta_0^k(\theta_1^k)^2 \frac{\mathrm{d}^n}{\mathrm{d}a^n}\left(\mathcal{A}'(\theta_1^k)\right)^\top \\ \vdots \end{bmatrix}$$

For $\tilde{\mathbf{X}}$, note that:

$$\frac{\mathrm{d}^n}{\mathrm{d}a^n}\left(\left[\frac{1}{2}s\mathbf{I}+\mathbf{M}\right]\mathcal{X}(s)\right)=\left[\frac{1}{2}s\mathbf{I}+\mathbf{M}\right]\frac{\mathrm{d}^n}{\mathrm{d}a^n}(\mathcal{X}(s))+\sum_{k=0}^{n-1}\binom{n}{k}\frac{\mathrm{d}^{n-k}}{\mathrm{d}a^{n-k}}(\mathbf{M})\frac{\mathrm{d}^k}{\mathrm{d}a^k}(\mathcal{X}(s))$$

hence we can solve for $\frac{\mathrm{d}}{\mathrm{d}a}(\mathcal{X}(s))$ from

$$\left[\frac{1}{2}s\mathbf{I}+\mathbf{M}\right]\mathrm{d}^n a\left(\mathcal{X}(s)\right)+\mathrm{d}^n a\left(\mathcal{X}(s)\right)\left[\frac{1}{2}s\mathbf{I}+\mathbf{M}\right]^\top=\mathbf{e}_r\,\mathrm{d}^n a\left(\mathcal{A}(s)\right)^\top+\mathrm{d}^n a\left(\mathcal{A}(s)\right)\mathbf{e}_r^\top-\sum_{k=0}^{n-1}\binom{n}{k}\left(\frac{\mathrm{d}^{n-k}}{\mathrm{d}a^{n-k}}(\mathbf{M})\frac{\mathrm{d}^k}{\mathrm{d}a^k}(\mathcal{X}(s))+\frac{\mathrm{d}^k}{\mathrm{d}a^k}(\mathcal{X}(s))\frac{\mathrm{d}^{n-k}}{\mathrm{d}a^{n-k}}(\mathbf{M})^\top\right)$$

A.3 Localization Proofs

Definitions and terminology: In order to compare the effects of demand factors j and k, we compare their relative effects on bond prices. Suppose demand factor k is more concentrated on long-maturity bonds compared to demand factor j ($\theta_1^j > \theta_1^k$). Consider the effect of factor k on long-maturity bonds relative to its own effects on short-maturity bonds. If this relative movement is the same as factor j, then we say that demand factors have "global" effects on the yield curve. If instead the relative effect of factor k on long-maturity bonds is larger than that of factor j (and similarly, the relative effect of factor j on short-maturity bonds is larger than that of factor k), we say that demand factors have "local" effects on the yield curve.

We formalize this logic as follows. Let

$$\mathcal{B}_j(s,t)\equiv\frac{\mathcal{A}_j(s)}{\mathcal{A}_j(t)} \tag{A6}$$

This vector is the weighted average response of bond prices with Laplace frequency parameter s, relative to the weighted average response of bond prices with Laplace frequency parameter t. The weights in the Laplace transform are given by $e^{-s\tau}$, so $s > t$ implies that $\mathcal{A}_j(s)$ has more weight on short-maturity bonds than $\mathcal{A}_j(t)$. Hence, if $s > t$ and $\mathcal{B}_j(s,t) > \mathcal{B}_k(s,t)$, then we have that the j-demand factor has a relatively larger impact on short-maturity yields, compared to the k-demand factor. If $s < t$ and $\mathcal{B}_j(s,t) > \mathcal{B}_k(s,t)$, then we have that the j-demand factor has a relatively larger impact on long-maturity yields, compared to the k-demand factor.

Hence, demand factors have "global" effects if $\mathcal{B}_j(s,t) = \mathcal{B}_k(s,t)$ for all demand factors j,k and frequency weights s,t. Demand factors have "local" effects if $\mathcal{B}_j(s,t) > \mathcal{B}_k(s,t)$ for demand factors j,k such that $\theta_1^j > \theta_1^k$ and frequency weights $s > t$.

Before stating and proving our results formally, we preview and discuss the results.

Proposition 1 shows that demand shocks have global effects when arbitrageurs approach risk-neutrality ($a \to 0$) or when demand factors are risk-free ($\sigma_\beta = 0$). Proposition 1 further shows that the first-order effects of increasing risk aversion do not lead to a localization of demand shocks. That is, in a neighborhood around $a = 0$, increasing risk aversion does change the global nature of demand shocks.

Proposition 2 shows that the second-order effects of increasing risk aversion increase the localization of demand shocks. That is, for large enough values of risk aversion $a \gg 0$, demand shocks become localized. Proposition 2 also shows that with infinite risk aversion, demand shocks become fully localized. Note that this is a "discontinuous" result; the model is no longer arbitrage-free.

Assumptions:

1. The "general equilibrium" effects of imperfect arbitrage are not too large near $a = 0$: $\lim_{a\to 0} \mathrm{d}^n/\mathrm{d}a^n \, (\mathbf{\Gamma}) \approx 0$.
2. The state dynamics and correlation matrices are diagonal: $\mathbf{\Gamma} = \text{diag}\begin{bmatrix}\dots & \gamma_{j,j} & \dots\end{bmatrix}$ and $\mathbf{\Sigma} = \text{diag}\begin{bmatrix}\dots & \sigma^2_{j,j} & \dots\end{bmatrix}$.
3. Demand factors are identical besides the location of $\theta(\tau)^k$. That is, $\theta^j_0 = \theta^k_0$, $\gamma_{j,j} = \gamma_{k,k}$, and $\sigma^2_{j,j} = \sigma^2_{k,k}$ for $j, k > 1$.

Assumption 1 and 2 are for analytical tractability (and for instance hold trivially in partial equilibrium models such as Vayanos and Vila (2009)). Note that Assumption 1 does not imply that demand factors have no macroeconomic implications, but only assumes that changes in risk aversion in a neighborhood around risk-neutrality do not lead to changes in the dynamics of the model. Assumption 3 implies that besides the location in maturity space, demand factors are symmetric.

In order to simplify notation, define $\lim_{a=0} \frac{\mathrm{d}^n}{\mathrm{d}a^n}(x) \equiv \mathrm{d}_0 x$ for any model object x. Assumption 1 implies that as $a \to 0$,

$$\begin{aligned}
\mathbf{M} &\to \mathbf{\Gamma}^\top \\
\mathrm{d}_0\mathbf{M} &= \left\{\tilde{\mathbf{X}} - \tilde{\mathbf{Y}}\right\}\mathbf{\Sigma} \\
\mathrm{d}_0^n\mathbf{M} &= n\left\{\mathrm{d}_0^{n-1}\tilde{\mathbf{X}} - \mathrm{d}_0^{n-1}\tilde{\mathbf{Y}}\right\}\mathbf{\Sigma}
\end{aligned}$$

and hence we can recursively solve for all derivatives with respect to a at $a = 0$.

With these assumptions, we have that as $a \to 0$, $\mathbf{M}$ is also diagonal and so is $s\mathbf{I} + \mathbf{M}$. To simplify notation, define the vector and matrix equations

$$[\mathbf{g}(s)]_i \equiv \frac{1}{s + \gamma_{i,i}}, \quad [\mathbf{G}(s)]_{i,j} \equiv \frac{1}{s + \gamma_{i,i} + \gamma_{j,j}} \tag{A7}$$

and note that Assumption 3 implies that for all $j, k, m, n > 1$:

$$\mathbf{g}_j(s) = \mathbf{g}_k(s), \quad \mathbf{G}_{j,k}(s) = \mathbf{G}_{m,n}(s)$$

Using this notation, we have that

$$\lim_{a\to 0} \mathcal{A}(s) \equiv \mathcal{A}^0(s) = \frac{1}{s} \cdot \mathbf{g}(s) \circ \mathbf{e}_r = \left[\frac{1}{s(s+\gamma_{11})} \quad 0 \quad \dots \quad 0\right]^\top \tag{A8}$$

$$\lim_{a\to 0} \mathcal{A}'(s) \equiv \mathcal{A}^{0\prime}(s) = -\mathbf{g}(s) \circ \left[\frac{1}{s^2}\mathbf{e}_r + \mathcal{A}(s)\right] = \left[-\frac{2s+\gamma_{11}}{s^2(s+\gamma_{11})^2} \quad 0 \quad \dots \quad 0\right]^\top \tag{A9}$$

where $\circ$ denotes the Hadamard (element-wise) product. Further,

$$\mathrm{d}_0^n \mathcal{A}(s) = -\mathbf{g}(s) \circ \sum_{k=0}^{n-1} \binom{n}{k} \mathrm{d}_0^{n-k} \mathbf{M} \mathrm{d}_0^k \mathcal{A}(s) \tag{A10}$$

$$\mathrm{d}_0^n \mathcal{A}'(s) = -\mathbf{g}(s) \circ \left(\mathrm{d}_0^n \mathcal{A}(s) + \sum_{k=0}^{n-1} \binom{n}{k} \mathrm{d}_0^{n-k} \mathbf{M} \mathrm{d}_0^k \mathcal{A}'(s)\right) \tag{A11}$$

We also can characterize the limit of $\mathcal{X}(s)$:

$$\lim_{a\to 0} \mathcal{X}(s) \equiv \mathcal{X}^0(s) = \mathbf{G}(s) \circ \left(\mathbf{e}_r \mathcal{A}(s)^\top + \mathcal{A}(s)\mathbf{e}_r^\top\right) \tag{A12}$$

and recursively the derivatives are found from:

$$\mathrm{d}_0^n \mathcal{X}(s) = \mathbf{G}(s) \circ \left(\mathbf{e}_r \mathrm{d}_0^n \mathcal{A}(s)^\top + \mathrm{d}_0^n \mathcal{A}(s)\mathbf{e}_r^\top \sum_{k=0}^{n-1} \left(\mathrm{d}_0^{n-k} \mathbf{M} \mathrm{d}_0^k \mathcal{X}(s) + \mathrm{d}_0^k \mathcal{X}(s) \mathrm{d}_0^{n-k} \mathbf{M}^\top\right)\right) \tag{A13}$$

In particular, equations (A9) and (A12) imply:

$$\lim_{a\to 0} [\tilde{\mathbf{X}}]_{i,j} = \begin{cases} 2\alpha_0 \mathcal{A}_1^0(\alpha_1) \mathbf{G}_{1,1}(\alpha_1) & \text{if } i = j = 1 \\ 0 & \text{otherwise} \end{cases}$$

$$\lim_{a\to 0} [\tilde{\mathbf{Y}}]_{i,j} = \begin{cases} -\theta_0^j (\theta_1^j)^2 \mathcal{A}_1^{0\prime}(s) & \text{if } i > 1, j = 1 \\ 0 & \text{otherwise} \end{cases}$$

$$\implies [\mathrm{d}_0 \mathbf{M}]_{i,j} = \begin{cases} 2\sigma_{1,1}^2 \alpha_0 \mathcal{A}_1^0(\alpha_1) \mathbf{G}_{1,1}(\alpha_1) & \text{if } i = j = 1 \\ \sigma_{1,1}^2 \theta_0^j (\theta_1^j)^2 \mathcal{A}_1^{0\prime}(s) & \text{if } i > 1, j = 1 \\ 0 & \text{otherwise} \end{cases}$$

So $\mathrm{d}_0\mathbf{M}$ is zero everywhere except the first column, which we denote $\mathrm{d}_0\mathbf{M}_1$. Then

$$\mathrm{d}_0\mathcal{A}(s) = -\mathbf{g}(s) \circ \mathrm{d}_0\mathbf{M}_1 \cdot \mathcal{A}_1^0(s) \tag{A14}$$

$$\mathrm{d}_0\mathcal{A}'(s) = -\mathbf{g}(s) \circ \mathrm{d}_0\mathbf{M}_1 \circ \left(\mathcal{A}_1^{0\prime}(s) - \mathbf{g}(s) \cdot \mathcal{A}_1^0(s)\right) \tag{A15}$$

and

$$\mathrm{d}_0^2\mathcal{A}(s) = -\mathbf{g}(s) \circ \left(\mathrm{d}_0^2\mathbf{M}_1 \cdot \mathcal{A}_1^0(s) + 2\mathrm{d}_0\mathbf{M}_1 \cdot \mathrm{d}_0\mathcal{A}_1^0(s)\right) \tag{A16}$$

$$\mathrm{d}_0^2\mathcal{A}'(s) = -\mathbf{g}(s) \circ \left(\mathrm{d}_0^2\mathbf{M}_1 \cdot (\mathcal{A}_1^{0\prime}(s) - \mathbf{g}_1(s)\mathcal{A}_1^0(s)) + 2\mathrm{d}_0\mathbf{M}_1 \cdot (\mathrm{d}_0\mathcal{A}_1^{0\prime}(s) - \mathbf{g}_1(s)\mathrm{d}_0\mathcal{A}_1^0(s))\right) \tag{A17}$$

The following Lemma derives some useful algebraic properties of the model.

Lemma 1. *For $n \geq 2$, the ratio*

$$\frac{\mathrm{d}_0^n\mathcal{A}_j(s)}{\mathrm{d}_0\mathcal{A}_j(s)} = n\frac{\mathrm{d}_0^{n-1}\mathcal{A}_1(s)}{\mathcal{A}_1^0(s)} + \frac{\mathrm{d}_0^n\mathbf{M}_{j,1}}{\mathrm{d}_0\mathbf{M}_{j,1}} + \frac{\sum_{k=1}^{n-2}\binom{n}{k}\left[\mathrm{d}_0^{n-k}\mathbf{M}\mathrm{d}_0^k\mathcal{A}(s)\right]_j}{\mathrm{d}_0\mathbf{M}_{j,1}\mathcal{A}_1^0(s)} \tag{A18}$$

Proof. We have that

$$\frac{\mathrm{d}_0^n\mathcal{A}_j(s)}{\mathrm{d}_0\mathcal{A}_j(s)} = \frac{\left[\sum_{k=0}^{n-1}\binom{n}{k}\mathrm{d}_0^{n-k}\mathbf{M}\mathrm{d}_0^k\mathcal{A}(s)\right]_j}{\mathrm{d}_0\mathbf{M}_{j,1}\mathcal{A}_1^0(s)}$$

Since $\mathrm{d}_0\mathbf{M}$ is zero everywhere besides the first column, we have that $\mathrm{d}_0\mathbf{M}\mathbf{x}(s) = \mathrm{d}_0\mathbf{M}_1 \cdot \mathbf{x}_1(s)$ for any vector function $\mathbf{x}(s)$. Hence

$$\frac{\left[\mathrm{d}_0\mathbf{M}\mathrm{d}_0^n\mathcal{A}(s)\right]_j}{\mathrm{d}_0\mathbf{M}_{j,1}\mathcal{A}_1^0(s)} = \frac{\mathrm{d}_0^n\mathcal{A}_1(s)}{\mathcal{A}_1^0(s)}$$

which is independent of j.

Since $\mathcal{A}^0(s)$ is zero everywhere besides the first element, we have that $\mathbf{Q}\mathcal{A}^0(s) = \mathbf{Q}_1 \cdot \mathcal{A}_1^0(s)$ for any matrix $\mathbf{Q}$, where $\mathbf{Q}_1$ is the first column of $\mathbf{Q}$. Hence

$$\frac{\left[\mathrm{d}_0^n\mathbf{M}\mathcal{A}^0(s)\right]_j}{\mathrm{d}_0\mathbf{M}_{j,1}\mathcal{A}_1^0(s)} = \frac{\mathrm{d}_0^n\mathbf{M}_{j,1}}{\mathbf{M}_{j,1}}$$

which is independent of s.

In particular, equation (A18) implies that for $n = 2$, the ratio is additively separable in the demand factor index j and the Laplace frequency weight s.

□

Proposition 1 ("Global" Demand Shocks)**.** *Demand shocks have "global" effects under (near) risk-neutrality, or when demand is risk-free.*

(a) For any demand factors j, k and Laplace frequency parameters s, t, we have that

$$\lim_{a \to 0} \left(\mathcal{B}_j(s,t) - \mathcal{B}_k(s,t) \right) = 0$$

(b) Assume $\mathbf{\Sigma}_{j,j} = 0$ for all demand factors j (but $\sigma_r^2 > 0$ and $a > 0$). For any demand factors j, k and Laplace frequency parameters s, t, we have that

$$\mathcal{B}_j(s,t) = \mathcal{B}_k(s,t)$$

(c) For any demand factors j, k and Laplace frequency parameters s, t, we have that

$$\lim_{a \to 0} \frac{\mathrm{d}}{\mathrm{d}a} \left(\mathcal{B}_j(s,t) - \mathcal{B}_k(s,t) \right) = 0$$

Proof. (a) For $j > 1$, $\mathcal{A}_j(s) = 0$ when $a = 0$, so apply L'Hopital's rule to equation (A6):

$$\lim_{a \to 0} \mathcal{B}_j(s,t) = \frac{\mathrm{d}_0 \mathcal{A}_j(s)}{\mathrm{d}_0 \mathcal{A}_j(t)} \tag{A19}$$

Equation (A14) implies that the ratio

$$\frac{\mathrm{d}_0 \mathcal{A}_j(s)}{\mathrm{d}_0 \mathcal{A}_j(t)} = \frac{\mathbf{g}_j(s) \mathcal{A}_1^0(s)}{\mathbf{g}_j(t) \mathcal{A}_1^0(t)}$$

and from Assumption 3, $\mathbf{g}_j(s) = \mathbf{g}_k(s)$ for any $j > 1, k > 1$. Hence

$$\frac{\mathrm{d}_0 \mathcal{A}_j(s)}{\mathrm{d}_0 \mathcal{A}_j(t)} = \frac{\mathrm{d}_0 \mathcal{A}_k(s)}{\mathrm{d}_0 \mathcal{A}_k(t)}$$

and the result follows.

A useful corollary of this result that $\lim_{a \to 0} \mathcal{B}_j(s,t) > 0$, since $\mathcal{A}_1(s) > 0$ and $\mathbf{g}(s) > 0$ (element-wise).

(b) When demand is risk-free, $\mathbf{\Sigma}$ is zero everywhere except for the first element (equal to σ_r^2). Hence, we have that

$$a \cdot \left\{ \tilde{\mathbf{X}} - \tilde{\mathbf{Y}} \right\} \mathbf{\Sigma} = a \sigma_r^2 \cdot \left[\tilde{\mathbf{X}}_1 - \tilde{\mathbf{Y}}_1 \quad \mathbf{0} \quad \dots \quad \mathbf{0} \right]$$

where $\tilde{\mathbf{X}}_1, \tilde{\mathbf{Y}}_1$ are the first columns of $\tilde{\mathbf{X}}$ and $\tilde{\mathbf{Y}}$. Since $\mathbf{\Gamma}$ is diagonal, for any $a > 0$, $\mathbf{M} \equiv \mathbf{\Gamma}^\top + a \cdot \left\{ \tilde{\mathbf{X}} - \tilde{\mathbf{Y}} \right\} \mathbf{\Sigma}$ is zero everywhere except the first column and diagonal.

Therefore, the $j > 1$ element of $\mathcal{A}(s)$ is given by

$$\mathcal{A}_j(s) = \frac{1}{s}\left[(s\mathbf{I} + \mathbf{M})^{-1}\right]_{j,1} = \frac{a\sigma_r^2(\tilde{\mathbf{Y}}_{j,1} - \tilde{\mathbf{X}}_{j,1})}{s(s+\gamma_{j,j})(s+\gamma_{1,1}+a\sigma_r^2\tilde{\mathbf{X}}_{1,1})}$$
$$\implies \mathcal{B}_j(s,t) = \frac{t(t+\gamma_{j,j})(t+\gamma_{1,1}+a\sigma_r^2\tilde{\mathbf{X}}_{1,1})}{s(s+\gamma_{j,j})(s+\gamma_{1,1}+a\sigma_r^2\tilde{\mathbf{X}}_{1,1})}$$

Then the result follows since $\gamma_{j,j} = \gamma_{k,k}$ for $j, k > 1$ (by Assumption 3).

(c) Differentiating equation (A6) (and applying L'Hopital's rule and removing terms equal to zero in the limit) gives

$$\mathrm{d}_0\mathcal{B}_j(s,t) = \frac{\mathrm{d}_0^2\mathcal{A}_j(s)\mathrm{d}_0\mathcal{A}_j(t) - \mathrm{d}_0^2\mathcal{A}_j(t)\mathrm{d}_0\mathcal{A}_j(s)}{2\mathrm{d}_0\mathcal{A}_j(t)^2}$$

Equation (A19) and the corollary from the proof of (a) implies

$$\lim_{a\to 0}\mathcal{B}_j(s,t) = \frac{\mathrm{d}_0\mathcal{A}_j(t)}{\mathrm{d}_0\mathcal{A}_j(s)} = \frac{\mathrm{d}_0\mathcal{A}_k(t)}{\mathrm{d}_0\mathcal{A}_k(s)} = \lim_{a\to 0}\mathcal{B}_k(s,t) > 0$$

Hence

$$\frac{\mathrm{d}_0\mathcal{A}_j(t)}{\mathrm{d}_0\mathcal{A}_j(s)}\mathrm{d}_0\mathcal{B}_j(s,t) = \frac{1}{2}\left(\frac{\mathrm{d}_0^2\mathcal{A}_j(s)}{\mathrm{d}_0\mathcal{A}_j(s)} - \frac{\mathrm{d}_0^2\mathcal{A}_j(t)}{\mathrm{d}_0\mathcal{A}_j(t)}\right)$$
$$\frac{\mathrm{d}_0\mathcal{A}_j(t)}{\mathrm{d}_0\mathcal{A}_j(s)}\mathrm{d}_0\mathcal{B}_k(s,t) = \frac{1}{2}\left(\frac{\mathrm{d}_0^2\mathcal{A}_k(s)}{\mathrm{d}_0\mathcal{A}_k(s)} - \frac{\mathrm{d}_0^2\mathcal{A}_k(t)}{\mathrm{d}_0\mathcal{A}_k(t)}\right)$$

From the Lemma 1, we have that

$$\frac{1}{2}\frac{\mathrm{d}_0^2\mathcal{A}_j(s)}{\mathrm{d}_0\mathcal{A}_j(s)} = \frac{1}{2}\frac{\mathrm{d}_0^2\mathbf{M}_{j,1}}{\mathrm{d}_0\mathbf{M}_{j,1}} + \frac{\mathrm{d}_0\mathcal{A}_1(s)}{\mathcal{A}_1^0(s)}$$

which is additively separable in terms which are a function of j and s. The result follows.

□

Proposition 2 ("Localized" Demand Shocks)**.** *Demand shocks have "local" effects far from risk-neutrality, and are fully localized under infinite risk aversion.*

(a) Suppose $\mathbf{\Sigma}_{j,j} > 0$. For any demand factors j, k and Laplace frequency parameters s, t, we have that

$$\lim_{a\to 0}\operatorname{sgn}\frac{\mathrm{d}^2}{\mathrm{d}a^2}(\mathcal{B}_j(s,t) - \mathcal{B}_k(s,t)) = \operatorname{sgn}(s-t)(\theta_1^j - \theta_1^k)$$

(b) When risk aversion $a = \infty$:

$$\frac{\mathrm{d}\log P_t^{(\tau)}}{\mathrm{d}\beta_t^k} = \frac{\theta^k(\tau)}{\alpha(\tau)}, \quad \frac{\mathrm{d}\log P_t^{(\tau)}}{\mathrm{d}r_t} = 0$$

Proof. (a) Differentiating equation (A6) (and applying L'Hopital's rule and removing terms equal to zero in the limit) gives

$$\mathrm{d}_0^2\mathcal{B}_j(s,t) = \frac{1}{6\mathrm{d}_0\mathcal{A}_j(t)^3}\left(3\mathrm{d}_0^2\mathcal{A}_j(t)^2\mathrm{d}_0\mathcal{A}_j(s) - 3\mathrm{d}_0^2\mathcal{A}_j(s)\mathrm{d}_0^2\mathcal{A}_j(t)\mathrm{d}_0\mathcal{A}_j(t) + 2\mathrm{d}_0^3\mathcal{A}_j(s)\mathrm{d}_0\mathcal{A}_j(t)^2 - 2\mathrm{d}_0^3\mathcal{A}_j(t)\mathrm{d}_0\mathcal{A}_j(t)\mathrm{d}_0\mathcal{A}_j(s)\right)$$

Using the results from Prop 1, we can scale and rewrite as

$$\frac{\mathrm{d}_0\mathcal{A}_j(t)}{\mathrm{d}_0\mathcal{A}_j(s)}\mathrm{d}_0^2\mathcal{B}_j(s,t) = \frac{1}{3}\left(\frac{\mathrm{d}_0^3\mathcal{A}_j(s)}{\mathrm{d}_0\mathcal{A}_j(s)} - \frac{\mathrm{d}_0^3\mathcal{A}_j(t)}{\mathrm{d}_0\mathcal{A}_j(t)}\right) + \frac{1}{2}\left(\frac{\mathrm{d}_0^2\mathcal{A}_j(t)}{\mathrm{d}_0\mathcal{A}_j(t)}\right)\left(\frac{\mathrm{d}_0^2\mathcal{A}_j(t)}{\mathrm{d}_0\mathcal{A}_j(t)} - \frac{\mathrm{d}_0^2\mathcal{A}_j(s)}{\mathrm{d}_0\mathcal{A}_j(s)}\right)$$
$$\frac{\mathrm{d}_0\mathcal{A}_j(t)}{\mathrm{d}_0\mathcal{A}_j(s)}\mathrm{d}_0^2\mathcal{B}_k(s,t) = \frac{1}{3}\left(\frac{\mathrm{d}_0^3\mathcal{A}_k(s)}{\mathrm{d}_0\mathcal{A}_k(s)} - \frac{\mathrm{d}_0^3\mathcal{A}_k(t)}{\mathrm{d}_0\mathcal{A}_k(t)}\right) + \frac{1}{2}\left(\frac{\mathrm{d}_0^2\mathcal{A}_k(t)}{\mathrm{d}_0\mathcal{A}_k(t)}\right)\left(\frac{\mathrm{d}_0^2\mathcal{A}_j(t)}{\mathrm{d}_0\mathcal{A}_j(t)} - \frac{\mathrm{d}_0^2\mathcal{A}_j(s)}{\mathrm{d}_0\mathcal{A}_j(s)}\right)$$

and note that the final parenthetical term in each expression is identical (from Prop 3).

Focusing on the third-order terms, from Lemma 1 we have that

$$\frac{1}{3}\frac{\mathrm{d}_0^3\mathcal{A}_j(s)}{\mathrm{d}_0\mathcal{A}_j(s)} = \frac{\mathrm{d}_0^2\mathcal{A}_1(s)}{\mathcal{A}_1^0(s)} + \frac{1}{3}\frac{\mathrm{d}_0^3\mathbf{M}_{j,1}}{\mathbf{M}_{j,1}} + \frac{\left[\mathrm{d}_0^2\mathbf{M}\mathrm{d}_0\mathcal{A}(s)\right]_j}{\mathrm{d}_0\mathbf{M}_{j,1}\mathcal{A}_1^0(s)}$$

The final term in the sum can be written

$$\frac{\left[\mathrm{d}_0^2\mathbf{M}\mathrm{d}_0\mathcal{A}(s)\right]_j}{\mathrm{d}_0\mathbf{M}_{j,1}\mathcal{A}_1^0(s)} = \sum_{m=1}^{J}\left[\frac{\left[\mathrm{d}_0^2\mathbf{M}\right]_{j,m}}{\mathrm{d}_0\mathbf{M}_{j,1}}\right]\cdot\left[\frac{\mathrm{d}_0\mathcal{A}_m(s)}{\mathcal{A}_1^0(s)}\right] \equiv \mathbf{u}_j^\top\mathbf{v}(s)$$

and hence

$$\frac{1}{3}\left(\frac{\mathrm{d}_0^3\mathcal{A}_j(s)}{\mathrm{d}_0\mathcal{A}_j(s)} - \frac{\mathrm{d}_0^3\mathcal{A}_j(t)}{\mathrm{d}_0\mathcal{A}_j(t)}\right) - \frac{1}{3}\left(\frac{\mathrm{d}_0^3\mathcal{A}_k(s)}{\mathrm{d}_0\mathcal{A}_k(s)} - \frac{\mathrm{d}_0^3\mathcal{A}_k(t)}{\mathrm{d}_0\mathcal{A}_k(t)}\right) = \left[\mathbf{u}_j - \mathbf{u}_k\right]^\top\left[\mathbf{v}(s) - \mathbf{v}(t)\right]$$

Further, from Lemma 1,

$$\begin{aligned}\left(\frac{\mathrm{d}_0^2\mathcal{A}_j(t)}{\mathrm{d}_0\mathcal{A}_j(t)} - \frac{\mathrm{d}_0^2\mathcal{A}_k(t)}{\mathrm{d}_0\mathcal{A}_k(t)}\right) &= \frac{\mathrm{d}_0^2\mathbf{M}_{j,1}}{\mathrm{d}_0\mathbf{M}_{j,1}} - \frac{\mathrm{d}_0^2\mathbf{M}_{k,1}}{\mathrm{d}_0\mathbf{M}_{k,1}} \\ &\equiv [\mathbf{u}_j - \mathbf{u}_k]_1 \\ \frac{1}{2}\left(\frac{\mathrm{d}_0^2\mathcal{A}_j(t)}{\mathrm{d}_0\mathcal{A}_j(t)} - \frac{\mathrm{d}_0^2\mathcal{A}_j(s)}{\mathrm{d}_0\mathcal{A}_j(s)}\right) &= \frac{\mathrm{d}_0\mathcal{A}_1(t)}{\mathcal{A}_1^0(t)} - \frac{\mathrm{d}_0\mathcal{A}_1(s)}{\mathcal{A}_1^0(s)} \\ &\equiv -[\mathbf{v}(s) - \mathbf{v}(t)]_1\end{aligned}$$

Therefore, we have that

$$\frac{\mathrm{d}_0\mathcal{A}_j(t)}{\mathrm{d}_0\mathcal{A}_j(s)}\left(\mathrm{d}_0^2\mathcal{B}_j(s,t) - \mathrm{d}_0^2\mathcal{B}_k(s,t)\right) = \sum_{m=2}^{J}[\mathbf{u}_j - \mathbf{u}_k]_m[\mathbf{v}(s) - \mathbf{v}(t)]_m$$

Dealing with each vector separately: first, we have that

$$\begin{aligned}\mathbf{v}(s) = \frac{\mathrm{d}_0\mathcal{A}(s)}{\mathcal{A}_1^0(s)} &= -\mathbf{g}(s) \circ \mathrm{d}_0\mathbf{M}_1 \\ \implies \mathbf{v}(s) - \mathbf{v}(t) &= -\mathrm{d}_0\mathbf{M}_1 \circ (\mathbf{g}(s) - \mathbf{g}(t))\end{aligned}$$

Next, the j, m element of $\mathrm{d}_0^2\mathbf{M}$ is

$$[\mathrm{d}_0^2\mathbf{M}]_{j,m} = \left(\alpha_0[\mathrm{d}_0\mathbf{X}]_{j,m} + \theta_0^j(\theta_1^j)^2\mathrm{d}_0\mathcal{A}'_m(\theta_1^j)\right)\sigma^2_{m,m}$$

(and recall that $\theta_0^1 = 0$). We have that

$$\begin{aligned}\frac{[\mathrm{d}_0\mathbf{X}]_{j,m}}{\mathrm{d}\mathbf{M}_{j,1}} &= \begin{cases} -\left(\mathbf{g}_j(\alpha_1)\mathcal{A}_1^0(\alpha_1) + \mathcal{X}_{1,1}^0(\alpha_1)\right)\mathbf{S}_{j,1}(\alpha_1) & \text{if } m = 1 \\ 0 & \text{otherwise} \end{cases} \\ &= \frac{[\mathrm{d}_0\mathbf{X}]_{k,m}}{\mathrm{d}\mathbf{M}_{k,1}}\end{aligned}$$

where the second equality follows from Assumption 3.

Recall $\mathrm{d}_0\mathbf{M}_{j,1} = \sigma_r^2\theta_0^j(\theta_1^j)^2[\mathrm{d}_0\mathcal{A}'(\theta_1^j)]_1$, hence we can write

$$\begin{aligned}-\frac{\theta_0^j(\theta_1^j)^2}{\mathrm{d}\mathbf{M}_{j,1}}\mathrm{d}_0\mathcal{A}'(\theta_1^j) &= -\mathrm{d}_0\mathbf{M}_1 \circ \mathbf{g}(\theta_1^j) \circ \left(1 + \mathbf{g}(\theta_1^j)\frac{\theta_1^j}{1 + \theta_1^j\mathbf{g}_1(\theta_1^j)}\right) \\ &\equiv -\mathrm{d}_0\mathbf{M}_1 \circ \mathbf{h}(\theta_1^j)\end{aligned}$$

Therefore,

$$[\mathbf{u}_j - \mathbf{u}_k] = -\mathrm{d}_0\mathbf{M}_1 \circ \left(\mathbf{h}(\theta_1^j) - \mathbf{h}(\theta_1^k)\right)$$

which implies

$$[\mathbf{u}_j - \mathbf{u}_k] \circ [\mathbf{v}(s) - \mathbf{v}(t)] = (\mathrm{d}_0\mathbf{M}_1)^2 \circ (\mathbf{h}(\theta_1^j) - \mathbf{h}(\theta_1^k)) \circ (\mathbf{g}(s) - \mathbf{g}(t))$$

Hence, the sign of any element of the above vector is determined by the (element-wise) behavior of the functions $\mathbf{g}, \mathbf{h}$. From equation (A7), the function $\mathbf{g}_m(s)$ is decreasing in s for any element m. Further,

$$\begin{aligned} \mathbf{h}_m(x) &= \frac{3x^2 + 2(\gamma_{m,m} + \gamma_{1,1}) + \gamma_{m,m}\gamma_{1,1}}{(x + \gamma_{m,m})^2(2x + \gamma_{1,1})} \\ \implies \mathbf{h}'_m(x) &= -\frac{2x(x + \gamma_{1,1})(\gamma_{1,1} + \gamma_{m,m} + 3x)}{(x + \gamma_{m,m})^3(2x + \gamma_{1,1})^2} \end{aligned}$$

so $\mathbf{h}_m(x)$ is also decreasing in x for any element m. Thus, we have that

$$\operatorname{sgn}\left[(\mathbf{h}_m(\theta_1^j) - \mathbf{h}_m(\theta_1^k)) \cdot (\mathbf{g}_m(s) - \mathbf{g}_m(t))\right] = \operatorname{sgn}(\theta_1^j - \theta_1^k) \cdot (s - t)$$

and therefore the sum over the $m \geq 2$ elements has the same sign. The result follows.

(b) If $a = \infty$, arbitrageurs invest their entire wealth in the risk-free rate and hence hold no long-maturity bonds: $X_t^{(\tau)} = 0$ for all τ and t. Thus market clearing implies that habitat investors also take zero positions: $Z_t^{(\tau)} = 0$. Thus, the results follow from differentiating equation (6) with respect to any demand factor β_t^k or short rate r_t and setting to zero.

□

Appendix B Numerical Calibration Details

In this section we briefly describe the model and calibration of our numerical exercise.

B.1 Numerical Exercise Calibration

In our numerical model, we have that

$$\mathbf{y}_t = \begin{bmatrix} r_t \\ \beta_t^s \\ \beta_t^\ell \end{bmatrix}, \quad \mathbf{x}_t = \begin{bmatrix} \pi_t \\ x_t \end{bmatrix}, \quad \boldsymbol{\sigma} = \begin{bmatrix} \sigma_r & 0 & 0 \\ 0 & \sigma_{\beta^s} & 0 \\ 0 & 0 & \sigma_{\beta^\ell} \end{bmatrix}$$

The dynamics matrix is given by

$$\boldsymbol{\Upsilon} = \begin{bmatrix} \kappa_r & 0 & 0 & -\kappa_r\phi_\pi & -\kappa_r\phi_x \\ \phi_{r,\beta} & \kappa_\beta & 0 & 0 & 0 \\ \phi_{r,\beta} & 0 & \kappa_\beta & 0 & 0 \\ 0 & 0 & 0 & -\rho & \delta \\ -\varsigma^{-1}\hat{A}_r & -\varsigma^{-1}\hat{A}_{\beta^s}(\tau) & -\varsigma^{-1}\hat{A}_{\beta^\ell}(\tau) & \varsigma^{-1} & 0 \end{bmatrix} \tag{B1}$$

where

$$\hat{\mathbf{A}} \equiv \int_0^T \frac{\eta(\tau)}{\tau}\mathbf{A}(\tau)\,\mathrm{d}\tau \tag{B2}$$

This implies that the effective borrowing rate $\tilde{r}_t = \mathbf{y}_t^\top \hat{\mathbf{A}}$. Note that these coefficients are equilibrium (fixed point) objects.

B.2 Regression coefficients

Fama and Bliss (1987) perform the regression

$$\frac{1}{\Delta\tau}\log\left(\frac{P_{t+\Delta\tau}^{(\tau-\Delta\tau)}}{P_t^{(\tau)}}\right) - y_t^{(\Delta\tau)} = \alpha_{FB}^{(\tau)} + \beta_{FB}^{(\tau)}\left(f_t^{(\tau-\Delta\tau,\tau)} - y_t^{(\Delta\tau)}\right) + e_{t+\Delta\tau}^{(\tau)} \tag{B3}$$

The dependent variable is the log return on a zero-coupon bond with maturity τ held over a period $\Delta\tau$, in excess of the spot rate for maturity $\Delta\tau$. The independent variable is the slope of the term structure as measured by the difference between the forward rate between maturities $\tau - \Delta\tau$ and τ $f_t^{(\tau-\Delta\tau,\tau)}$, and the spot rate for maturity $\Delta\tau$.

Campbell and Shiller (1991) perform the regression

$$y_{t+\Delta\tau}^{(\tau-\Delta\tau)} - y_t^{(\tau)} = \alpha_{CS}^{(\tau)} + \beta_{CS}^{(\tau)}\frac{\Delta\tau}{\tau-\Delta\tau}\left(y_t^{(\tau)} - y_t^{(\Delta\tau)}\right) + e_{t+\Delta\tau} \tag{B4}$$

The dependent variable is the change, between times t and $t+\Delta\tau$, in the yield of a zero-coupon bond that has maturity τ at time t. The independent variable is the difference between the spot rates for maturities τ and $\Delta\tau$, normalized so that the regression coefficient β_{CS} is equal to one under the EH. CS find that β_{CS} is smaller than one, negative for most τ, and decreasing in τ.

Following Vayanos and Vila (2009), as $\Delta\tau \to 0$, the FB and CS regression coefficients in the model are given by:

$$\beta_{FB}^{(\tau)} \to \frac{\left[(\mathbf{M}-\boldsymbol{\Gamma}^\top)\mathbf{A}(\tau)\right]^\top \boldsymbol{\Sigma}^\infty \left[\mathbf{M}\mathbf{A}(\tau)\right]}{\left[\mathbf{M}\mathbf{A}(\tau)\right]^\top \boldsymbol{\Sigma}^\infty \left[\mathbf{M}\mathbf{A}(\tau)\right]} \tag{B5}$$

$$\beta_{CS}^{(\tau)} \to \frac{\left[\mathbf{A}(\tau)/\tau - (\boldsymbol{\Gamma}^\top - \mathbf{M})\mathbf{A}(\tau) - \mathbf{e}_r\right]^\top \boldsymbol{\Sigma}^\infty \left[\mathbf{A}(\tau)/\tau - \mathbf{e}_r\right]}{\left[\mathbf{A}(\tau)/\tau - \mathbf{e}_r\right]^\top \boldsymbol{\Sigma}^\infty \left[\mathbf{A}(\tau)/\tau - \mathbf{e}_r\right]} \tag{B6}$$

where $\mathbf{\Gamma}$ is from equation (A1) and $\mathbf{\Sigma}^{\infty}$ is the long-run (unconditional) variance of the state variables:

$$\begin{aligned} Var[\mathbf{y}_t] &= vec^{-1}\left[(\mathbf{\Gamma} \oplus \mathbf{\Gamma})^{-1} vec(\mathbf{\Sigma})\right] \equiv \mathbf{\Sigma}^{\infty} \\ Cov[\mathbf{y}_{t+s}, \mathbf{y}_t] &= \exp(-\mathbf{\Gamma} s)\mathbf{\Sigma}^{\infty} \end{aligned}$$

where $\oplus$ is the Kronecker sum. Note that under risk neutrality ($a = 0$), the matrices $\mathbf{M} = \mathbf{\Gamma}^{\top}$ so equation (B5) is equal to zero and (B6) is equal to 1 for all maturities τ. That is, the Expectations Hypothesis holds, and the slope of the term structure does not predict excess returns.

B.3 Moment-Matching Exercise

We estimate the unknown parameters to minimize the distance between the model-implied and empirical FB and CS regression coefficients. Given empirical estimates $\left\{\hat{\beta}_{FB}^{(\tau)}, \hat{\beta}_{CS}^{(\tau)}\right\}_{\tau=1}^{30}$ and combining the unknown parameters into a vector $\boldsymbol{\zeta}$, we conduct the following constrained minimization problem:

$$\min_{\boldsymbol{\zeta}, \mathbf{M}} \quad \sum_{\tau=1}^{30} \left(\hat{\beta}_{FB}^{(\tau)} - \beta_{FB}^{(\tau)}\right)^2 + \left(\hat{\beta}_{CS}^{(\tau)} - \beta_{CS}^{(\tau)}\right)^2 \tag{B7}$$

$$\text{s.t.} \quad H(\mathbf{M}; \boldsymbol{\zeta}) = \mathbf{0} \tag{B8}$$

where H characterizes the equilibrium of the model (defined by (A3)) and where we have made explicit the dependence on the unknown parameters $\boldsymbol{\zeta}$. Note that evaluating equations (B7) and (B8) at some set of points $\boldsymbol{\zeta}, \mathbf{M}$ involves the following computations:

1. Construct $\hat{\mathbf{A}}$ and $\mathbf{\Upsilon}$ from $\boldsymbol{\zeta}, \mathbf{M}$ in equations (B1) and (B2).
2. Compute the eigendecomposition of $\mathbf{\Upsilon}$ and form $\mathbf{\Gamma}$ from equation (A2).
3. Construct the model-implied coefficients from equations (B5) and (B6).
4. Compute the loss function (B7).
5. Compute the left-hand-side of the equilibrium root function (B8) (H, defined by (A3)).

Note that this approach chooses the unknown structural parameters $\boldsymbol{\zeta}$ and the endogenous parameters $\mathbf{M}$ jointly. The constraint (B8) imposes the equilibrium conditions of the model. Hence, our moment-matching exercise consists of minimizing the objective function (B7), subject to the equality constraints (B8). Finding a local solution is straightforward using off-the-shelf nonlinear constrained optimization algorithms. However, equations (B7) and (B8) are highly nonlinear and there is no reason to expect a local

minimization routine to converge to the global solution. Therefore, we use a global two-step basin hopping routine to find the global minimum. The routine consists of repeated local searches, where the starting points are chosen as stochastic perturbations from the previous local minimum. When a minimum is found that improves upon the previous minimum, this is taken as the new starting point. The algorithm also stochastically accepts minima which are not improvements over the previous minimum, which enhances the ability of the algorithm to jump away from areas of the parameter space with only local minima.

For our problem, the algorithm is as follows:

1. Initialize $\boldsymbol{\zeta}^0, \mathbf{M}^0$.
2. Given points $\boldsymbol{\zeta}^i, \mathbf{M}^i$, construct initial points $\widetilde{\boldsymbol{\zeta}}^i, \widetilde{\mathbf{M}}^i$ by stochastic perturbation. Find a minima $\widehat{\boldsymbol{\zeta}}, \widehat{\mathbf{M}}$ using a local constrained optimization routine.
3. Apply an acceptance test to $\widehat{\boldsymbol{\zeta}}, \widehat{\mathbf{M}}$ as a function of the value of the objective function compared to the previous minima. If accepted, set $\boldsymbol{\zeta}^{i+1} = \widehat{\boldsymbol{\zeta}}, \mathbf{M}^{i+1} = \widehat{\mathbf{M}}$. If not, keep $\boldsymbol{\zeta}^{i+1} = \boldsymbol{\zeta}^i, \mathbf{M}^{i+1} = \mathbf{M}^i$.
4. Record the global minimum from the set of local minima $\left\{\boldsymbol{\zeta}^i, \mathbf{M}^i\right\}$.
5. If no improvements to the global minimum have occurred in the previous I iterations, stop. Otherwise, return to step 2.

We estimate FB and CS coefficients separately for the non-crisis and crisis subsamples, for maturities $\tau = 1$ to 30 years. We use Gürkaynak et al. (2007) zero-coupon Treasury yields at the monthly frequency to estimate equations (B3) and (B4). In the non-crisis subsample, our unknown parameters consist of $\hat{\boldsymbol{\zeta}}^{NC} = \left[\hat{\kappa}_\beta^{NC} \quad \hat{\phi}_{r,\beta}^{NC} \quad \widehat{a\sigma^2 \cdot \alpha_0}^{NC} \quad \widehat{a\sigma^2 \cdot \theta_0}^{NC}\right]$. In the crisis sample, we fix the estimates of $\hat{\kappa}_\beta, \hat{\phi}_{r,\beta}$ to the values from the non-crisis sample and only re-estimate the risk-adjusted parameters $\hat{\boldsymbol{\zeta}}^{C} = \left[\widehat{a\sigma^2 \cdot \alpha_0}^{C} \quad \widehat{a\sigma^2 \cdot \theta_0}^{C}\right]$. The results are reported in Panels C and D of Table 5.

Appendix C Additional Figures and Tables

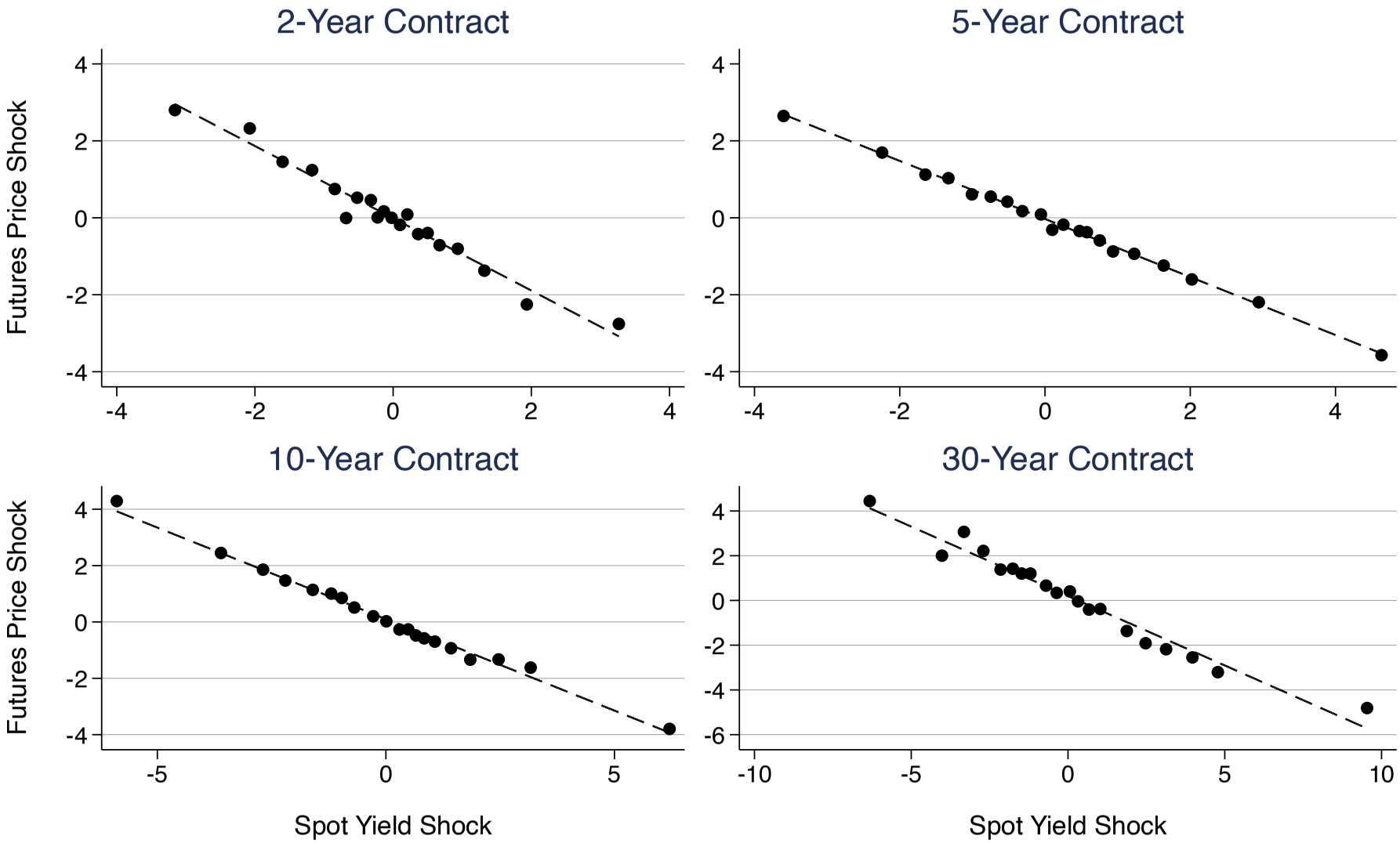

Figure C1: Demand Shock Comparison: Spot Yields and Futures

Notes: Comparison of intra-day changes in secondary market Treasury yields and Treasury futures, constructed using the same windows as described in equation (1). See Gorodnichenko and Ray (2017) for a detailed discussion of Treasury futures.

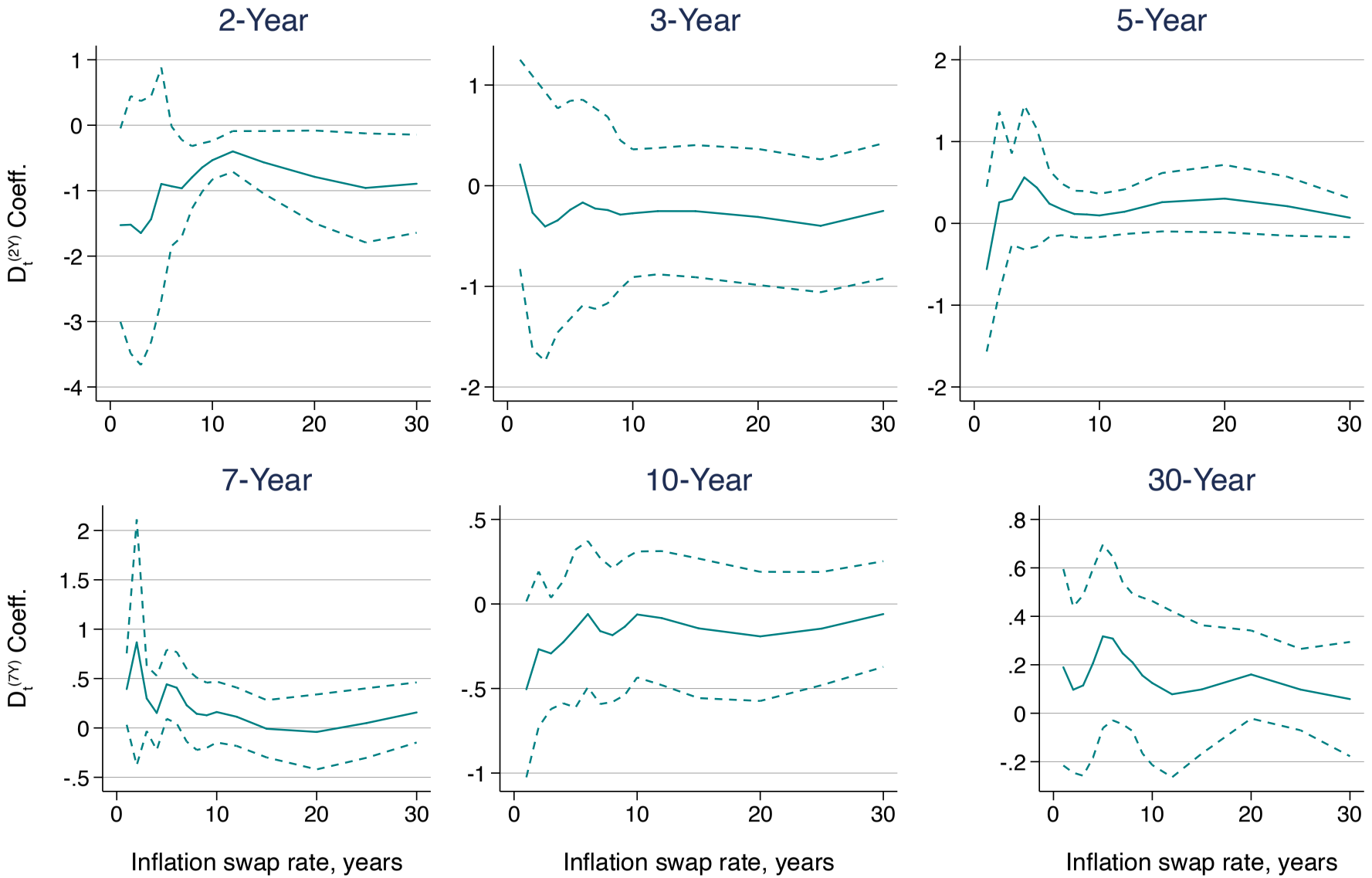

Figure C2: Inflation Swap Rates and Demand Shocks

Notes: Regressions of inflation swap rate changes on demand shocks $D_t^{(m)}$, run separately by maturities $m = 2, 3, 5, 7, 10, 30$ years. The solid line represents point estimates for inflation swaps of years $y = 1, \ldots, 30$; dotted lines denote 2-standard error (Newey-West, 9 lags) confidence intervals.

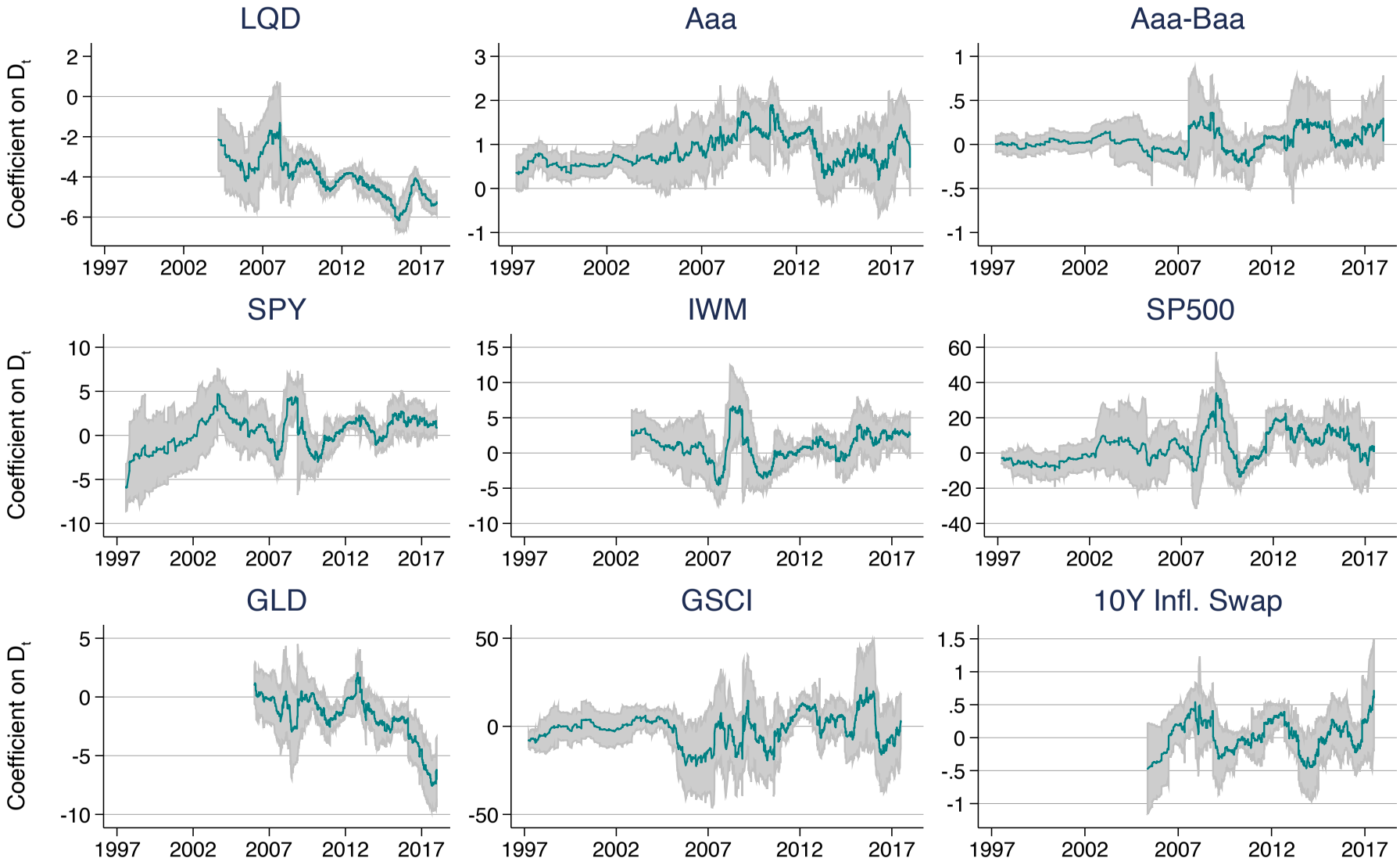

Figure C3: Rolling Regressions, Asset Prices

Notes: Rolling coefficient estimates of asset prices on auction demand shocks D_t (pooled across maturities). Each data point is from rolling estimates of the regressions reported in Table 4, using the 60 most recent auctions.

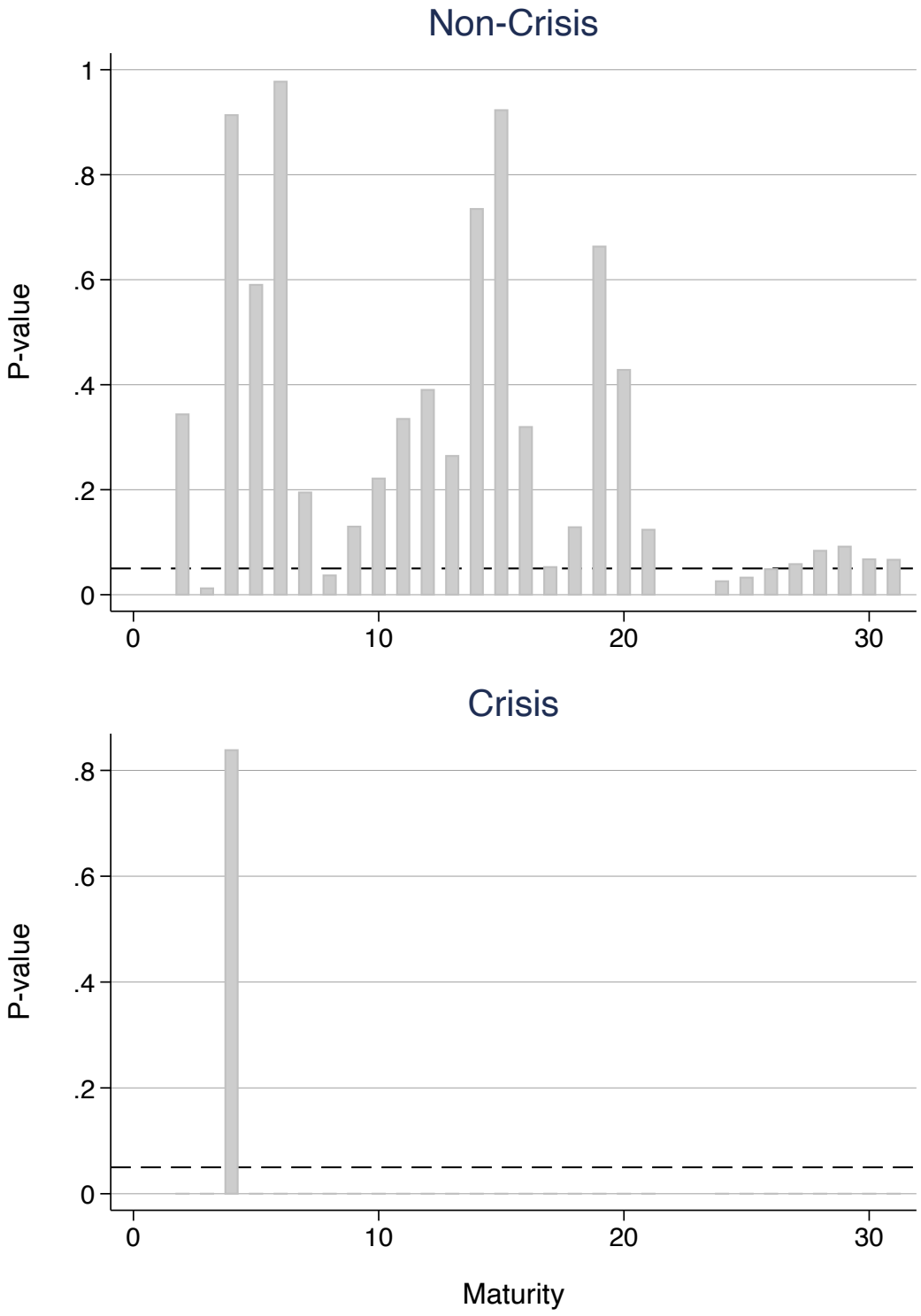

Figure C4: Model-Implied Preferred Habitat Coefficients, P-Values

Notes: P-values testing equality of coefficients from Figure 10.

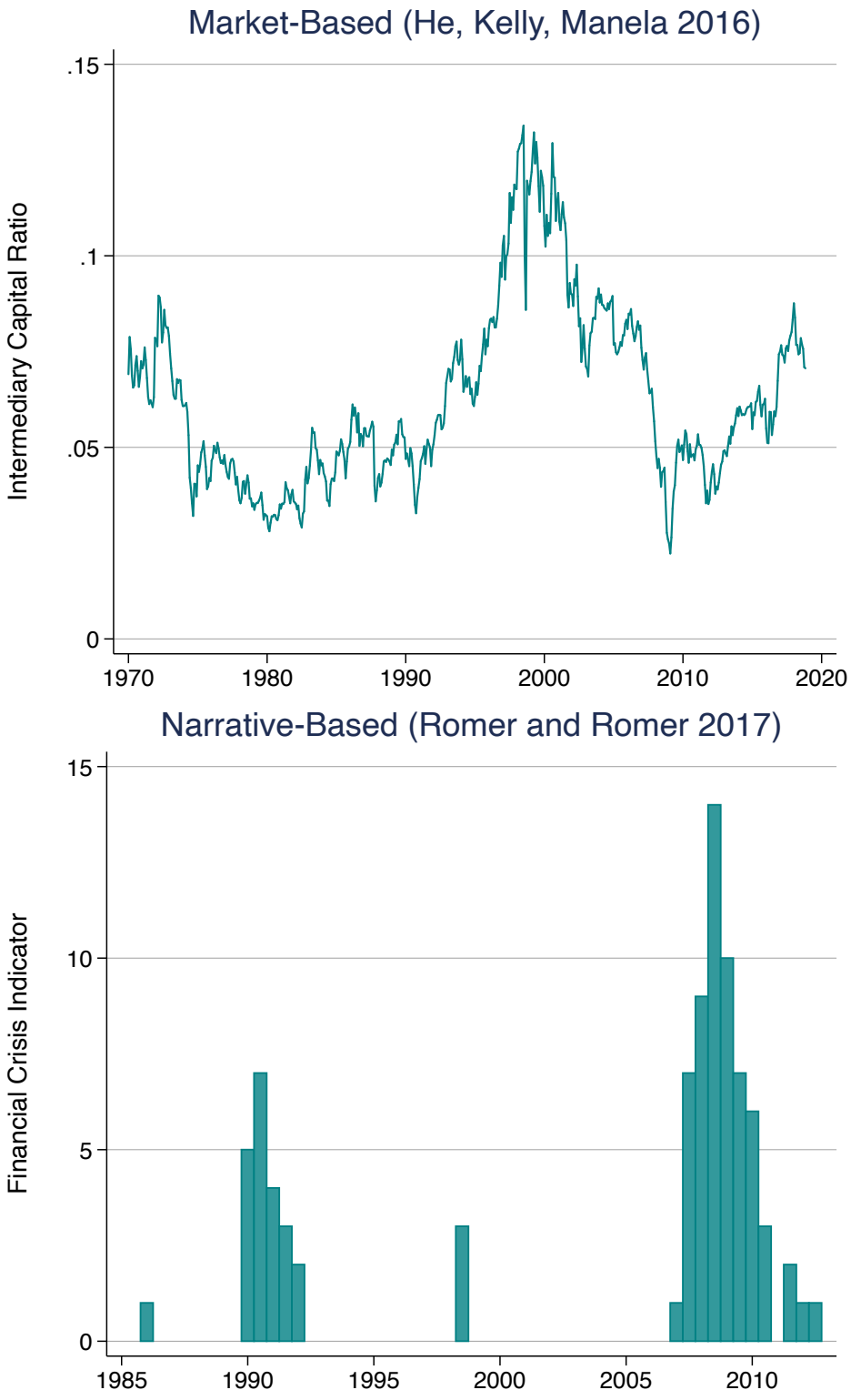

Figure C5: Alternative Measures of Financial Crises

Notes: Alternative measures of financial crises from He et al. (2016) (top panel) and Romer and Romer (2017) (bottom panel).

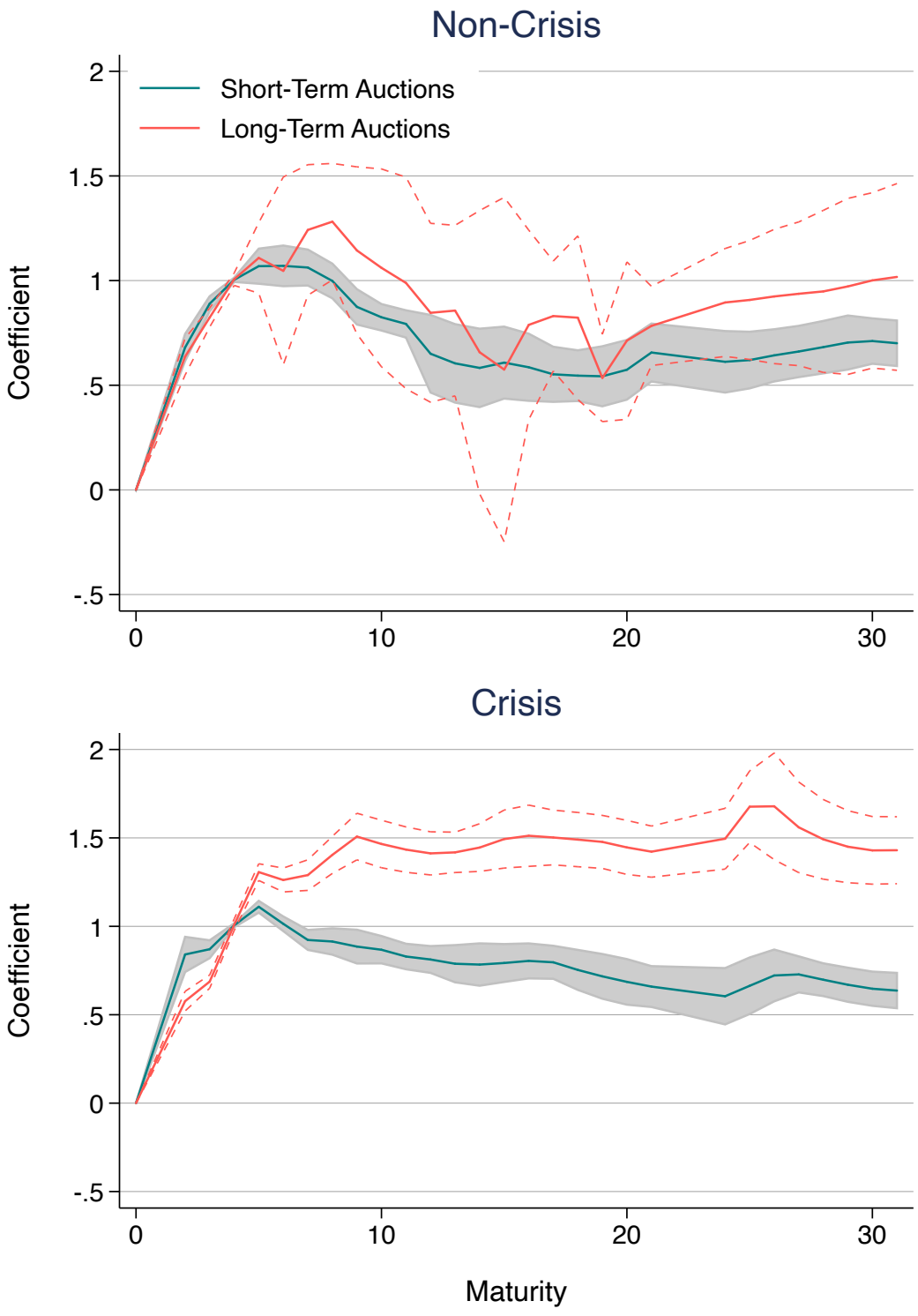

Figure C6: Localization Robustness: Market-Based Crises

Notes: Estimates of regression equation (15), identifying financial crises as periods in which the aggregate capital ratio from He et al. (2016) is low (≤ 0.055).

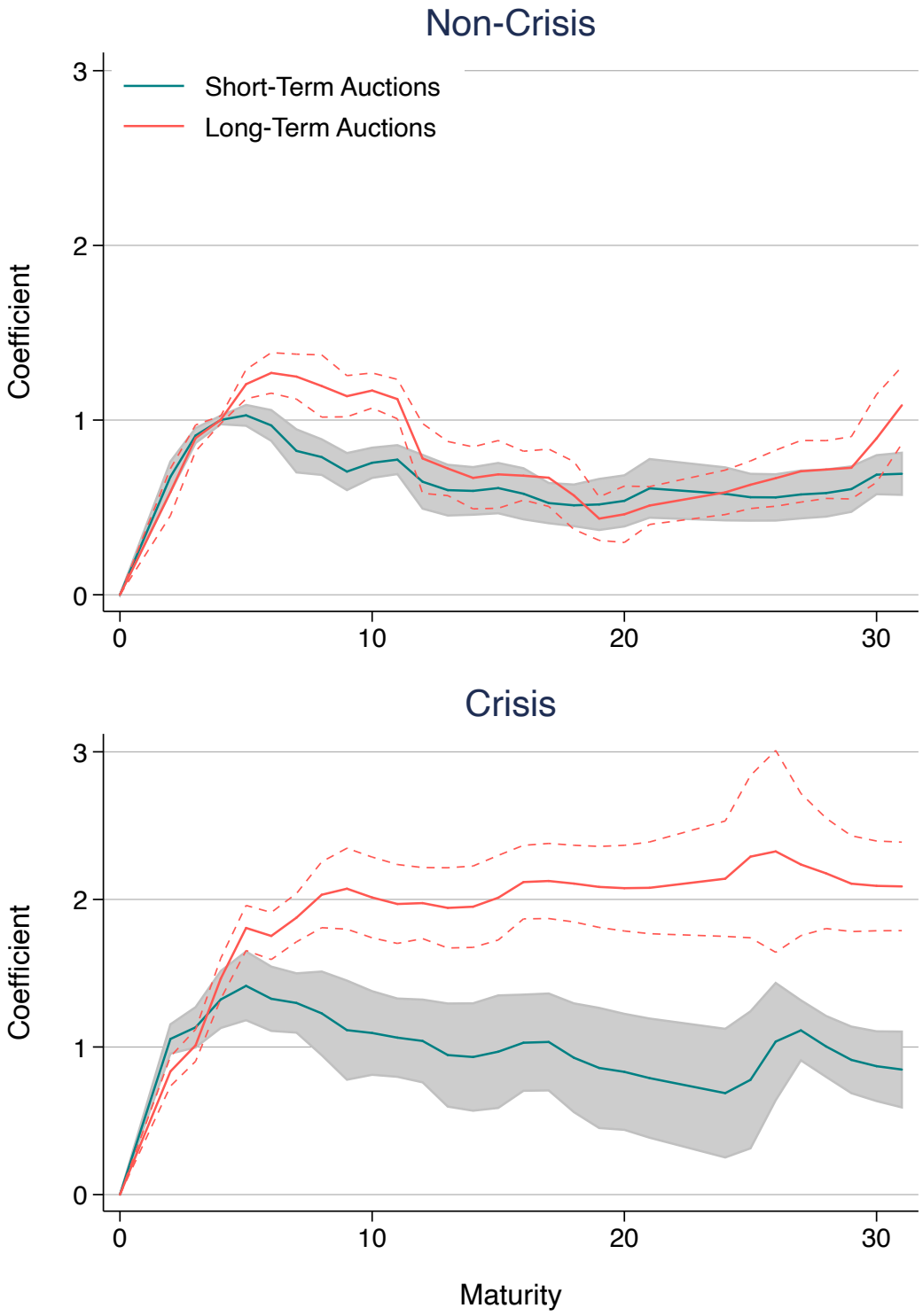

Figure C7: Localization Robustness: Market-Based Crises (Continuous)

Notes: Alternative specification of regression equation (15), where the crisis measure is treated as continuous (as measured by the aggregate capital ratio from He et al. (2016)). The measure is transformed to range from 0 to 1, and truncated so that values below 0.04 are set to 1 while values above 0.075 are set to 0.

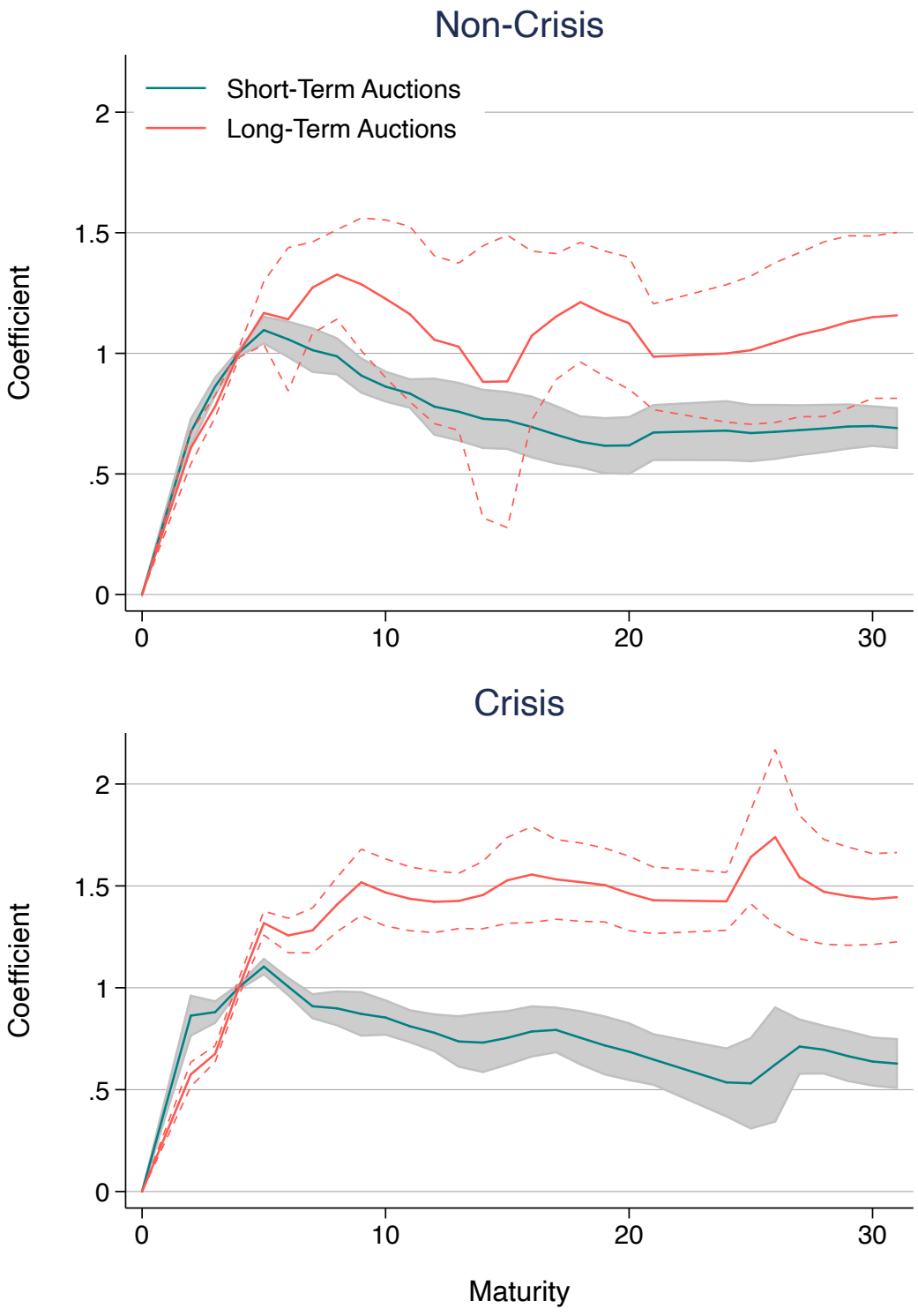

Figure C8: Localization Robustness: Narrative-Based Crises

Notes: Estimates of regression equation (15), identifying financial crises as periods identified by Romer and Romer (2017).

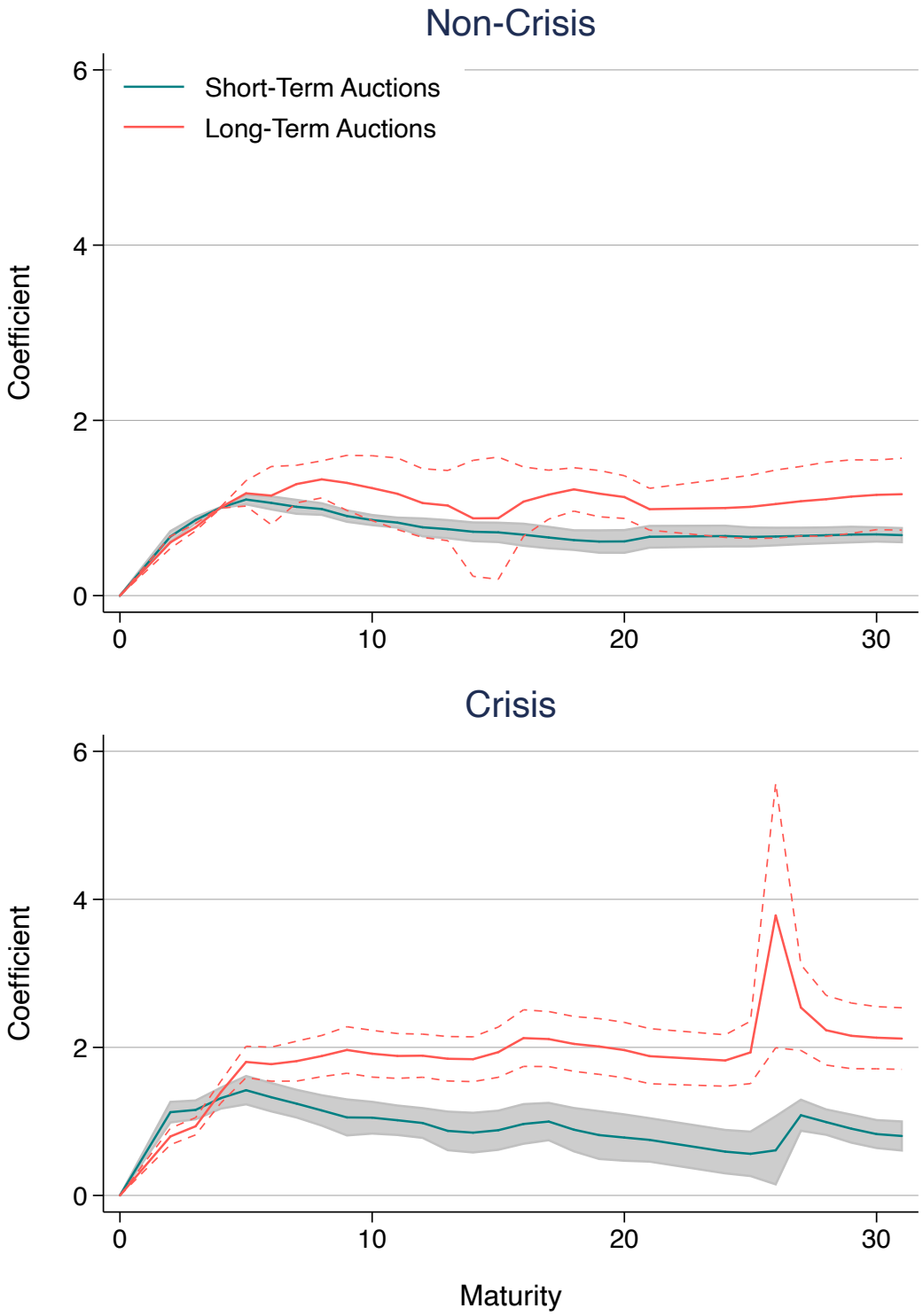

Figure C9: Localization Robustness: Narrative-Based Crises (Continuous)

Notes: Alternative specification of regression equation (15), where the crisis measure is treated as continuous (as measured by Romer and Romer (2017)). The measure is transformed to range from 0 to 1, and truncated so that values above 10 are set to 1.

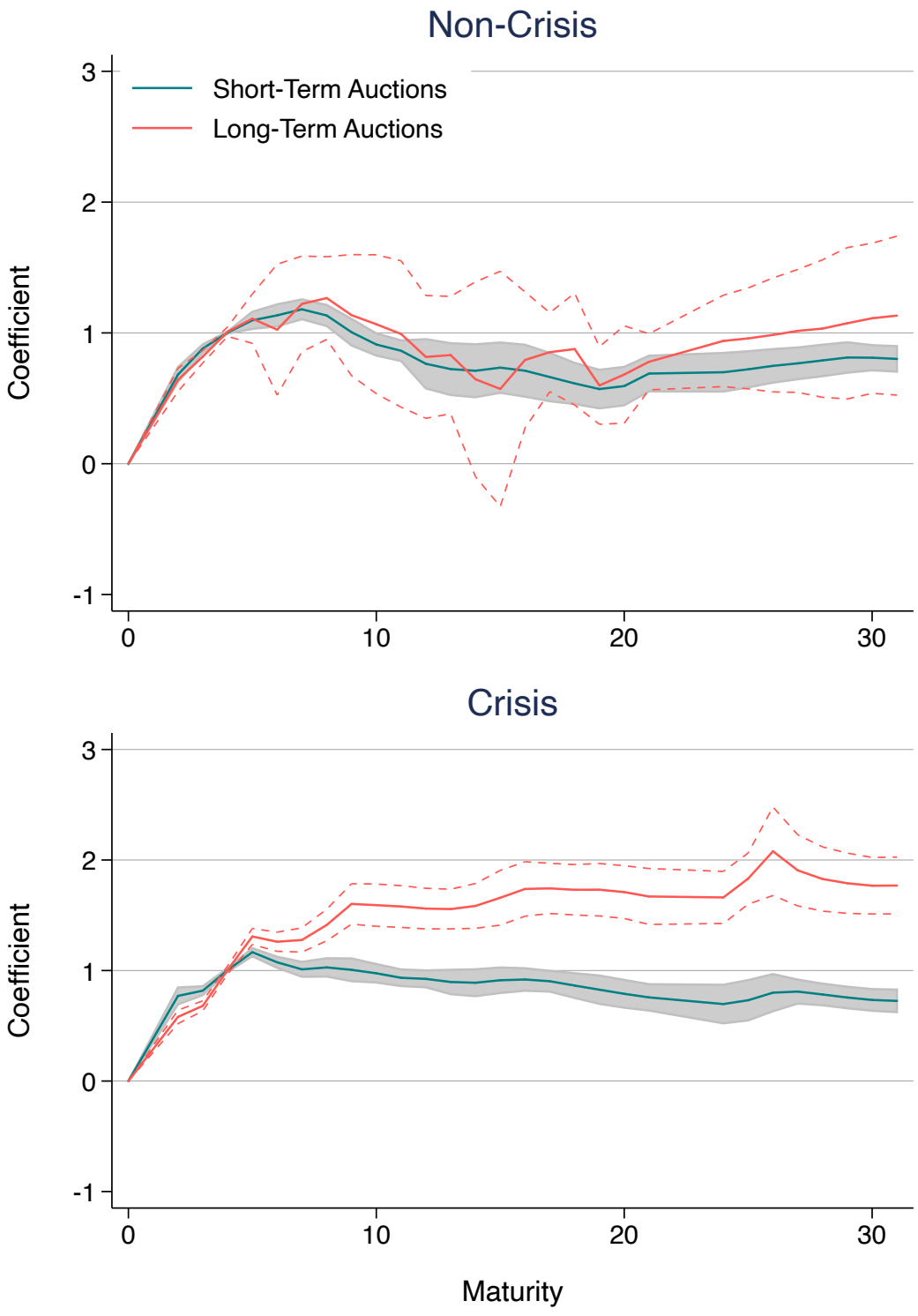

Figure C10: Localization Robustness: Long/Short Auctions

Notes: Estimates of regression equation (15), where short-maturity auctions are those with maturities 7 years or below, while long-maturity auctions are 10 years and above.

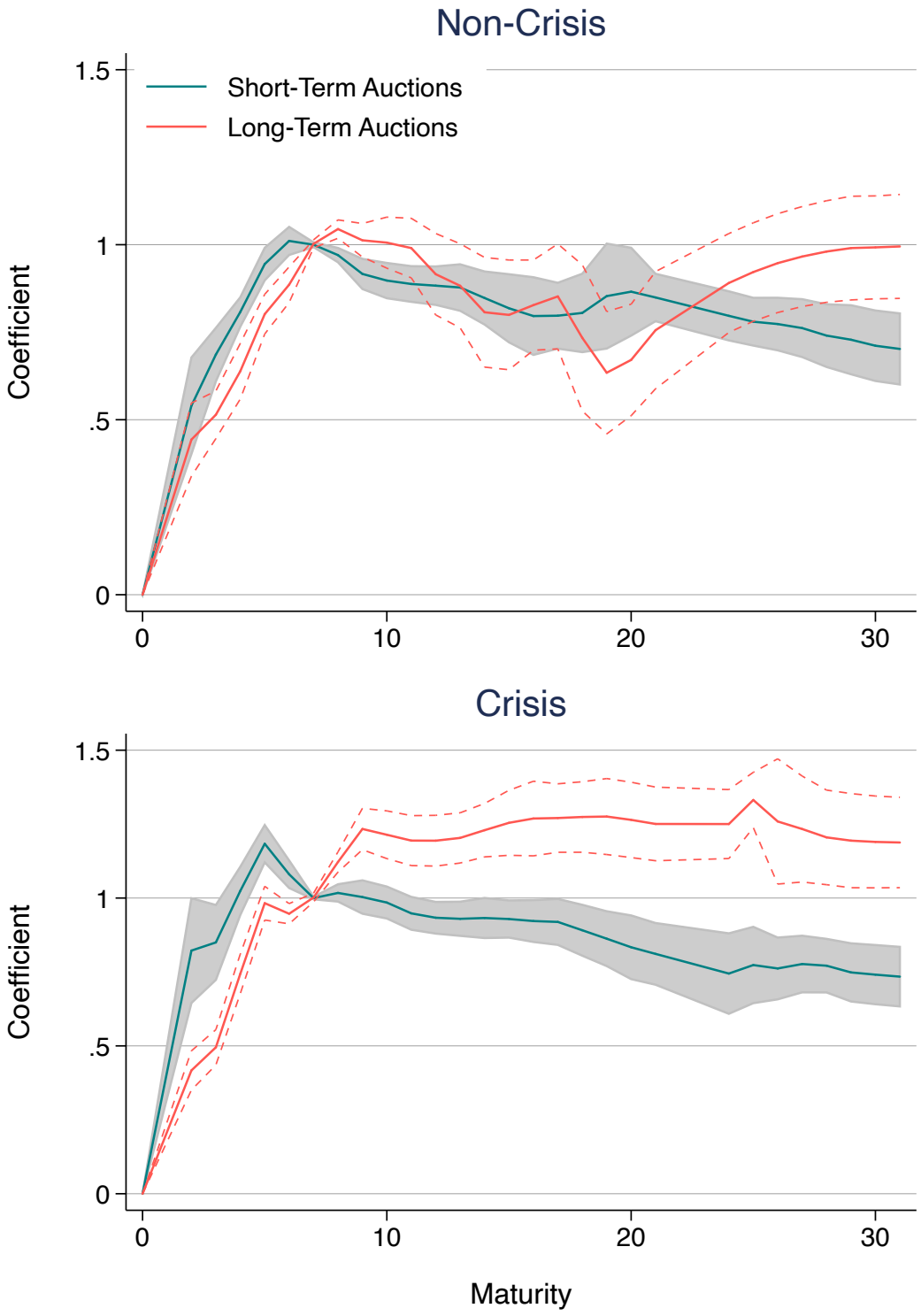

Figure C11: Localization Robustness: τ^*

Notes: Estimates of regression equation (15), where $\tau^* = 6$.

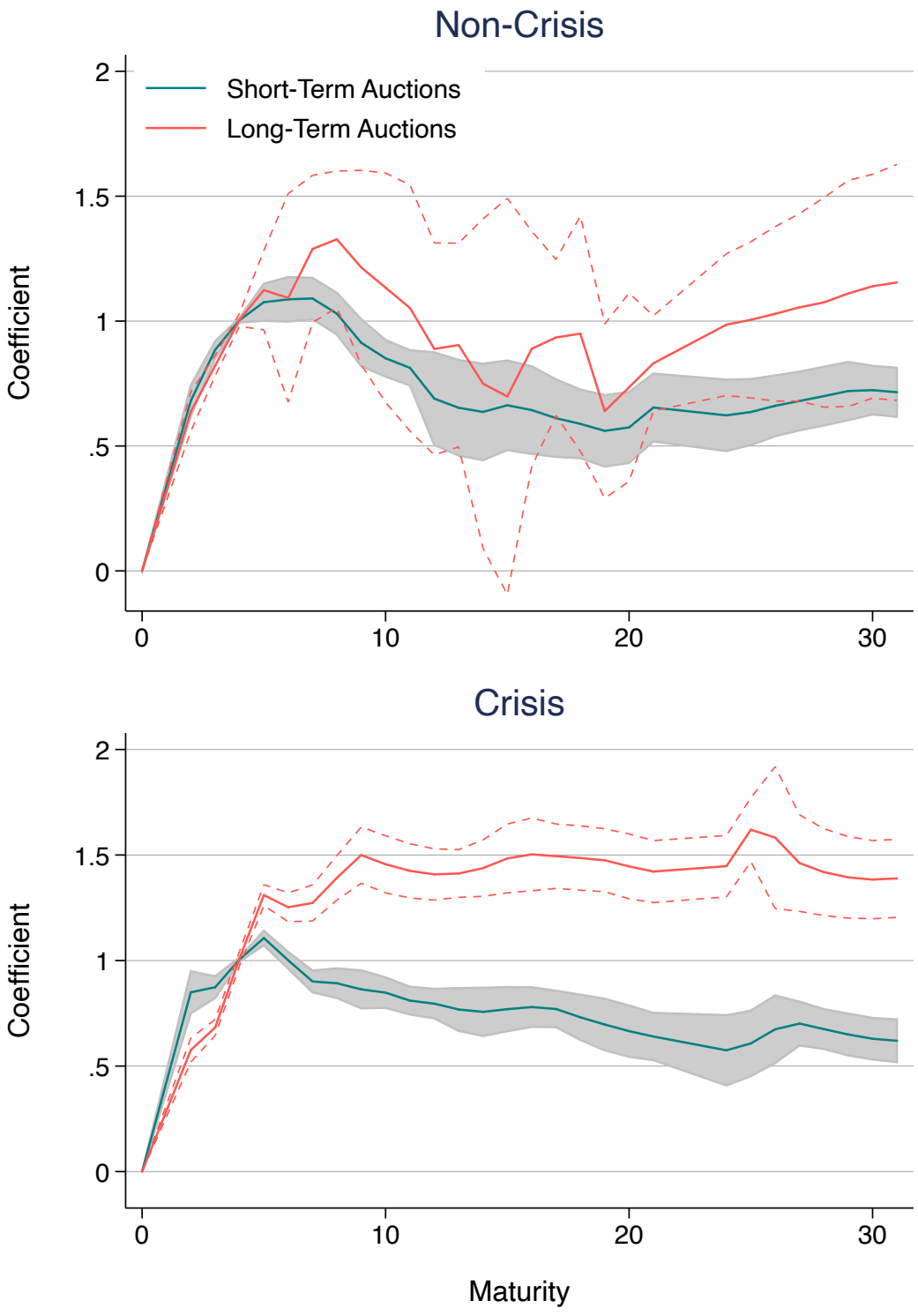

Figure C12: Localization Robustness: No QE Event Weeks

Notes: Estimates of regression equation (15), dropping auctions that occurred during the weeks of QE announcements.

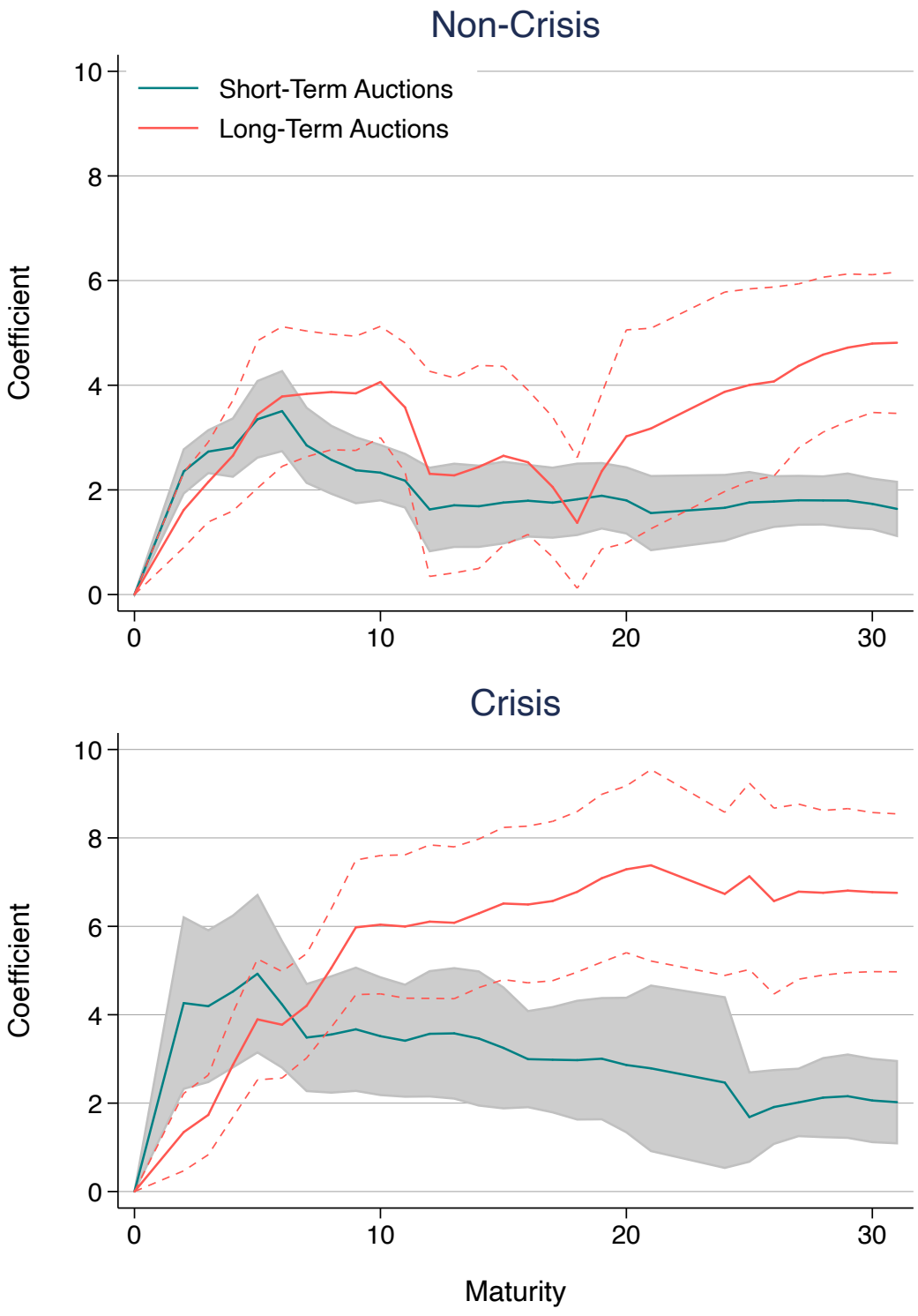

Figure C13: Localization Robustness: Bid-to-Cover

Notes: Estimates of the alternative localization regression equation (16), using the bid-to-cover ratio as a proxy of structural demand shocks (after controlling for its own four lags and flipping the sign).

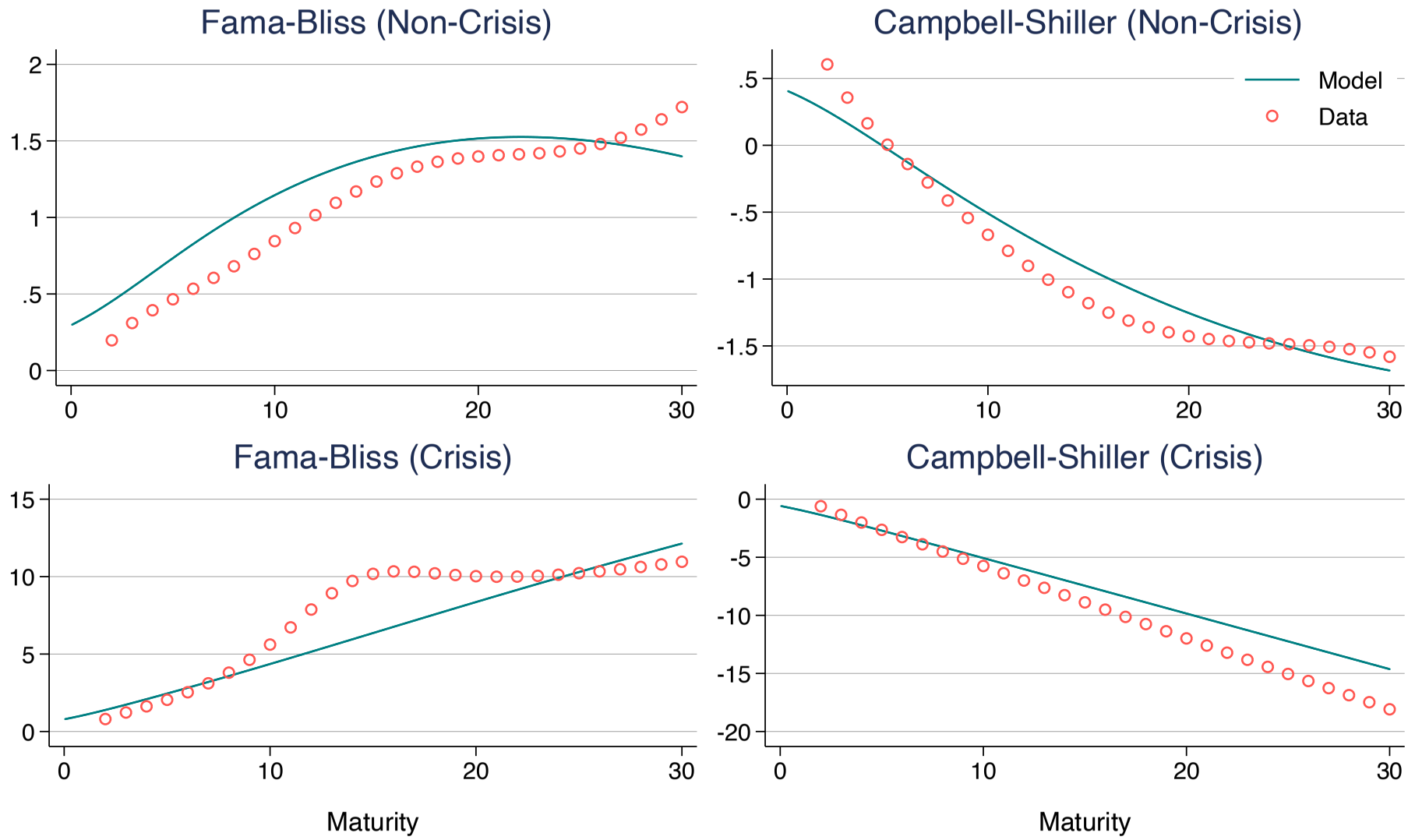

Figure C14: Model-Implied Term Structure Moments

Notes: comparison of targeted moments in the model (solid lines) with the data (scatter points). The targeted moments are regression coefficients across the term structure (maturity is on the x-axis): Fama-Bliss coefficients (left column) and Campbell-Shiller coefficients (right column), during periods of non-crisis (top row) and crisis (bottom row).

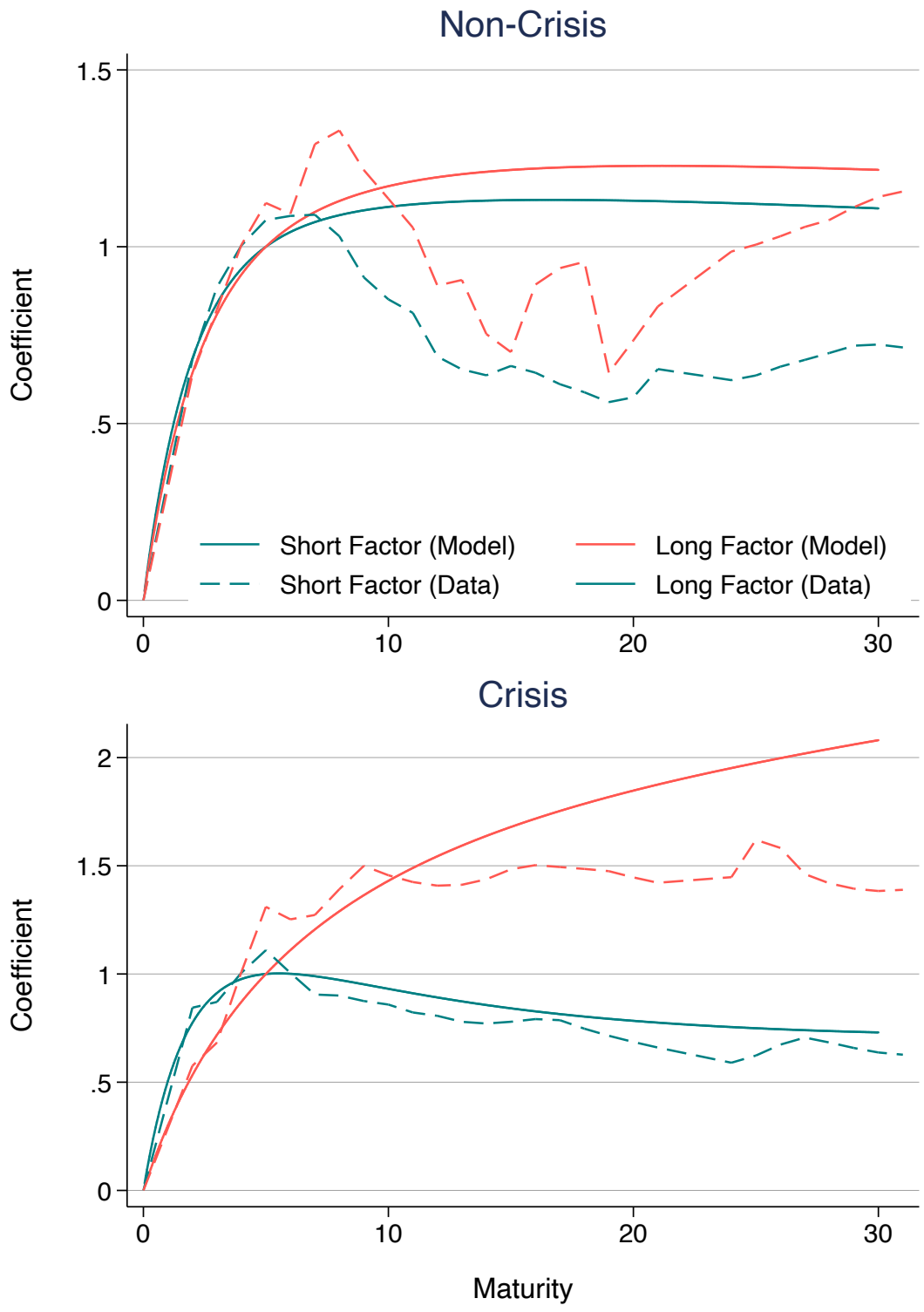

Figure C15: Localization Regression: Model vs. Data

Notes: Comparison of the empirical and model-implied localization coefficients from equation (15) (overlaying Figures 10 and 11).

Table C1: Asset Price Reactions to Demand Shocks (IV Specification)

Asset type	Estimate (s.e.)	Obs.	F-stat	Sample
	(1)	(2)	(3)	(4)
Panel A: Corporate debt				
LQD	-4.25***	826	92.2	2002-2017
	(0.33)			
Corp. Aaa†	1.10***	1016	147.5	1995-2017
	(0.15)			
Corp. Baa†	1.14***	1016	147.5	1995-2017
	(0.14)			
Corp. C†	0.36	969	134.6	1997-2017
	(0.47)			
Panel B: Equities				
SPY	-1.04	1020	145.9	1995-2017
	(0.68)			
IWM	-0.84	872	108.0	2000-2017
	(0.94)			
SP500†	1.65	950	142.0	1995-2016
	(4.24)			
Russell 2000†	5.45	950	142.0	1995-2016
	(4.40)			
Panel C: Inflation and commodities				
GLD	-1.63***	771	67.1	2004-2017
	(0.58)			
GSCI†	-5.80	950	142.0	1995-2016
	(3.99)			
10Y Infl. Swap†	0.04	720	67.1	2004-2016
	(0.13)			
2Y Infl. Swap†	0.09	720	67.1	2004-2016
	(0.33)			
Panel D: Spreads and credit default swaps				
Aaa-Baa†	0.04	1016	147.5	1995-2017
	(0.06)			
LIBOR-OIS†	0.22	733	70.8	2003-2016
	(0.15)			
Auto CDS†	1.72	729	69.5	2004-2016
	(2.66)			
Bank CDS†	-0.40	729	69.5	2004-2016
	(0.26)			
VIX†	0.05	1016	147.5	1995-2017
	(0.06)			

Notes: The table repeats the regressions from Table 4, but instruments the demand shocks D_t with the surprise component of the bid-to-cover ratio. First-stage F-statistics are reported in column (3). Newey-West (9 lags) standard errors in parentheses.